GEOLOGICAL, ENGINEERING GEOLOGICAL AND GEOTECHNICAL STUDIES OF THE UPPER TRISHULI – 2 HYDROELECTRIC PROJECT RASUWA, CENTRAL NEPAL

A DISSERTATION

(COURSE NO.: GEO 617)

BY

KEDAR SHRESTHA

EXAM ROLL NO.: 6048

SUBMITTED TO

CENTRAL DEPARTMENT OF GEOLOGY

INSTITUTE OF SCIENCE AND TECHNOLOGY

TRIBHUVAN UNIVERSITY

KIRTIPUR, KATHMANDU

NEPAL

IN PARTIAL FULFILLMENT OF THE REQUIREMENTS FOR THE MASTER'S DEGREE OF SCIENCE IN GEOLOGY

(2012 A.D.)

Tel. No.: 4332449, 4333085
E-mail: tugeoology@wlink.com.np

TRIBHUVAN UNIVERSITY

CENTRAL DEPARTMENT OF GEOLOGY
OFFICE OF THE HEAD OF DEPARTMENT
Kirtipur, Kathmandu
Nepal

Date: 10th Shrawan, 2069

It is certified that MR. KEDAR SHRESTHA has worked satisfactorily for his Master's Degree dissertation under my guidance and supervision. He has worked enthusiastically with sincere interest. The dissertation entitled "GEOLOGICAL, ENGINEERING GEOLOGICAL AND GEOTECHNICAL STUDIES OF THE UPPER TRISHULI – 2 HYDROELECTRIC PROJECT, RASUWA, CENTRAL NEPAL" embodies the candidate's own work. I, hereby, recommend the dissertation for approval.

……..

Supervisor

Dr. Prakash Das Ulak

Associate Professor

Tel. No.: 4332449, 4333085
E-mail: tugeoology@wlink.com.np

TRIBHUVAN UNIVERSITY

CENTRAL DEPARTMENT OF GEOLOGY
OFFICE OF THE HEAD OF DEPARTMENT

Kirtipur, Kathmandu
Nepal

Date: 11th Bhadra, 2069

The dissertation presented by MR. KEDAR SHRESTHA entitled "GEOLOGICAL, ENGINEERING GEOLOGICAL AND GEOTECHNICAL STUDIES OF THE UPPER TRISHULI – 2 HYDROELECTRIC PROJECT, RASUWA, CENTRAL NEPAL" has been accepted as the partial fulfillment of requirements for the Master's Degree of Science in Geology.

……..	……..
Head	**Supervisor**
Dr. Lalu Prasad Paudel	Dr. Prakash Das Ulak
Associate Professor	Associate Professor
……..	……..
External Examiner	**Internal Examiner**
Tikaram Paudel	Naresh Kaji Tamrakar
Nepal Electrical Authority	Associate Professor

ACKNOWLEDGEMENTS

I wish to express my deep sense of gratitude to my Internal Guide, Dr. Prakash Das Ulak, Associate Professor, Tri-Chandra Multiple Campus, Tribhuvan University (TU) for his incredible supervision, consistent support, able guidance and useful suggestions throughout the dissertation preparation.

I am heartily thankful to Er. Kamalesh Pradhananga, IDS Energy Pvt. Ltd. for his logistic support and constant help. I am also thankful to Mr. Bhupati Neupane and Sobit Thapaliya for giving their precious time during field data acquisition and for the invaluable suggestion and encouragement during dissertation preparation.

I am equally thankful to my colleagues Mr. Prem Nath Paudel and Mr. Saunak Bhandari for their constant help in map preparation and invaluable discussion during dissertation preparation.

I am also indebted to all the teachers and staffs of Central Department of Geology, Tribhuvan University for their kind co-operation. The contributions made by different persons whose names are not cited above are also highly acknowledged for their kind help.

Finally, I express deep gratitude to my parents and family members for their prolong help, support and inspiration.

Kedar Shrestha

July, 2012

TABLE OF CONTENTS

LIST OF FIGURES

LIST OF TABLES

GEOLOGICAL, ENGINEERING GEOLOGICAL AND GEOTECHNICAL STUDIES OF THE UPPER TRISHULI – 2 HYDROELECTRIC PROJECT

RASUWA, CENTRAL NEPAL

KEDAR SHRESTHA

Central Department of Geology, Kirtipur, Kathmandu

Abstract

The Upper Trishuli – 2 Hydroelectric Project is located on the northern part of Rasuwa District, Central Nepal. Geographically, the study area extends from longitude 85° 17' 44" E to 85° 20' 37" E and latitude 28° 07' 36" N to 28° 10' 06" N. Its estimated capacity is 100 MW with net head of about 98 m.

The study is concerned with geological, engineering geological and geotechnical studies of the Upper Trishuli – 2 Hydroelectric Project. The rocks of the area belong to the Ranimatta Formation, Midland Group of Lesser Himalayan succession. They comprise quartzite, phyllite and schist. Most of the area comprise higher proportion of quartzite than that of phyllite The foliation plane of the area is along (020° to 040°) with dip amount of (45° to 30°).

All the hydraulic structures lie within the bedrock. The structures like desander basin and powerhouse are underground. The headrace tunnel alignment passes through two passive faults namely, Syo Khola Fault and Gre Khola Fault. Adjusted RMR and Q ranges from 46 to 64 and 1.68 to 8.66 respectively. Generally, rocks belong to poor to fair rock class.

Geotechnical studies include preliminary stress analysis and rock support design along the underground structures. Average in-situ deformation modulus ranges from 6.7865 to 22.719. Vertical and horizontal stress as well as horizontal to vertical ratio ranges from 0.74-3.9394, 1.5029-5.7050 and 0.623-3.262 respectively. Damage index varies from 0.0367 to 0.1158. Support design for construction of the headrace tunnel based on different system suggests the combination of local to systematic bolting and reinforced shotcrete as per requirement.

Geophysical survey shows the thickness of alluvial and colluvial overburden ranges from 15 m to 60m.

Construction material can be extracted from 14 sites while 4 sites are suitable for muck disposal.

CHAPTER 1

INTRODUCTION

Nepal has a huge hydropower potential. In fact, the perennial nature of Nepali rivers and the steep gradient of the country's topography provide ideal conditions for the development of some of the world's largest hydropower projects in Nepal. Based on the report of Water and Energy Commission Secretariat, WECS (2011), the estimated hydropower potential of Nepal is 83,000 MW. Out of this estimated potential, 114 projects with a combined capacity of 45,610 MW have been identified as economically feasible. The recent estimate at 40% dependable flows for the Run-of-River (ROR) hydropower potential in Nepal stands at 53,836 MW. At present, the NEA has a total installed electricity generation capacity of about 689 MW. Out of this, the hydropower capacity stands at 632 MW.

Geologically, Nepal lies within the most tectonically active mountain belts and fragile part of the world. The most seismically active zone had suffered various geological disasters. The high relief, steep gradient of stream, monsoonal rainfall and flood, frequent earthquakes and fragile nature of terrain causes the higher rate of erosion and are the factors aggravating the situation. These phenomena made the region more vulnerable to the mass movement. The infrastructures built in these conditions are very susceptible to the failure. Considering these adverse natural conditions and its negative impacts on infrastructures, the geological study is quite essential for the construction of hydropower structures in Nepal.

The present work has been carried out for the partial fulfillment of the requirements for the Master's Degree of Science in Geology with the permission from the Upper Trishuli – 2 Hydroelectric Project. The study is focused concerning the significant geological factors at and around the project area. Most of the study is confined to the area where the major hydraulic structures such as headworks, headrace tunnel, powerhouse and tailrace has been planned to construct. The dissertation is the outcome of overall 3 weeks of fieldwork and about 16 weeks of laboratory and table work.

The organization of the report closely follows the guideline provided by the Central Department of Geology. The dissertation comprises eight chapters and three annexes. The first chapter includes a brief introduction of the project, location, accessibility,

topography and drainage, climate, flora and fauna and socio-economic condition of the area. The second chapter includes the objectives and methodology adopted during the study. The third chapter deals with the geology of the study area. The fourth chapter describes the engineering geological condition of the study area. The fifth chapter includes the geotechnical studies of the underground structures. The sixth chapter deals with the subsurface investigation of the project area. The seventh chapter includes the description of construction materials. The conclusion is given in chapter eight. Salient features of the Upper Trishuli-2 HEP is given in Annex-I. Annex-II represents the photographs of the project area. Annex-III contains the geomechanical parameters of the study area.

1.1 Introduction of Upper Trishuli-2 Hydroelectric Project

The Upper Trishuli-2 Hydroelectric Project is the daily poundage Run-of-River type project having discharge of 1,041m^3/s. The proposed installed capacity of the project is 100 MW with underground power plant. The design net head is about 98 m. The headworks comprises of a 123.1 m long dam from which water is diverted into the underground desander basin having the dimension of 30m×15m×10.3m. The horse shoe shaped headrace tunnel is 3,170 m long having 7 m diameter. The surge shaft has 11 m diameter and 59.5 m height. The pressure pipe has 5m diameter and 155 m length. The proposed powerhouse is underground structure having dimension of 70m×17.6m×44.8m that accommodates two generating units of capacity 50 MW each. After the generation, water will be discharged to the Trishuli River through a tailrace tunnel of length 135 m.

1.2 Location

Politically, the study area (Fig. 1.1) lies in Rasuwa district of Bagmati zone in Central Development Region. Geographically, the study area extends from longitude 85° 17' 44" E to 85° 20' 37" E and latitude 28° 07' 36" N to 28° 10' 06" N. Geologically, the study area lies in Central Nepal Lesser Himalaya that includes the rocks of the Nawakot Complex.

1.3 Accessibility

The study area is accessible by Kathmandu – Trishuli – Somdang Road with the distance of 130 km to the northwest of Kathmandu. A number of foot trails connecting local villages facilitate to traverse in the different section of the headworks, headrace tunnel and powerhouse area.

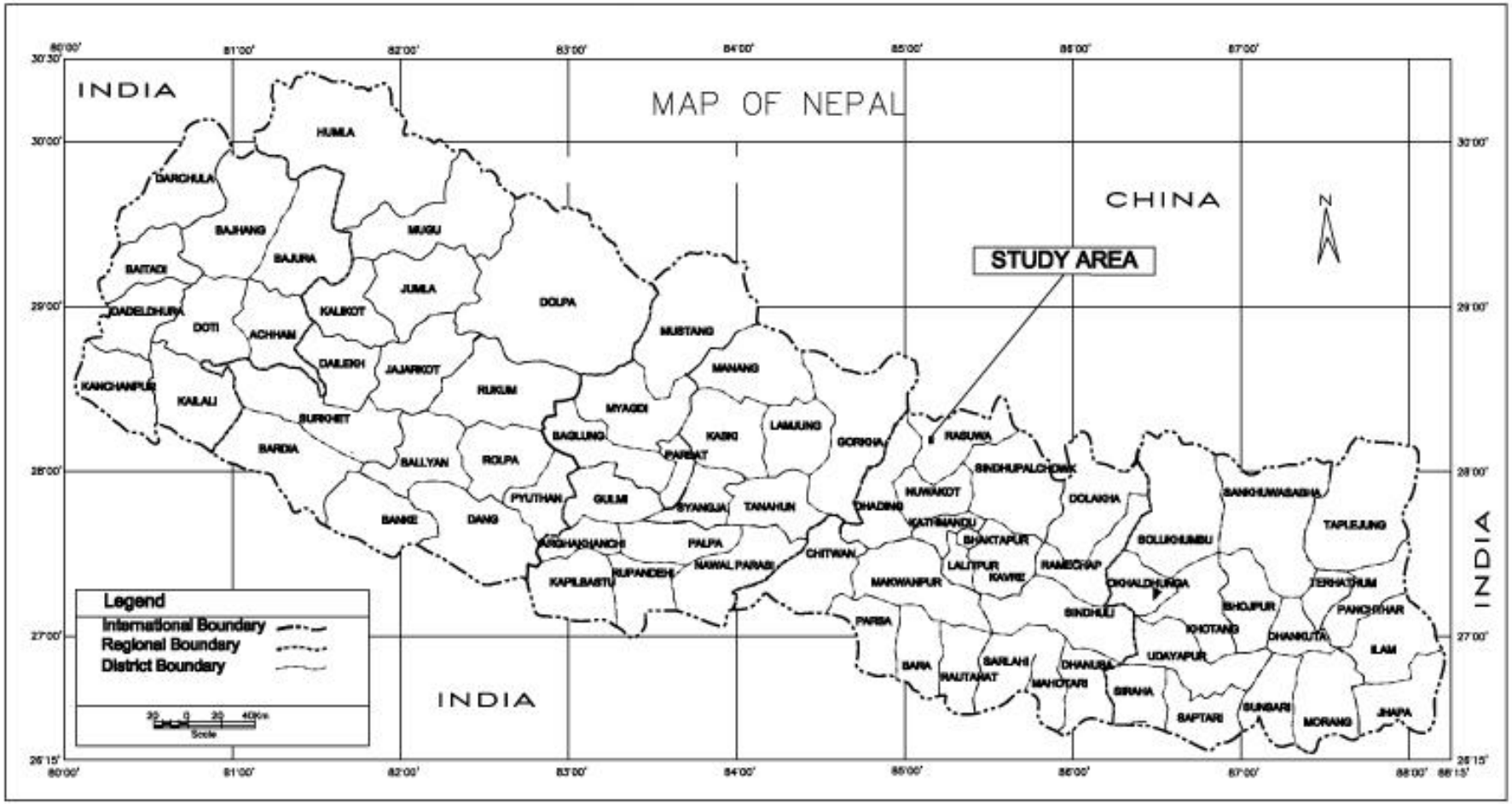

Fig. 1.1 Location map of the study area

1.4 Topography and Drainage

The study area is characterized by matured topography with ridges and spurs either forming cliffs or steep faces. The highest altitude is 2,546 m at Gre and the lowest one is 1,250 m at the confluence of Bhote Koshi River and Trishuli Khola. Most of the study area lies in V- shaped valley (Fig. 1.2) of the Bhote Koshi River. The right bank of the river is steeper than the left bank.

Fig. 1.2 V-shaped valley of the Bhote Koshi River around the project area as seen on the satellite image (Source: Google Earth, 2009)

The Bhote Koshi River (called as Trishuli River after the conflux of Bhote Koshi River and Trishuli Khola) is one of the major tributaries of Sapta Gandaki. It is snow fed as well as rain fed river. In the study area, it flows from northeast to southwest. The Kerung Himal and Langtang Himal are major mountain range in the basin. The major tributaries of Bhote Koshi River in the study area are Chilime River, Langtang River and Trishuli Khola. The overall drainage pattern of the area is dendritic (Fig. 1.3).

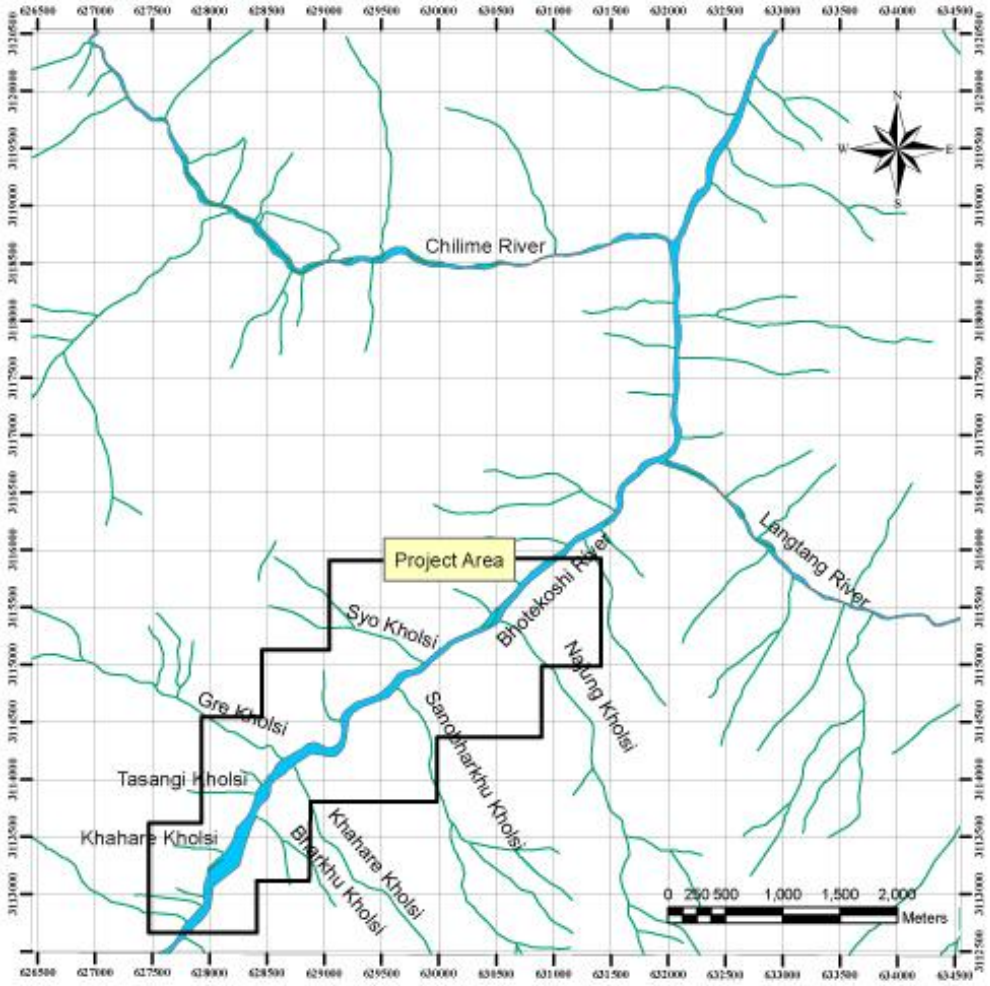

Fig. 1.3 Drainage map of the study area

1.5 Climate

The Himalayan range exhibits diversity in topography and climatic conditions. The fluctuation in both temperature and precipitation are due to a wide variation in elevation and exposure to sunlight. The basin in upper reaches is surrounded by high mountains and has an alpine climate. The High Himalayan Range (Ganesh Himal, Kerung Himal and Langtang Himal) essentially forms a barrier and exhibits very low precipitation in the north of this range. Hence, the upper catchment remains arid. In general, the amount of precipitation is highest to the south at the lower elevations and gradually decreases to the north with an increase in elevation. The lower catchment area has a sub-tropical to temperate climate. During monsoon period, the area receives about 85% of the total annual precipitation (source: Langtang National Park).

1.6 Flora and Fauna

The vegetation in the area changes with elevation, temperature and rainfall. Sub-tropical vegetation characterized by Sal (*Shorea robusta*) forest in southern part is gradually taken over by hill forest (2,000-2,600 m) consisting of Chirpine, Rhododendron and Nepalese alder. The temperate zone (2,600-3,000 m) is covered by oak forest to old growth forest of silver fir, hemlock and larch in the lower sub-alpine zone (3,000-3,600 m). Throughout these zones different species of Rhododendron such as *R. arboretum*, *R. barbatum*, *R. campanulatum* and *R. lepidotum* form a colourful under story.

The area's high meadows provide summer habitat for numerous ungulate species such as musk deer and Himalayan tahr. The area is also well known for its populations of red panda, Himalayan black bear, snow leopard, wild dog, ghoral, serow and more than 250 species of birds.

1.7 Socio-Economic Condition

Most people of the area depend upon agriculture and livestock rearing. The major agricultural products are potato, maize, buckwheat, millet as well as other seasonal vegetables. Tamang, Brahmin, Gurung and Sherpa are the major ethnic groups living in the area. The economic condition is relatively sound. Villages are popular for tourism for their Tamang culture, tradition, cultural sites and pilgrimage sites.

CHAPTER 2

OBJECTIVES AND METHODOLOGY

The present study is concerned with geological, engineering geological and geotechnical investigation of Upper Trishuli-2 Hydroelectric Project for the purpose of dissertation writing which is solely an academic.

2.1 Objectives

The main objective of the present study is to collect geological, engineering geological and geotechnical information in order to assess the technical prospect of Upper Trishuli-2 Hydroelectric Project. The objectives of the study are summarized below.

- To study regional geological condition of the study area
- To study engineering geological condition of the study area and prepare engineering geological map of the project area in the scale of 1:10,000.
- To assess and classify the rock mass surrounding the underground structures so that support system can be quantified.
- To carry out statistical analysis of joints and their interpretation
- To carry out preliminary study to find out in-situ stress conditions along the alignment of the underground structures using geotechnical parameters.
- To carry out subsurface investigation along the structures like desander basin, powerhouse area etc.
- To identify construction material sites.

2.2 Methodology

To achieve the stated objectives, the methodology adopted during the study can be broadly divided into four topics:

1) Desk study
2) Field study
3) Laboratory work and
4) Data processing, interpretation and report writing

2.2.1 Desk Study

Topographic maps, preliminary published and unpublished reports and journals, field manuals and established theories related to the present study were collected and studied in detail. The topographic map, 2885 14, Dhunche, (scale 1:50,000), published by the Government of Nepal, Department of Survey in 1996 were used for the study. In addition, the topographic map (scale 1:10,000) of the project area provided by the Upper Trishuli-2 HEP was also used for the preparation of Engineering Geological map.

The study provides some preliminary information as well as facilities to formulate the schedule and general route of the field work. Published and unpublished papers, reports and dissertation available on Central Department of Geology provide a concept on geological, engineering geological and geotechnical conditions of the study area. Based on available information, an investigation program was scheduled for the field works.

2.2.2 Field Study

The field study was carried out in two stages: (a) reconnaissance survey and (b) detail survey.

2.2.2.1 Reconnaissance survey

The desk survey was followed by four day reconnaissance survey. In this survey, information collected from the desk study was verified and various reconnaissance geological traverses were taken. After the reconnaissance study, the plan for detail study was initiated.

2.2.2.2 Detail survey

The 16 day detail survey covered regional geology of the study area and engineering geological mapping along the headworks site, headrace tunnel and powerhouse site with required geotechnical data collection. Brunton compass, geological hammer, measuring tape, dil. HCl, GPS and altimeter were used for this purpose. Generally, the traverses were made along the Bhote Koshi River and its tributaries, foot trails and spurs. The field study included the following main activities.

- Detail measurement of the rock discontinuities using Brunton compass, hammer and measuring tape.
- Detail measurement of geotechnical parameters required for rock mass classification.

- Detail mapping of rock outcrops, surficial deposits and geomorphological features for the preparation of engineering geological map.
- Collection of rock samples from different locations for the laboratory test.

2.2.3 Laboratory Work

The laboratory test (point load test) of rock samples was done in NEA Geotechnical Laboratory.

2.2.4 Data Processing, Interpretation and Report Writing

All the data and information obtained during desk study, field investigation and laboratory test were then refined and analyzed. Engineering geological map, slope stability analyses were prepared using different computer software such as AutoCad, Arc View GIS and DIPS.

The rock strength analysis for the underground structure was carried out using RocLab software. All of the data and maps were then used for the interpretation geological, engineering geological and geotechnical condition of study area. Finally the report was prepared in accordance with the guidelines provided by Central Department of Geology, Tribhuvan University.

CHAPTER 3

GEOLOGY OF THE STUDY AREA

The Himalaya was generated because of the collision of the northward moving Indian Plate with the Asian (Eurasian) Plate. This process of orogeny is still continued, mountains still being formed. Geographically, the Himalayan range lies between its eastern and western syntaxis as represented by the Namche Barwa and Naga Parbat. It is bounded by Yalu Tsangpo and Indus River in the north while the Main Frontal Thrust is the southern boundary. It is divided into five-section from west to east (Gansser, 1964). They are: Punjab, Kumaon, Nepal, Sikkim – Bhutan and NEFA Himalaya.

3.1 Geology of Nepal Himalaya

Nepal Himalaya covers the central most sector of 2,400 km long southwardly convex Himalaya mountain arc and extends for about one third (800 km) of its total length running from the Mechi River in the east to the Mahakali River in the west (Gansser, 1964). It is divided into five major tectonic zones that extend approximately parallel to each other, each characterized by their own lithology, tectonics, structures and geological history. From south to north, they are: Terai, Sub - Himalaya, Lesser Himalaya, Higher Himalaya and Tethys Himalaya. It is also divided into four traverse geological zones namely Eastern Nepal, Central Nepal, Western Nepal and Far Western Nepal separated by a major river. Fig. 3.1 depicts generalized regional geological map of the Nepal Himalaya.

3.1.1 Terai Zone

This zone represents the northern edge of the Indo-Gangetic alluvial plain and forms the southernmost tectonic division of Nepal. It is a foreland basin which is delineated by Himalayan Frontal Thrust (HFT) in the north. Geologically, the Terai plain is covered by Pleistocene-Recent Alluvium. The average thickness of the deposit is about 1,500 m. Geomorphologically, from north to south, Terai zone is sub-divided into Northern (Bhabar), Middle (Marshy) and Southern zones.

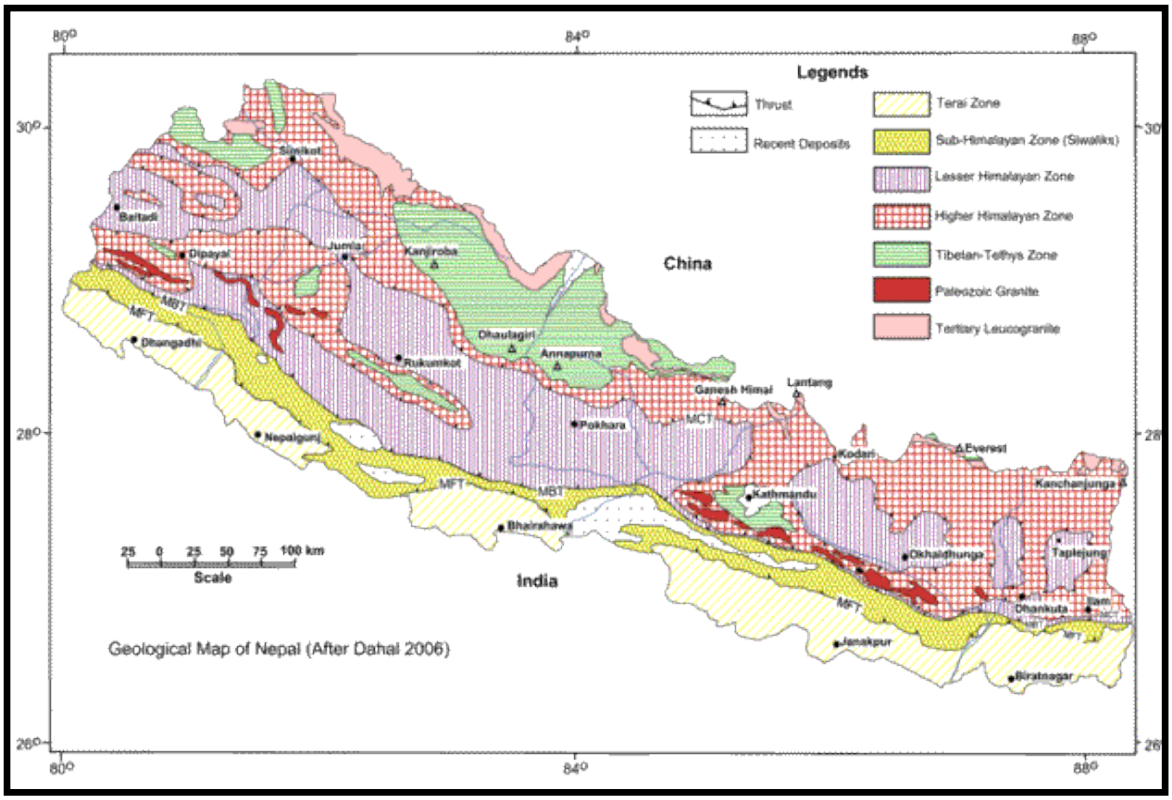

Fig. 3.1 Generalized geological map of Nepal Himalaya (after Dahal, 2006)

3.1.2 Sub Himalayan Zone (Siwalik)

The Sub-Himalayan Sequence borders the Indo-Gangetic Floodplain along the Himalayan Frontal Fault and is dominated by thick Late Tertiary mollassic deposits known as the Siwaliks that resulted from the accumulating fluvial deposits on the southern front of the evolving Himalaya. It is delineated by the Himalayan Frontal Thrust (HFT) and Main Boundary Thrust (MBT) in south and north respectively.

In Nepal, it extends throughout the country from east to west in the southern part. This zone is sub-divided into the Lower Siwalik, Middle Siwalik and Upper Siwalik (Auden, 1935). The Lower Siwalik comprises ash grey and red-brown, fine-grained sandstone with pseudo-conglomerate containing pebbles of Siwalik fragments, inter-bedded with purple, grey mudstone and siltstone. A few vertebrate fossil remains have been reported from central and central west Nepal (West *et al*., 1978, 1981; Munthe *et al*., 1983). The Middle Siwalik comprises relatively coarse, arkosic to lithic, grey sandstone with small proportion of green and grey mudstone and siltstone. Sandstone is “salt and pepper” type in appearance and is thick bedded and cross laminated toward the top. Occasionally, it consists of grit and conglomerate beds in the middle and upper part of the sequence. Coalified plant logs, leaf impressions and some mollusc are found in sandstone, mudstone and siltstone (West *et al*., 1975; Corvinus, 1988). The Upper Siwalik comprises dominant

coarse conglomerate beds with minor sandstone and mudstone beds. Conglomerate consists of pebble, cobble and boulder of gneiss, schist, granite and quartzite of the Higher Himalaya, limestone, phyllite, slate and sandstone of the Lesser Himalaya and sandstone of the Lower and Middle Siwaliks.

3.1.3 Lesser Himalayan Zone

The northernmost boundary of the Siwaliks Group is marked by the Main Boundary Thrust (MBT), over which the low grade metasedimentary rocks of the Lesser Himalaya overlie. The Lesser Himalaya, also called the Lower Himalaya, or the Midlands, is a thick (about 7 km) section of para – autochthonous crystalline rocks made up of low to medium grade rocks. These proterozoic clastic rocks (Parrish and Hodges, 1996) are subdivided into two groups. Argillo – arenaceous rocks dominate the lower half of the succession, whereas the upper half consists of both carbonate and siliciclastic rocks (Hagen, 1969; Le Fort, 1975; Stocklin, 1980). The Lesser Himalaya thrust over the Siwalik along the MBT to the south and is overlained by the allochthonous thrust sheets of Kathmandu and HHC along the MCT.

3.1.4 Higher Himalayan Zone

This zone extends from the MCT to Tibetan-Tethys zone and runs throughout the country. This zone consists of almost 10 km thick succession of the crystalline rocks, commonly called the Himal Group. This group sequence can be divided into four main units, as Kyanite - Sillimanite gneiss, Pyroxenic marble and gneiss, Banded gneiss and Augen gneiss in the ascending order (Bordet, Colchen and Le Fort 1972).

The Higher Himalayan sequence has been variously named. French workers used the term Dalle du Tibet (Tibetan Slab) for this unit (Le Fort, 1975; Bordet, Colchen and Le Fort, 1972). Hagen (1969) called them Khumbu Nappes and Lumbasumba Nappes. Arita (1983) calls it the Himalayan Gneiss Group and it lies above the MCT II or the upper MCT.

The High Himalayan Crystalline (HHC) units are mainly composed of kyanite to sillimanite grade gneisses intruded by High Himalayan leucogranites at structurally higher levels (Upreti, 1999). Throughout much of the range, the unit is divided into three formations (Pêcher and Le Fort, 1986). In Central Nepal (Guillot, 1999), the upper Formation III consists of augen orthogneisses, whereas the middle Formation II are

calcsilicate gneisses and marbles and the basal Formation I are kyanite and sillimanite bearing metapelites, gneisses and metagreywackes with abundant quartzite.

The gneiss of Higher Himalayan Zone (HHZ) is a thick continuous sequence of about 5 to 15 km (Guillot, 1999). The northern part is marked by North Himalayan Normal Fault (NHNF), which is also known as South Tibetan Detachment System (STDS). At its base, it is bounded by the MCT. The protolith of the HHC is interpreted to be Late Proterozoic clastic sedimentary rocks deposited on the northern Indian margin (Parrish and Hodges, 1996).

3.1.5 Tibetan - Tethys Zone

The Tibetan - Tethys Himalayas generally begins from the top of the Higher Himalayan Zone and extends to the north in Tibet. In Nepal, these fossiliferous rocks are well developed in Thak Khola (Mustang), Manang and Dolpa area. This zone is about 40km wide and composed of fossiliferous sedimentary rocks such as shale, sandstone and limestone etc.

The north of the Annapurna and Manaslu ranges in Central Nepal consists of metasediments that overlie the Higher Himalayan Zone along the South Tibetan Detachment System. It has undergone very little metamorphism except at its base where it is close to the Higher Himalayan crystalline rocks. The rocks are currently presumed to be 7400 m (Fuchs, Widder and Tuladhar, 1988). The rocks of the Tibetan Tethys Series (TSS) consist of a thick and nearly continuous Lower Paleozoic to Lower Tertiary marine sedimentary succession. The rocks are considered to be deposited in a part of the Indian passive continental margin (Liu and Einsele, 1994).

3.2 Review of previous works in the study area

Lesser Himalayan succession of Nepal Himalaya has been studied by various geoscientists. From the early time, geological investigations around Lesser Himalaya received a high priority. Compared to western counterparts, more study has been carried out in eastern parts of Nepal Himalaya.

The earliest note on the geology of Central Nepal was given by Medlicott (1875) who took a traverse from Amlekhgunj through Kathmandu to Nuwakot. Auden (1935) is one of the earliest workers who has given a fairly detail geology of Central Nepal. Hagen as early as 1951 described the geological structures of Central Nepal who later extended his work to entire country (Hagen, 1969).

Although many researchers have worked in Central Nepal, very few carried out their research in the present study area. A brief review of previous works of the area is given below.

- Stöcklin and Bhattarai (1977) and Stöcklin (1980) prepared a regional geological map and divided the rocks of Central Nepal into the Nawakot Complex and the Kathmandu Complex separated by the Mahabharat Thrust (MT). Based on aerial photo interpretation and fieldwork, they stated the MT as the southward extension of the MCT.
- Colchen *et al.*, (1980, 1986) carried out the mapping of Annapurna-Manaslu-Ganesh Himal area. The map is further modified by Rai (2001). According to them, the Higher Himalayan succession is made up of medium to high grade metamorphic rocks such as sillimanite schist and gneiss, kyanite schist and gneiss whereas the Lesser Himalayan sequence contains essentially phyllite, quartzite and graphitic schist. They delineated the MCT between Ganesh Himal and the Kaligandaki River.
- Department of Mines and Geology (DMG, 1987) prepared the geological map (Fig. 3.4) of Central Nepal and subdivided the whole area into Kathmandu Group and Midland Group.
- Macfarlane *et al.*, (1992) carried out structural analysis of the MCT in and around the Syaphrubesi area. This is the first major geological work in the study area. They divided schist, augen gneiss, quartzite and carbonate rocks of the Lesser Himalaya into eleven formations. The MCT passing near the confluence of the Bhote Koshi and Langtang Khola separates these Lesser Himalayan rocks with the Higher Himalayan Gneisses. They traced a series of four more or less parallel faults within the MCT zone.
- Parrish and Hodges (1996) studied isotope of U-Pb and Sm-Nd sample from Langtang area, Central Nepal. They separated the Lesser and Higher Himalayan sequence on the basis of Sm-Nd isotopic analysis. The Greater and Lesser Himalayan sequences are juxtaposed along a structurally complex shear zone, up to 3.7 km thick, representing the MCT system.
- Rai (1998, 2001) prepared a geological map of Central Nepal including Syaphrubesi area. He studied the pressure temperature evolution in Gosainkunda

region and divided into Gosainkunda Crystalline Sequence and Lesser Himalayan Sequence separated by the MCT.

- Takagi *et al.*, (2003) have studied about the kinematic history of the Main Central Thrust in the Langtang area, Central Nepal (Fig. 3.2). They have worked in detail around the MCT zone and divided the area into three major tectono-lithostratigraphic units. The Lower and Middle units were included in Lesser Himalayan Sequence and the Upper unit was included in the Higher Himalayan Sequence.

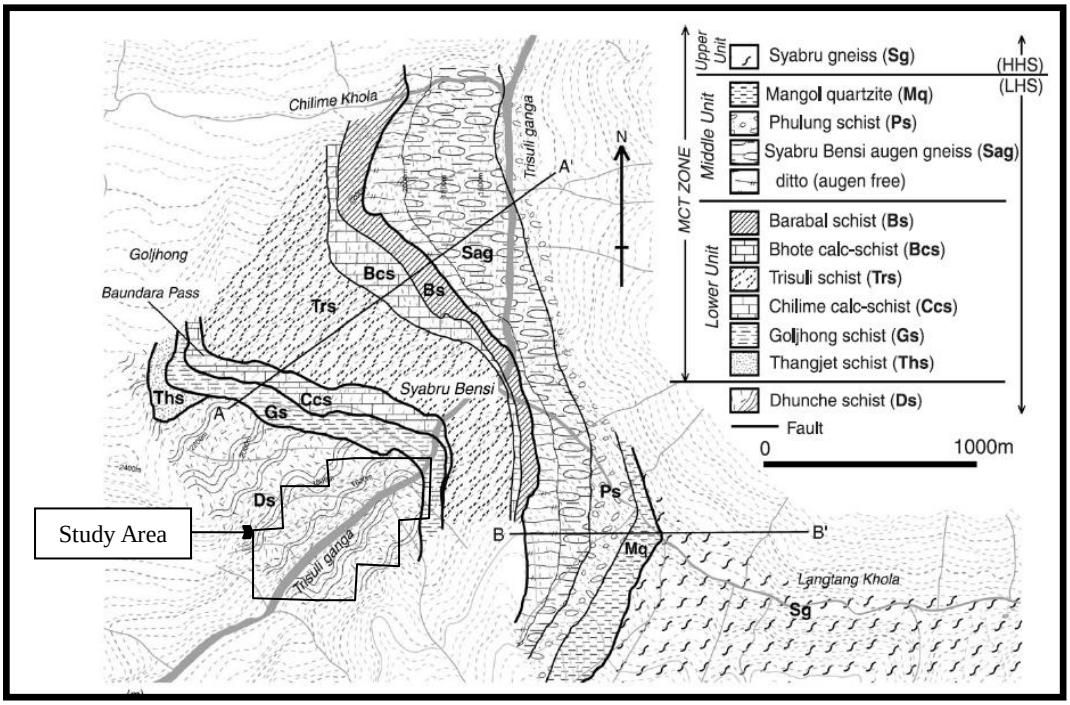

Fig. 3.2 Geological map of the study area after Takagi *et al.*, (2003)

- Kohn *et al.*, (2005) studied the northern part of the area (Syaphrubesi to Langtang village). They divided the area into two major tectonic divisions; the Lesser Himalayan Sequence and the Higher Himalayan Sequence (Fig. 3.3). According to them, MCT and Ramgadh Thrust (RT) are two major thrust. The MCT divides the whole area into the Lesser Himalayan Sequence and the Higher Himalayan Sequence whereas the RT separates massive marble and calc-schist with Orthogneiss and Al-rich schist.

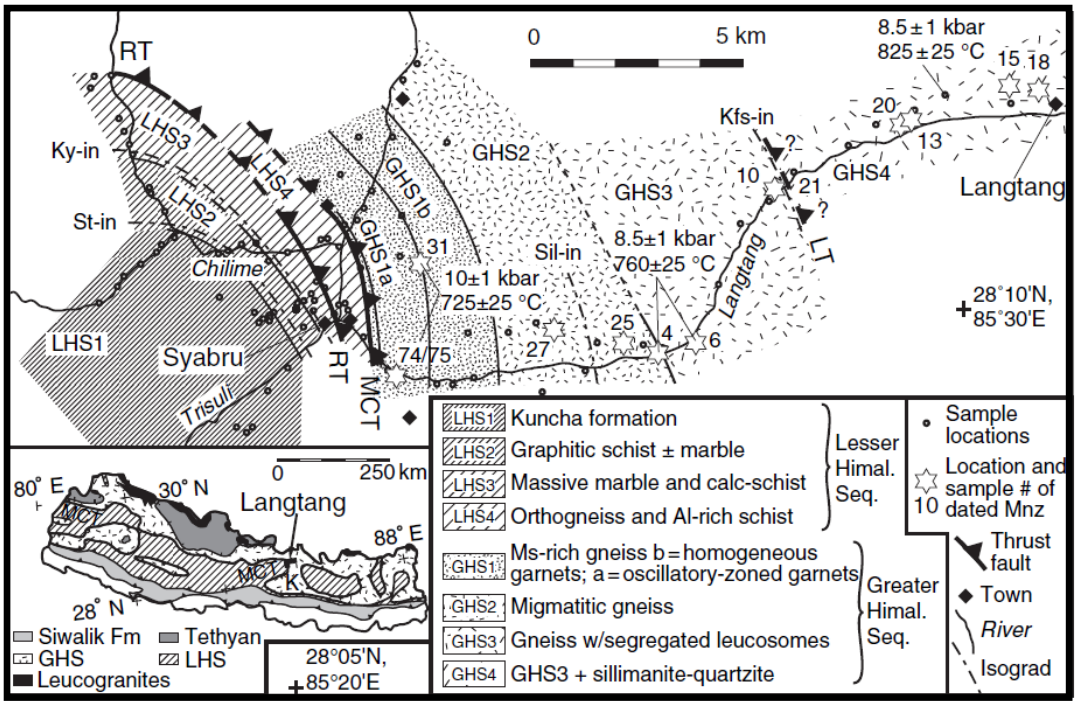

Fig. 3.3 Geological map of the Langtang Valley after Kohn *et al.,* (2005)

3.3 Regional Geology of the study area

The Bhote Koshi River area between Syaphrubesi and Dhunche is located in the Lesser Himalaya, Central Nepal, consists of low-grade metamorphic rocks (Fig. 3.4) e.g. intercalation of grey, fine- to medium-grained quartzite and greenish grey, pencil grey phyllite as well as schist and also the gritty phyllite. Generally, the ratio of quartzite is greater than phyllite. Structurally, the Main Central Thrust (MCT) is situated about 3 km north of the project area that passes through the north of Syaphrubesi Bazaar. The lithostratigraphy of the area is given in Table 3.1 and Fig. 3.4.

3.4 Lesser Himalaya

Generally, the Lesser Himalaya consists of low-grade metasedimentary rocks. The Lesser Himalaya is divided into the Midland and Kathmandu Groups based on the metamorphism of the rocks and tectonics of the area.

Table 3.1: Lithostratigraphy of Lesser Himalaya, Central Nepal (after DMG, 1987)

Group	Formation	Main Lithology	Thickness (m)	Age
Higher Himalaya				
Main Central Thrust (MCT)				
Midland	Ulleri	Gneiss	800	Pre-Cambrian to Cambrian
	Lakharpata	Limestone/Dolomite	500-1,000	
	Syanja	Phyllite /Dolomite	800	
	Galyang	Phyllite/Quartzite	1000	
	Naudanda Quartzite	Quartzite	400	
	Ranimatta *	Phyllite, Quartzite	3000+	
Main Boundary Thrust (MBT)				
Siwalik Group				

*Rock exposed in project area

3.4.1 Midland Group

This group comprises six litho-units (Fig. 3.4) which consist of phyllite, dolomite and metasedimentary rocks.

3.4.1.1 Ranimatta Formation (Rm) comprises alteration of greenish grey to dark grey, crenulated phyllite, phyllitic schist and grey to greenish grey, fine- to medium-grained quartzite. This formation attains more than 3 km thickness. The project area lies within this formation. The proportion of quartzite and phyllite varies place to place in the study area. This formation is equivalent to the Kuncha Formation, Lower Nawakot Group of Stocklin and Bhattarai, 1977.

3.4.1.2 Naudadada Quartzite (Nd) is represented by the presence of thick-bedded, white, coarse-grained quartzite with frequently developed ripple marks and cross lamina. Total thickness of the litho-unit is about 400m.

3.4.1.3 Galyang Formation (Gl) is characterized by the presence of dark grey to black phyllite and spotted white, fine-grained quartzite. Total thickness of the litho-unit is about 1,000 m.

3.4.1.4 Syanja Formation (Sy) is characterized by grey metasandstone intercalated with dark grey phyllite and dolomite. Total thickness of the litho-unit is about 800 m.

3.4.1.5 Lakharpata Formation (Lk) characterized by the presence of bluish-grey, fine-grained dolomite and dolomitic limestone. Total thickness of this litho-unit is about 500 to 1,000 m.

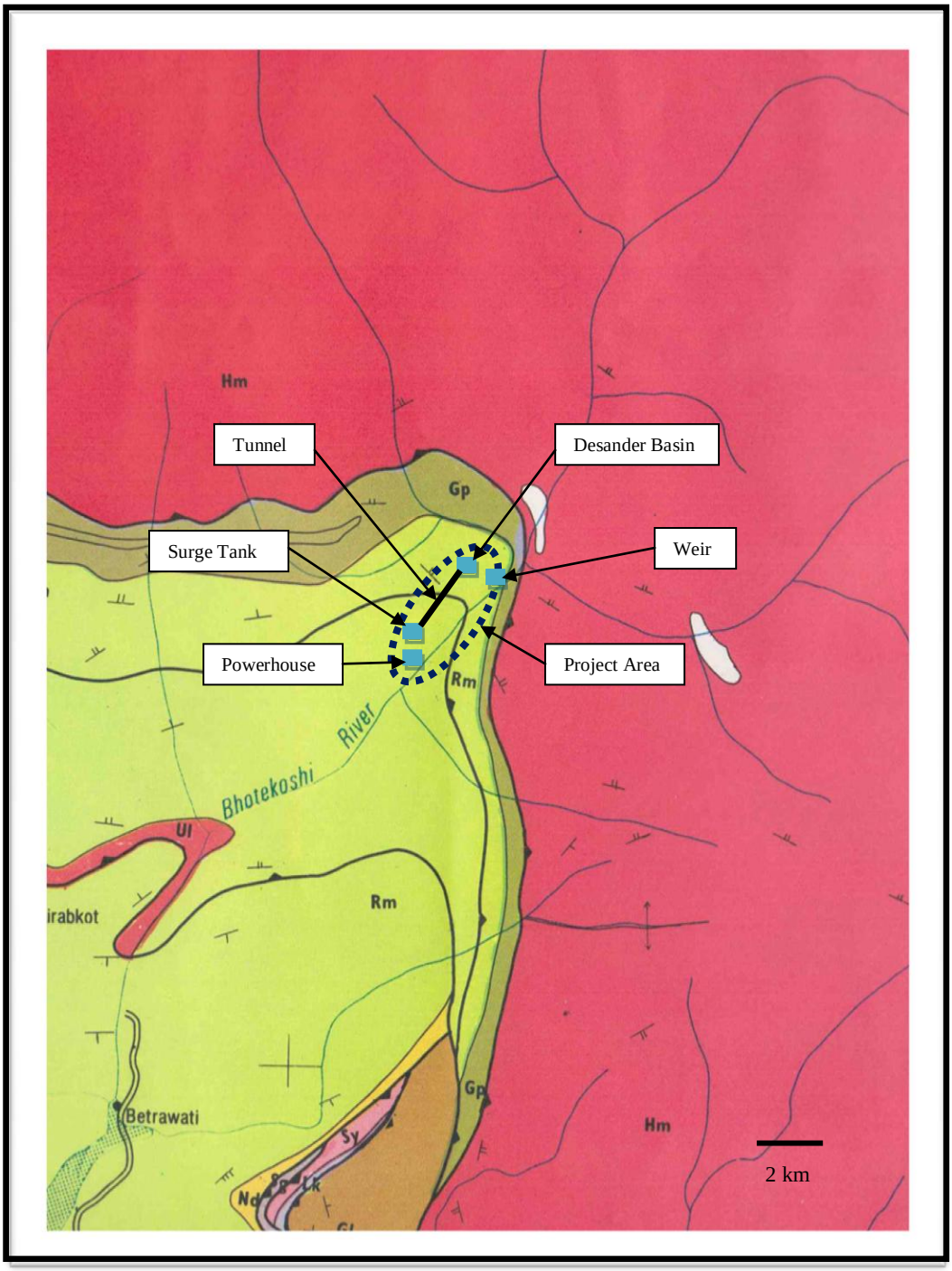

Fig. 3.4 Geological map of study area (DMG, 1987)

3.4.1.6 Ulleri Formation (Ul) is comprised of thick and monotonous augen gneiss. It has thickness of about 800 m.

3.5 Geological Structures

Fig. 3.4 shows the major geological structures in the project area. Among them, the Main Central Thrust (MCT) is the main geological structure. Other structures include Syo Khola Fault, Gre Khola Fault, Fold, Foliation and Joints.

3.5.1 Main Central Thrust (MCT)

The MCT striking NE-SW with an average dip of 40° to 45° follows nearly parallel to the Langtang Khola, north of Syaphrubesi Bazaar. It separates the high-grade metamorphic rocks of the Higher Himalaya to the north and low-grade metamorphic rocks of the Midland Group to the south. The thrust is located about 3 km north of the proposed weir axis area and about 7 km south from powerhouse area of the project.

3.5.2 Syo Khola Fault

Nearly east-west directed this fault has developed within the rocks of Ranimatta Formation and is dipping towards north direction. This fault passes through the Syo Khola. The right bank of the Syo Khola is very steep as compared to the left bank. The fault is not active.

3.5.3 Gre Khola Fault

Just downstream from the confluence of Bhote Koshi River and Syo Khola, east-west directed fault has developed within the rocks of Ranimatta Formation. The fault dips toward north direction and passes through the Gre Khola. The fault is passive.

3.5.4 Fold

Regional folds are not reported around the study area. But, minor and micro folds can be seen. These folds that developed in the intercalation of quartzite and phyllite do not directly affect the project structures along the tunnel alignment.

3.5.5 Foliation

The trend of the foliation plane of the study area is along northeast direction (020° to 040°) with dip amount (30° to 45°).

3.5.6 Joints

Three to four joint sets are common in study area. Most of the joint sets are developed in Quartzite. These joint sets form various wedges.

3.6 Detail Geology of the Project Area

The proposed area belongs to the Lesser Himalayan rocks of the Ranimatta Formation and is located about 3 km south of the Main Central Thrust. It lies between Syaphrubesi and Dhunche villages (Fig. 3.4). The lithounit is comprised of thick-bedded, grey quartzite intercalated with thin to thick bedded dark grey to pencil grey phyllite. In

general, 80% of the rocks are quartzite and remaining rocks are phyllite. The dip directions of rocks vary from 020° to 040° and dipping 30° to 45°. The proposed structures like powerhouse, desander basin, approach tunnel alignment and diversion tunnel alignment will be underground. The powerhouse and tailrace structures are located in thick beds of quartzite and phyllite while the intake and weir axis area is located partly in bedrock and partly in the recent and old alluvial deposits. Colluvial deposits are sparsely found in the project area. Remarkable area of the project is shown in the photographs (Annex II).

3.6.1 Reservoir Area

The proposed area is located in the rocks of the Ranimatta Formation. The area extends up to the bridge crossing the Bhote Koshi River along the Galchhi-Syaphrubesi Road at Syaphrubesi. Most of the area is covered with old alluvial and colluvial deposits. Along the proposed area, thick bedded, fine- to medium-grained quartzite intercalates with phyllite. Thickness of quartzite ranges from 0.5 to 3 m whereas phyliite is from 0.2 to 0.5 m. Coarse-grained, grey gritty phyllite with thickness of 1 to 3 m can also be seen in the proposed area.

3.6.2 Intake and Weir Axis Area

Among the three proposed options for the weir axis, the upper option (option I) is located about 0.6 km downstream from the Bhote Koshi Bridge along Galchhi-Syaphrubesi Road. Similarly, the middle option (option II) and lower option (option III) lies at about 0.8 and 1.7 km downstream from the bridge.

3.6.2.1 Option I (Upper Dam site area)

Geologically, the area is located in the rocks of the Ranimatta Formation, Lesser Himalaya. Along the right bank, the proposed area is characterized by thick bedded, fine- to medium-grained, grey quartzite intercalated with grey and gritty phyllite. Thickness of quartzite varies from 0.2 to 2 m while that of phyllite is from 0.1 to 0.5 m. The proportion of quartzite is greater than phyllite (85:15). Superficially, the right bank is covered with colluvial as well as old alluvial deposits. There is very little chance of finding bedrocks along the left bank. Right bank is quite steep compared to left one.

The intake area is located on the bedrock but initially falls on the colluvial deposits along the right bank of the Bhote Koshi River. Thick bedded quartzite intercalated with phyllite can be seen at the proposed area.

3.6.2.2 Option II (Middle Dam site area)

The proposed area is located at about 200 m downstream from the option I. The right bank consists of intercalation of quartzite and phyllite of the Ranimatta Formation whereas the left bank consists of old alluvial and colluvial deposits. Thick recent alluvial deposits are seen on the river bed. The ratio of quartzite is greater than that of phyllite (90:10). Characters of the rocks are same as the rocks found in the option I. Right bank has vertical topography with barren land and the left bank has gentle to steep slope covered with forested area.

The intake area falls on thick bedded quartzite. Thickness of quartzite ranges from 1 to 2 m. The topography is gentle at lower part but the upper part is almost vertical.

3.6.2.3 Option III (Lower Dam site area)

The proposed area is located at about 900 m downstream from the option II or about 200 m downstream from Syo Khola confluence. The right bank consists of intercalation of grey quartzite (0.5 to 2 m thick) and dark grey phyllite (0.1 to 0.4 m thick). Ratio of the quartzite is greater than that of phyllite. The left bank consists of old alluvial and colluvial deposits. Both the banks have steep (82°) topography with barren land in the right bank and forested land in the left bank.

The area of the intake belongs to the rocks of the Ranimatta Formation. The area is composed of thick quartzite beds.

In the present study, among three options proposed for dam, middle one reveals good site for large storage capacity. The upper proposed site might create backwash effect of water which may be problematic situation for both powerhouse area of Chilime Hydroelectic Project and Syaphrubesi Bazaar. Similarly, the lower proposed site creates head loss of about 20 m which lowers the total capacity of hydropower by 20 MW. Thus, middle proposed site is suitable for dam.

3.6.3 Approach Tunnel Alignment Area (Option II)

The proposed approach tunnel alignment area for the option II is located in the right bank of Bhote Koshi River. It connects the intake and underground desander basin. Based on surface geology, the area lies on thick and monotonous quartzite and phyllite of Ranimatta Formation. The proportion of quartzite is greater than that of phyllite.

3.6.4 Diversion Tunnel Alignment Area (Option II)

Since the left bank of the Bhotekshi River lies in the Buffer zone of Langtang National Park, the proposed diversion tunnel alignment area is located on the right bank of the river. The area is composed of thick quartzite and phyllite/schist. The proportion of quartzite is greater than phyllite. The length of diversion tunnel is about 500 m.

3.6.5 Desander Basin Area (Option II)

The proposed underground desander basin is located on the right bank of the Bhote Koshi River at about 300 m from the confluence of Syo Khola and Bhote Koshi River. Geologically, the area belongs to the Ranimatta Formation. The area is characterized by thick bedded quartzite intercalated with thin bedded phyllite. Individual thickness of quartzite and phyllite vary from 0.5 to 2 m and 0.1 to 0.5 m respectively. The proportion of quartzite is greater than phyllite (80:20).

3.6.6 Portal Inlet Area (Option II)

The proposed portal inlet area is located on the right bank of the Bhote Koshi River. The area is characterized by thick bedded quartzite intercalated with thin bedded phyllite. The proportion of quartzite is greater than that of phyllite.

3.6.7 Headrace Tunnel Alignment Area

The proposed tunnel alignment follows the right bank of the Bhote Koshi River. It lies entirely in the rocks of the Ranimatta Formation. Quartzite covers 80% of the total tunnel alignment whereas phyllite covers only 20%. Thin layers (< 1 m) of colluvial deposits are placed along the hill slope of the rocks. Thickness of the quartzite varies from 0.5 to 2 m whereas the phyllite varies from 0.1 to 0.5 m.

Along the section between weir axis and Syo Khola, Syo Khola and Gre Khola and Gre Khola and Tasangi Khola, the proportion of quartzite is greater than that of phyllite. But, the section between Tasangi Khola and Khahare Khola shows the ratio of phyllite is greater than that of quartzite.

3.6.8 Surge Tank and Surge Shaft Area

The proposed surge tank and surge shaft area are located on the right bank of the Bhotkoshi River at about 100 m upstream from the confluence of Trishuli River and Bhote Koshi River. The area is characterized by fine- to medium-grained, grey quartzite and phyllite of the Ranimatta Formation. Superficially, thin layers of colluvial deposits

cover the proposed surge tank area. The proportion of quartzite is greater than that of phyllite (70:30). The topography of the area is quite steep.

3.6.9 Powerhouse and Tailrace Tunnel Alignment Area

The proposed powerhouse and tailrace tunnel alignment area lie on the right bank of the Bhote Koshi River, about 100 m upstream from the confluence of the Trishuli River and Bhote Koshi River. The area is characterized by fine- to medium-grained, grey quartzite intercalated with phyllite of the Ranimatta Formation. Thickness of quartzite varies from 0.2 to 2 m whereas phyliite ranges from 0.1 to 0.5 m. The ratio of quartzite is greater than that of phyllite (70:30). Thick old alluvial deposits are present in the right bank of the river. The boulders are mostly comprised of gneiss and quartzite.

3.6.10 Adit-1 Area

The proposed adit area is located on the right bank of the Gre Khola. The area lies in beds of quartzite and phyllite of the Ranimatta Formation. But, thin layers of colluvial and alluvial deposits are present along the hill slope. The bedrocks are thin to thick bedded. Road connecting to adit area first passes through old alluvial and colluvial deposits which finally interact with the rocks of the Ranimatta Formation.

3.6.11 Adit-2 and 3 Areas

The proposed adit areas are located on the right bank of Bhote Koshi River at about 500 m upstream from the confluence of Trishuli Khola and Bhote Koshi River. The proposed area is characterized by thin to thick bedded quartzite and phyllite of the Ranimatta Formation. But, thin layers of colluvial deposits cover the rocks along the hill slope. Road connecting to the adit areas initially run over the old alluvial and colluvial deposits and then finally over the rocks.

3.6.12 Geomorphology

The Bhote Koshi River is one of the major tributary of the Trishuli River. It originates from the watershed of the southern flank of the Kerung Himal, Tibet. The catchment area of the river has very rugged topography. It is characterized by sharp crested ridges and medium to very steep slopes. Very little spaces are available for gently sloping lowlands in the valley. Majority of catchment lies along the slopes. Lowlands constitute nearly 5% of the total catchment while ridge constitute less than 1%. Within the catchment area, there are a large number of passive as well as active landslides. Deposits are mainly

composed of angular to sub-rounded boulders, cobbles and gravels which were brought down by the rivers and deposited as alluvial mixed with colluvial deposits. They are composed of gneiss, quartzite, granite etc. The slopes of river valley vary from 70° to 80°.

CHAPTER 4

ENGINEERING GEOLOGY OF THE STUDY AREA

Rock mass classifications form the backbone of the empirical design approach and are widely employed in rock engineering. In fact, on many projects, the classification approach serves as the practical basis for the design of complex underground structures (Bieniawski, 1989). Rock mass classifications are widely used in engineering at the preliminary design stages and, if applied properly, represent a powerful tool of estimating rock mass quality and stability, selecting underground support system and predicting some behavioral characteristics of rocks.

4.1 Review of Rock Mass Classifications

Rock mass classifications schemes have been developed for over 100 years since Ritter (1879) attempted to formalize an empirical approach to tunnel design, in particular for determining support requirements. But, the earliest reference to the use of rock mass classification system for engineering purpose is the rock load theory published by Terzaghi (1946). Only the support element in this system was steel arches. Deere (1964) proposed a quantitative index of rock mass quality based upon core recovery by diamond drilling. This Rock Quality Designation (RQD) has come to be very widely used and has been shown to be particularly useful in classifying rock masses for the selection of tunnel support. This is the first numerical form of a system which is an index of assessing rock quality quantitatively by estimating the core recovery percentage. Since then, the multi-parameter classification schemes by Wickham *et al*., (1972), Bieniawski (1973, 1989) and Barton *et al.,* (1974) were developed from civil engineering case histories in which all of the components of the engineering geological characters of the rock mass were included. Depending upon the purpose, various classifications and rating systems have been practiced (Table 4.1).

Table 4.1: Various rock mass classification systems

Name of Classification	Author and first version	Country of origin	Applications
Rock Load Theory	Terzaghi (1946)	USA	Tunnel with steel support
Stand up time	Lauffer (1958)	Austria	Tunneling
RQD	Deere *et al.* (1964)	USA	Core logging tunneling
RSR concept	Wickham *et al.* (1972)	USA	Tunnel with steel support
RMR-system (CSIR)	Bieniawski (1974)	South Africa	Tunnel, mines, foundations etc.
Q-system	Barton *et al.*(1974)	Norway	Tunnel, large chambers
Mining RMR	Laubscher (1975)		Mining
Slope mass rating	Romana (1985)	Spain	Slopes
Geological Strength Index (GSI)	Hoek *et al.* (1995)		Mines and tunnel
Rock Mass Index (RMI)	Palmström (1995)	Norway	Rock engineering, communication, characterization

4.2 Rock Mass Classification along the tunnel alignment of underground structures

The rock mass classification systems adopted for the present study are Rock Mass Rating (RMR), after Bieniawski (1989) and Q-system after Barton *et al.* (1974). Based on computed 'Q' and 'RMR' values (Table 4.2), the rock mass can be classified into very good to excellent, good, fair, poor, very poor, extremely poor and exceptionally poor rock zones. The calculated values can be used for rock support in the headrace tunnel alignment and underground structures.

The rock mass classification has been carried out along underground structures like desander basin area, alignment of the headrace tunnel, surge tank area and powerhouse area based on the detailed joint mapping of the surface outcrop. The joint analysis on the different tunnel sections have been carried out on the basis of detailed measurement of all relevant geo-mechanical elements and discontinuities such as joints and foliation plane.

Geological Strength Index (GSI) of the rock mass of the project area is calculated on the basis of RMR. GSI value is used to measure the rock mass strength parameters.

Table 4.2: Rock Mass Classification

$RMR \approx 9 \times \ln Q + 44$ **(Bieniawski, 1989);** $RMR = 15 \times \log Q + 50$ **(Barton, 1995)**					
Descriptions		**Range of Q-values**		**Range of RMR-values**	
Rock Class	**Quality descriptions**	**Minimum**	**Maximum**	**Minimum**	**Maximum**
Class I	Very good to excellent	100	1000	85	100
Class II	Good	10	100	65	85
Class III	Fair	4	10	56	65
Class IV	Poor	1	4	44	56
Class V	Very poor	0.1	1	35	44
Class VI	Extremely poor	0.01	0.1	20	35
Class VII	Exceptionally poor	0.001	0.01	5	20

4.2.1 Rock Strength

Strength is fundamental quantitative engineering property of rock which is the amount of the applied stress at failure or rupture. The stability of an underground excavation depends upon the relationship between the stress and strength of the rock. The stress applied may be compressive, shear or tensile in the application which give rise to compressive, shear or tensile strength. The strength of the rocks of the study area has been estimated by two methods. They are field identification method (Table 4.3) and point load test in the lab.

Rock samples were collected from the different location on the study area (Fig. 4.4). Total seven samples were collected for the point load test. The point load index calculated on laboratory is used to calculate the Uniaxial Compressive Strength (UCS) of the intact rock. The result thus obtained is used for determining geological and geotechnical parameters of the rock mass. The summary of the laboratory test of the rock samples are presented in Table 4.4.

Table 4.3: Field estimates of Uniaxial Compressive Strength of the Rock (Marinos and Hoek, 2001)

Term	**Uniaxial Compressive Strength (MPa)**	**Point Load Index (MPa)**	**Field estimate of strength**	**Examples**
Extremely Strong	> 250	> 10	Specimen can only be chipped with a geological hammer	Fresh basalt, chert, diabase, gneiss, granite, quartzite
Very Strong	100 – 250	4 – 10	Specimen requires many blows of geological hammer to fracture it	Amphibolite, sandstone, basalt, gabbro, gneiss, granodiorite, peridotite, rhyolite, tuff
Strong	50 – 100	2 – 4	Specimen requires more than on blow to fracture it	Limestone, marble, sandstone, schist
Medium strong	25 – 50	1 – 2	Cannot be scrapped or peeled with a pocket knife. Specimen can be fractured with a single blow from a geological hammer	Concete, phyllite, schist, siltstone
Weak	5 – 25	**	Can be peeled with a pocket knife with difficulty, shallow indentation made by firm blow with point of a geological hammer	Chalk, claystone, potash, marl, siltstone, shale, rocksalt
Very weak	1 – 5	**	Crumbles under firm blows with point of geological hammer, can be peeled by a pocket knife	Highly weatherd or altered rock, shale
Extremely weak	0.25 – 1	**	Indented by thumb nail	Stiff fault gouge

** Point load tests on rocks with a Uniaxial Compressive Strength below 25 MPa

Table 4.4: Summary of the point load test of the rock samples on laboratory

Structure	Chainage	Rock type	Location	Point Load Index (MPa)	Uniaxial Compressive Strength (MPa)
Intake		Quatzite >> Phyllite	S1	5.92	137.344
Headrace Tunnel	Ch. 0+411.46 m – 0+734.701 m	Quatzite >> Phyllite	S2	5.62	130.384
	Ch. 0+734.701 m – 2+179.50 m	Quatzite >> Phyllite	S3	4.98	115.536
	Ch. 2+179.50 m – 2+614.65 m	Quatzite >> Phyllite	S4	5.238	121.522
	Ch. 2+614.65 m – 3+212.93 m	Quatzite << Phyllite	S5	4.02	93.264
	Ch. 3+212.93 m – 3+580.87 m	Quatzite >> Phyllite	S6	4.982	115.582
Powerhouse		Quatzite >> Phyllite	S7	4.853	112.59

4.2.2 Rock Mass Rating (RMR)

Bieniawski (1976) published the details of a rock mass classification called the Geomechanics Classification or the Rock Mass Rating (RMR) system. The six parameters used to classify a rock mass using RMR system are:

- Uniaxial Compressive Strength of a rock material
- Rock Quality Designation (RQD)
- Spacing of discontinuities
- Condition of discontinuities
- Groundwater conditions
- Orientation of discontinuities

The strength of the rock samples are obtained from the laboratory test. All of the remaining parameters of the rock mass classification are taken in the field. These parameters are classified into various sub-categories that have been assigned different relative rating values. The RMR distribution along the tunnel alignment of the underground structures is shown in Fig. 4.1 and 4.3. The summary of the RMR system is presented in Table 4.5. The value of GSI is calculated from the following relation.

GSI = RMR_{89} – 5…….. (4.1) where, RMR_{89} = Rock Mass Classification

Table 4.5: Adjusted Rock Mass Rating (RMR) of the study area

Location	Rating for						RMR value	GSI	Rock class	Definition
	Strength of intact rock material	Rock Quality Designation (RQD)	Spacing of discontinuities	Condition of discontinuities	Groundwater condition	Orientation of discontinuities				
Reservoir area										
Both banks	15	12	15	17	17	-15	64	59	III	Fair
Intake and Weir Axis Area										
Right bank	17	15	15	17	12	-15	59	54	III	Fair
Approach / Diversion Tunnel Alignment Area										
Right bank	15	15	15	15	17	-15	62	57	III	Fair
Portal Inlet and Desander Basin Area										
Right bank	15	15	17	15	17	-15	64	59	III	Fair
Headrace Tunnel Alignment Area										
Portal Inlet to Syo Khola (Ch. 0+411.46m – 0+734.701m)	17	15	15	15	15	-15	62	57	III	Fair
Syo Khola to Gre Khola (Ch. 0+734.701m – 2+179.50m)	17	15	15	15	12	-15	59	54	III	Fair
Gre Khola to Tasangi Khola (Ch. 2+179.50m – 2+614.65m)	15	17	15	15	15	-15	62	57	III	Fair
Tasangi Khola to Khahare Khola (Ch. 2+614.65m – 3+212.93m)	12	12	15	15	12	-20	46	41	IV	Poor
Khahare Khola to Surge Tank (Ch. 3+212.93m – 3+580.87m)	15	17	12	15	17	-15	61	56	III	Fair
Surge Tank / Powerhouse /Tailrace Tunnel Area										
Right bank	15	12	15	15	15	-15	57	52	III	Fair

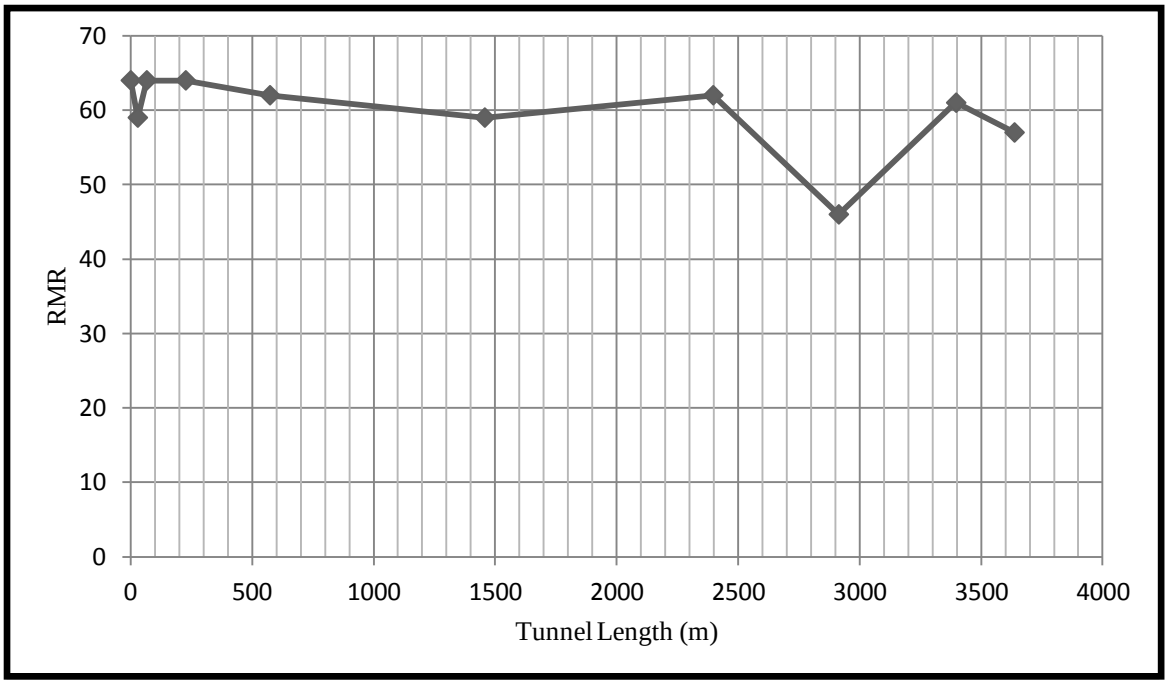

Fig. 4.1 Distribution of RMR along the tunnel alignment of underground structures

4.2.3 Rock Tunneling Quality Index (Q)

The Q value is obtained by the relation proposed by Barton *et al.*, (1974) of the Norwegian Geotechnical Institute for the determination of the rock mass characteristics and tunnel support requirement.

$$Q = (RQD/J_n) \times (J_r/J_a) \times (J_w/SRF)$$

Where,

RQD = Rock Quality Designation

J_n = Joint set number

J_r = Joint roughness number

J_a = Joint alteration number

J_w = Joint water reduction factor

SRF = Stress reduction factor

All of the parameters required for this classification are recorded in the field by using the table of rock tunneling quality index in which different rating values are assigned for each parameter. The value obtained from the Q system is presented in Table 4.6. Distribution of the Q along the tunnel alignment of the underground structures is shown in Fig. 4.2 and Fig. 4.3.

Table 4.6: Rock Tunneling Quality Index (Q) for the underground structures

Location	RQD	Joint Set Number (J_n)	Joint Set Roughness (J_r)	Joint Alteration Number (J_a)	Joint Water Reduction (J_w)	Stress Reduction Factor (SRF)	Q value	Rock Class	Rock Mass
Desander basin / Approach / Diversion Tunnel Alignment Area									
Right bank	62.2	16	1.5	3	1	0.4	4.86	III	Fair
Headrace Tunnel Alignment Area									
Portal Inlet to Syo Khola (Ch. 0+411.46m – 0+734.701m)	62.2	16	1.5	3	1	0.4	4.86	III	Fair
Syo Khola to Gre Khola (Ch. 0+734.701m – 2+179.50m)	55.6	18	3	3	2	0.8	3.86	III	Fair
Gre Khola to Tasangi Khola (Ch. 2+179.50m – 2+614.65m)	42.4	22	4	2	2	2	3.85	III	Fair
Tasangi Khola to Khahare Khola (Ch. 2+614.65m – 3+212.93m)	29.2	26	3	2	2	2	1.68	IV	Poor
Khahare Khola to Surge Tank (Ch. 3+212.93m – 3+580.87m)	58.9	17	5	2	2	2	8.66	III	Fair
Surge Tank / Powerhouse /Tailrace Tunnel Alignment Area									
Right bank	58.9	17	5	2	2	2	8.66	III	Fair

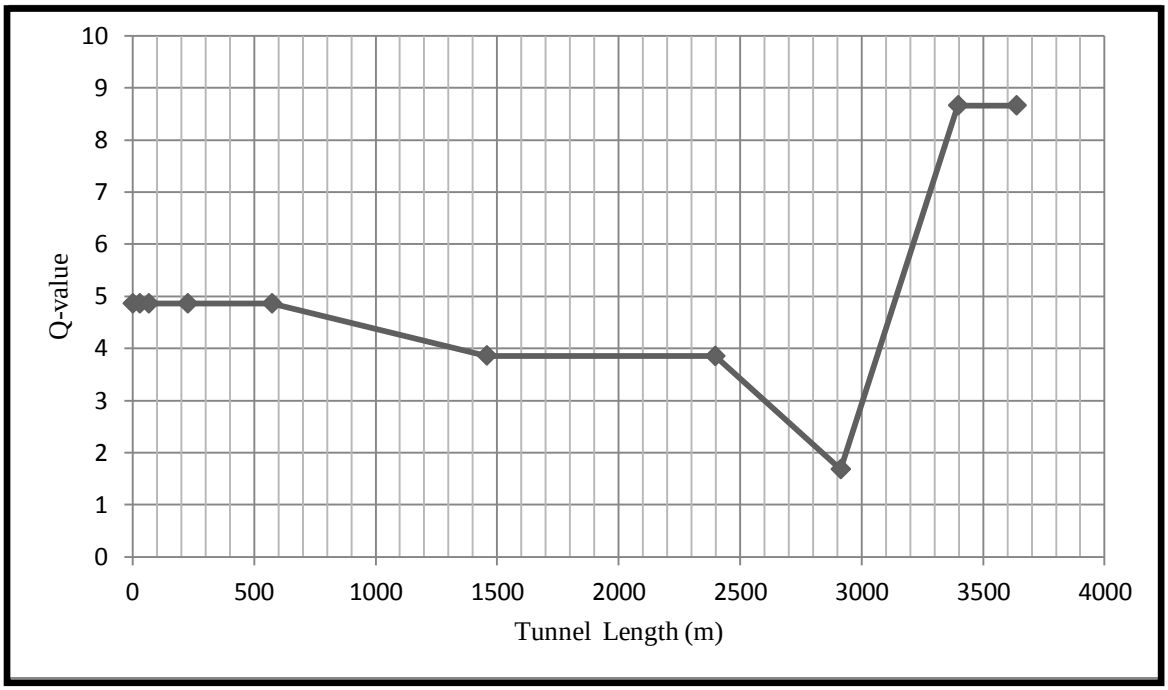

Fig. 4.2 Distribution of Q along the tunnel alignment of underground structures

4.2.4 Distribution of RMR and Q along the alignment of underground structure

The calculated RMR and Q value at the headworks area ranges from 59 to 64 and 4.85 to 4.86 respectively. Similarly, the calculated RMR and Q value along the headrace tunnel alignment area ranges from 46 to 62 and 1.68 to 8.66 respectively. But, the calculated RMR and Q value at the surge tank, powerhouse and tailrace tunnel alignment area are 57 and 8.66 respectively.

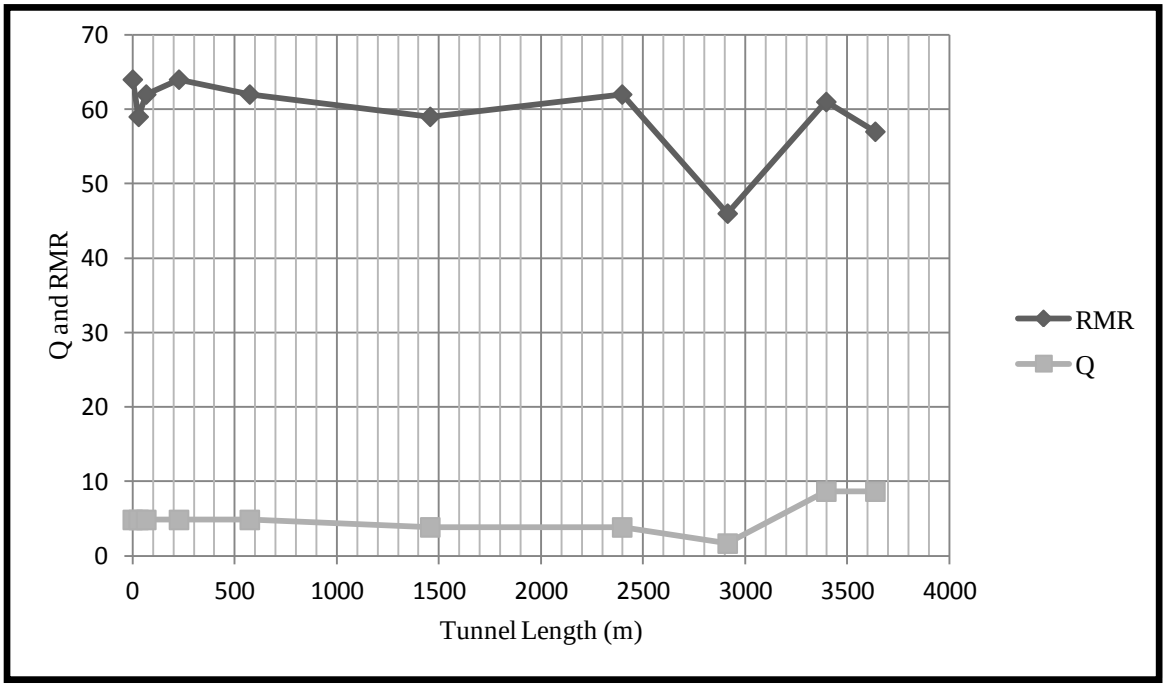

Fig. 4.3 Distribution of RMR and Q along the tunnel alignment of underground structures

4.3 Engineering Geology of the study area

Geological and engineering geological parameters were collected around the study area required for the study of underground structures. Rock mass classification and statistical analysis of joint sets were carried out to evaluate the engineering geological condition of the rock masses. Considering all parameters, the engineering geological map has been prepared in the scale of 1:10,000 (Fig. 4.4). Surface mapping reveals that the majority of the underground structures lie on the rock. Only few portions of the area are covered by colluviums deposits. Alluvial deposits at and around the river, consists of boulder and gravel mixed in sandy-silt matrix.

4.3.1 Engineering Geological Conditions of the Reservoir Area

Constructing a dam increases hydraulic head as well as provide sufficient storage for retaining high flows and flood water that can be released later at controlled rates to meet

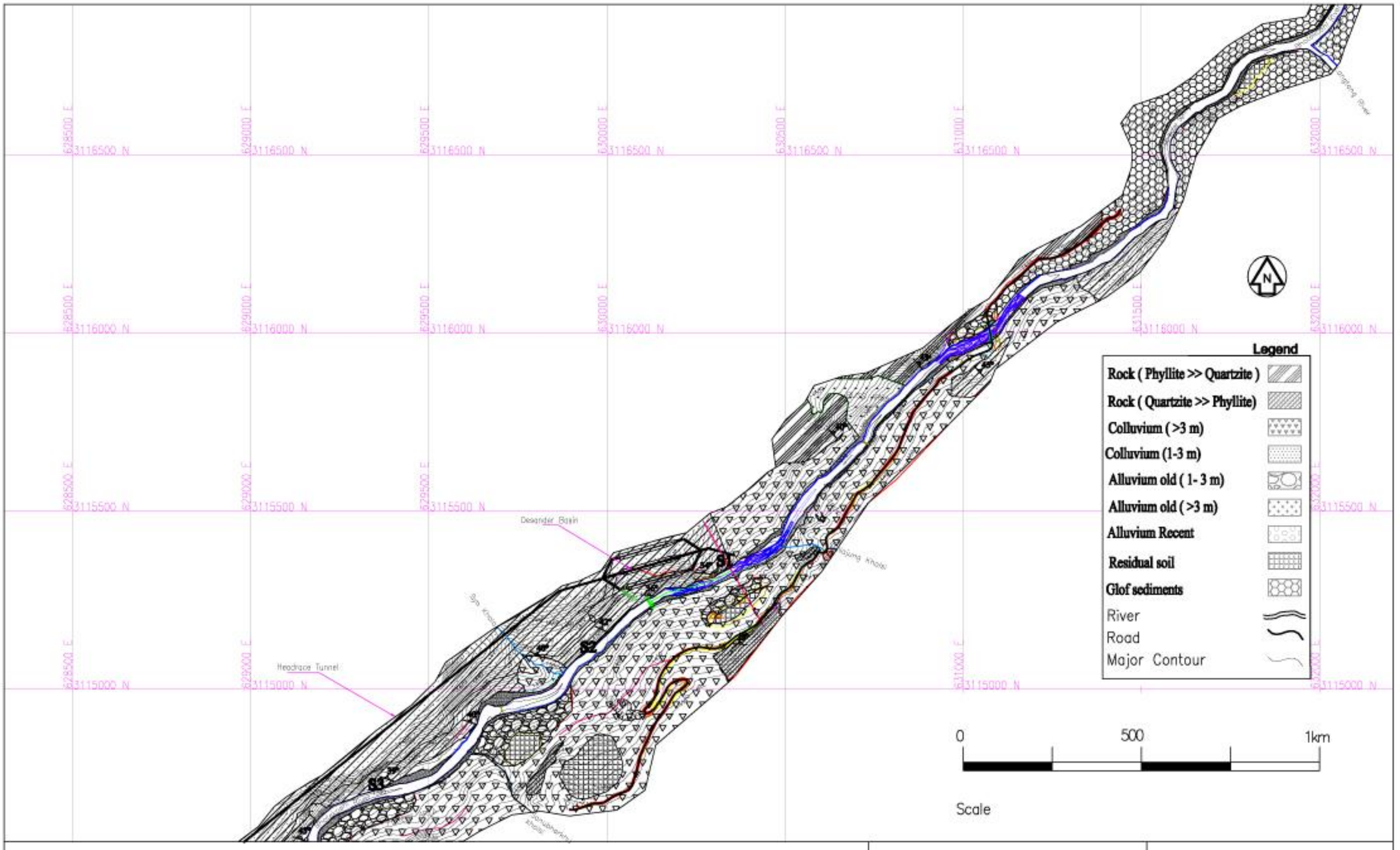

Fig. 4.4 Engineering Geological Map of the Upper Trishuli -2 Hydroelectric Project, Rasuwa

Prepared by
Kedar Shrestha

Sheet no. 1 of 2

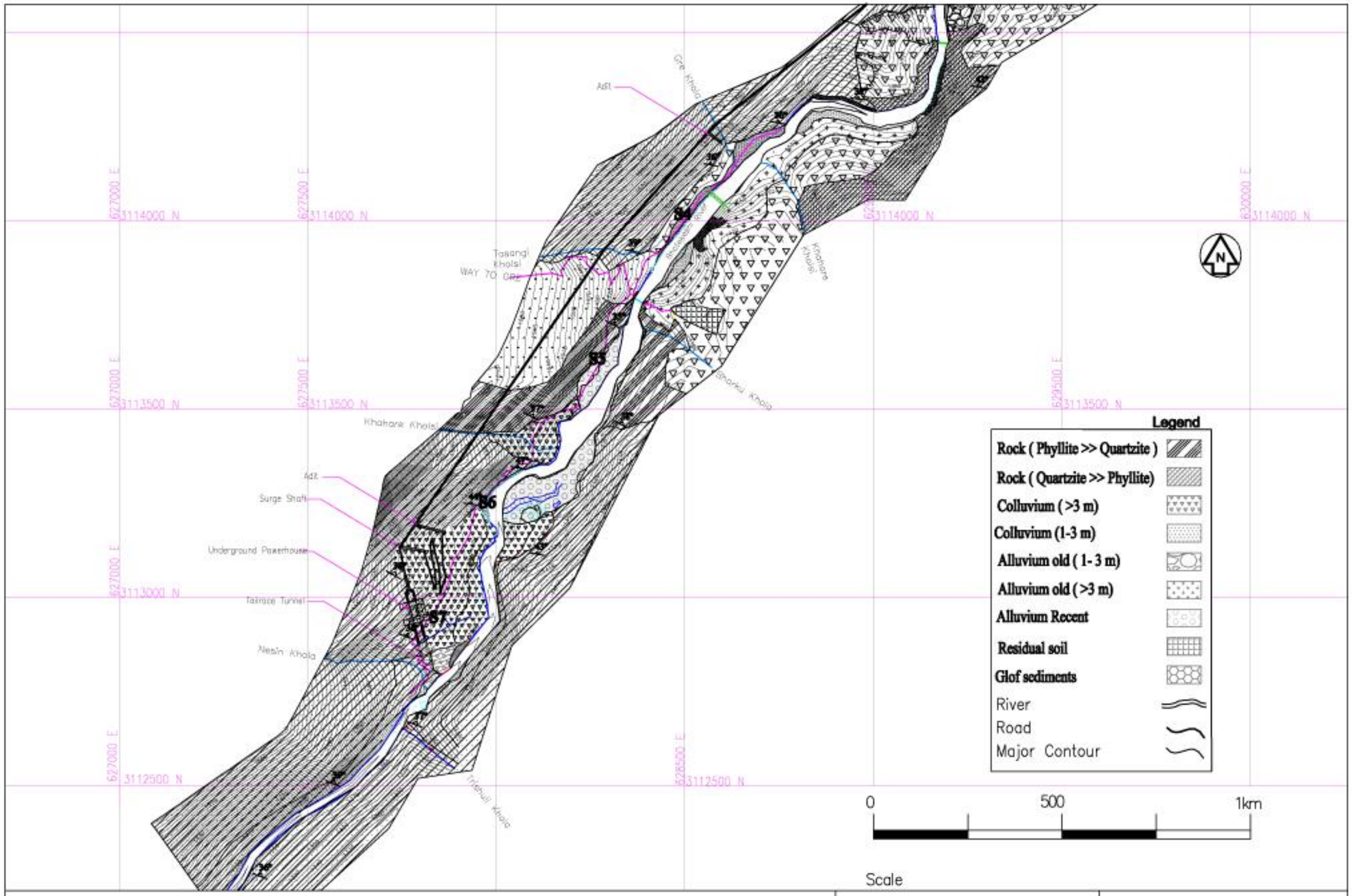

Fig. 4.4 Engineering Geological Map of the Upper Trishuli -2 Hydroelectric Project, Rasuwa

Prepared by
Kedar Shrestha

Sheet no. 2 of 2

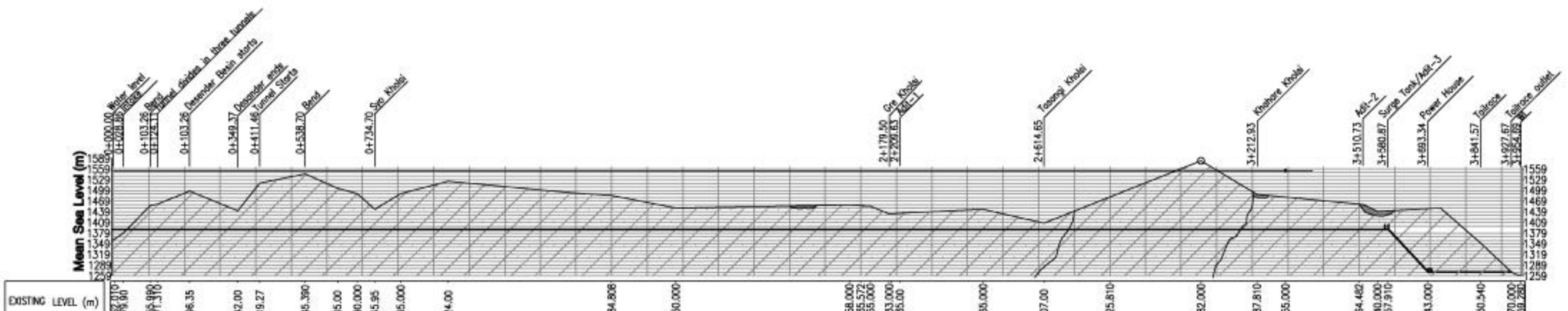

Rock Type	Quartzite>>phyllite	Quartzite>>phyllite	Quartzite>>phyllite	Quartzite>>phyllite	Quartzite<<phyllite	Quartzite>>phyllite	Quartzite>>phyllite
Weathering Pattern	Fresh–slightly	Fresh–slightly	Fresh–slightly	Fresh–slightly	Fresh–slightly	Fresh–slightly	Fresh–slightly
RMR Values	62	62	59	62	46	51	57
Rock Mass Classificationn	II	II	II	II	IV	II	II
Definition	Fair Rock	Fair Rock	Fair Rock	Fair Rock	Poor Rock	Fair Rock	Fair Rock
Q Value	4.86	4.86	3.86	3.85	1.68	8.66	8.66
Rock Mass Classificationn	II	II	II	II	IV	II	II
Definition	Fair Rock	Fair Rock	Fair Rock	Fair Rock	Poor Rock	Fair Rock	Fair Rock
Dip direction/Dip amount	036/42	036/42	019/39	021/36	038/35	009/50	029/38
Strike and Dip amount	126–306/42N	126–306/42N	109–289/39N	111–291/36N	128–306/35N	099–279/50N	119–299/38N
Support System	II	II	II	II	IV	II	II

Fig. 4.5 L-section of Upper Trishuli - 2 HEP, Rasuwa

Prepared by:
Kedar Shrestha

Scale Horizontal 1:1000 Vertical 1:1000

Legend

Rock (Quartzite >> Phyllite)

Rock (Quartzite << Phyllite)

Colluvium

peaking up power demand. The reservoir will provide regulation of the variable flow in the river.

In the present study, among three options proposed for dam, middle one reveals good site for large storage capacity. The area below elevation of 1362 m will be submerged by the construction of the dam. The total length of the reservoir is about 800m that reaches up to the bridge crossing Bhote Koshi River along the Galchhi-Syaphrubesi Road at Syaphrubesi. There is not any residential, historical and archeological important area found in the proposed submerged area. The area has no major tributary that can influx the large quantity of sediments on the reservoir. The present study does not reveal any indication of weakness zone, the potential shear zone and active faults as well as major instabilities along the river at the proposed reservoir area.

The right bank of the river is quite steep compared to the left one. The right bank consists of thick bedded, fine- to medium-grained quartzite bed intercalated with phyllite. Thickness of quartzite ranges from 0.5 to 3 m while that of phyllite ranges from 0.2 to 0.5 m. Coarse-grained, grey gritty phyllite with thickness of 1 to 3 m is also found in the study area. The rocks are covered by thin layers of colluvial deposits. The spacing of discontinuities is very large (Annex-III). Most of the area in left bank of the river is covered with old alluvial and colluvial deposits. These deposits are composed of gneiss, quartzite, phyllite and schist. The study shows the area consists of boulder (50%), cobble and pebble (30%) and sand (20%). On the slope the alluvial deposits are loose in nature and have no any calcareous cementing materials but represent the boulder mixed soil in engineering literature. To be clear about the subsurface geological condition, four ERT lines have been conducted.

4.3.1.1 Rock Classification

Geomechanical classification for jointed rock mass of the reservoir area using CSIR classification was carried out on the detailed surface discontinuity. Most of the Rock Mass Rating (RMR) of the headwork area falls in the range more than 64. It indicates the rock mass of the area is Class III type i.e. Fair Rock (Table 4.5).

4.3.1.2 Weathering and Strength

The rocks in the area are fresh to slightly weathered (Annex-III). The quartzite is strong and competent compared to phyllite. The Uniaxial Compressive Strength of the rock is greater than 137.344 MPa.

4.3.1.3 Slope Stability Condition

Slope stability assessment analysis of the hill slope was carried out on the basis of aerial photo interpretation and geological observations. About 149 measurements of discontinuities including foliation planes are measured. An analysis of these discontinuities using Lower Hemisphere Projection in Schmidt's equal area net is shown in Fig. 4.6.

The hill slope ranges from 70° to 75°. The attitude of foliation and joints in terms of dip direction and dip amount are: Foliation = 059°/43°, J_1 = 242°/68°, J_2 = 168°/58°. The dipping of foliation plane is favorable to the natural hill slope. The wedge formed by the intersection of the joints and foliation plane is stable. The wedge formed by the intersection of the joints J_1 and J_2, J_2 and J_3 and J_3 and J_1 are lateral wedges but the possibility of the failure is less. In general, the slope stability is good.

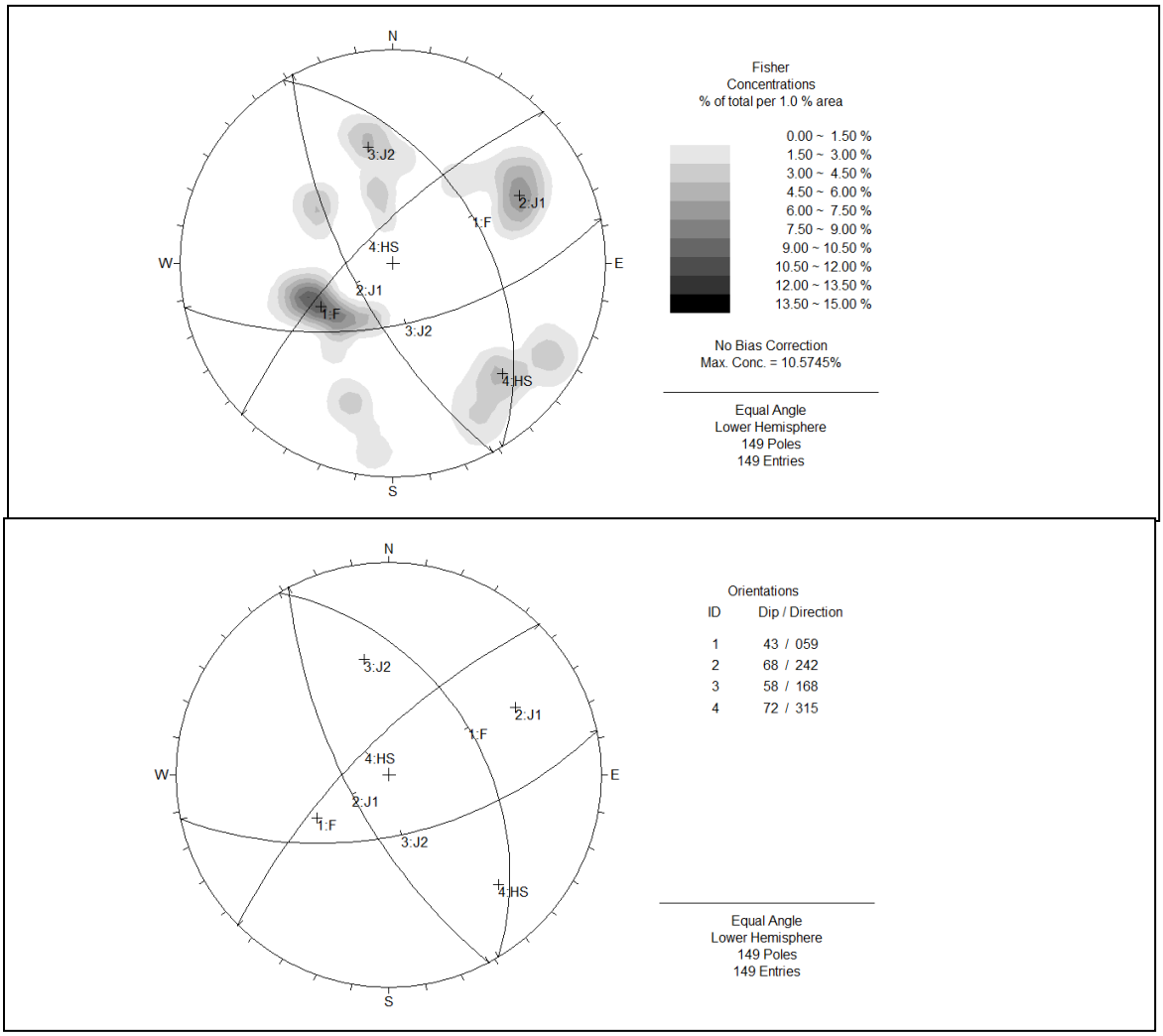

Fig. 4.6 Stereographic Projection of the rock mass exposed around the Reservoir Area

4.3.2 Engineering Geological Conditions of the Intake and Weir Axis Area

The weir is located at a straight course of the Bhote Koshi River. It is about 123.1 m long. The slope at both abutments varies considerably. The right bank is characterized by steep slope compared to left bank. Along the left bank, no rock outcrop exists. The area comprises old alluvial and colluvial deposits. But, the bed rock can be obtained at a depth of about 15 m. The study shows the area consists of boulder (50%), cobble and pebble (30%) and sand (20%). The boulders and gravels (80% gneiss and 20% schist) are generally sub-angular to sub-rounded in shape. Along the right bank, the outcrop consists of thick bedded, fine- to medium-grained quartzite intercalated with phyllite. Individual thickness of quartzite bed varies from 0.2 to 2 m. The spacing of the discontinuities is very large (Annex-III).

The proposed intake area is located on the right bank of the Bhote Koshi River. It consists of bedrocks of quartzite and phyllite. The topography is gentle at lower part but the upper part is almost vertical. To be clear about the subsurface geological condition, two ERT lines have been conducted.

4.3.2.1 Rock Classification

Geomechanical classification for jointed rock mass of the intake and weir axis area using CSIR classification was carried out on the detailed surface discontinuity. Most of the Rock Mass Rating (RMR) of the proposed area falls around 59. It indicates the rock mass of the area is Class III type i.e. Fair Rock (Table 4.5).

4.3.2.2 Weathering and Strength

The rocks along the river bank are fresh while at higher hill slope, they are slightly weathered (Annex-III). The quartzite is hard and competent in nature. The Uniaxial Compressive Strength of rock is 137.344 MPa.

4.3.2.3 Slope Stability Condition

Slope stability assessment analysis of the hill slope was carried out on the basis of aerial photo interpretation and geological observations. About 27 measurements of discontinuities including foliation planes are measured. An analysis of these discontinuities using Lower Hemisphere Projection in Schmidt's equal area net is shown in Fig. 4.7.

The hill slope ranges from 70° to 79°. The attitude of foliation and joints in terms of dip direction and dip amount are: Foliation = 016°/34°, J_1 = 224°/54°, J_2 = 131°/30° and J_3 = 069°/74°. The dipping of foliation plane is favorable to the natural hill slope. The wedge formed by the intersection of the joints and foliation plane is stable. The wedge formed by the intersection of the joints J_1 and J_2, J_2 and J_3 and J_3 and J_1 are lateral wedges but the possibility of the failure is less. In general, the slope stability is good.

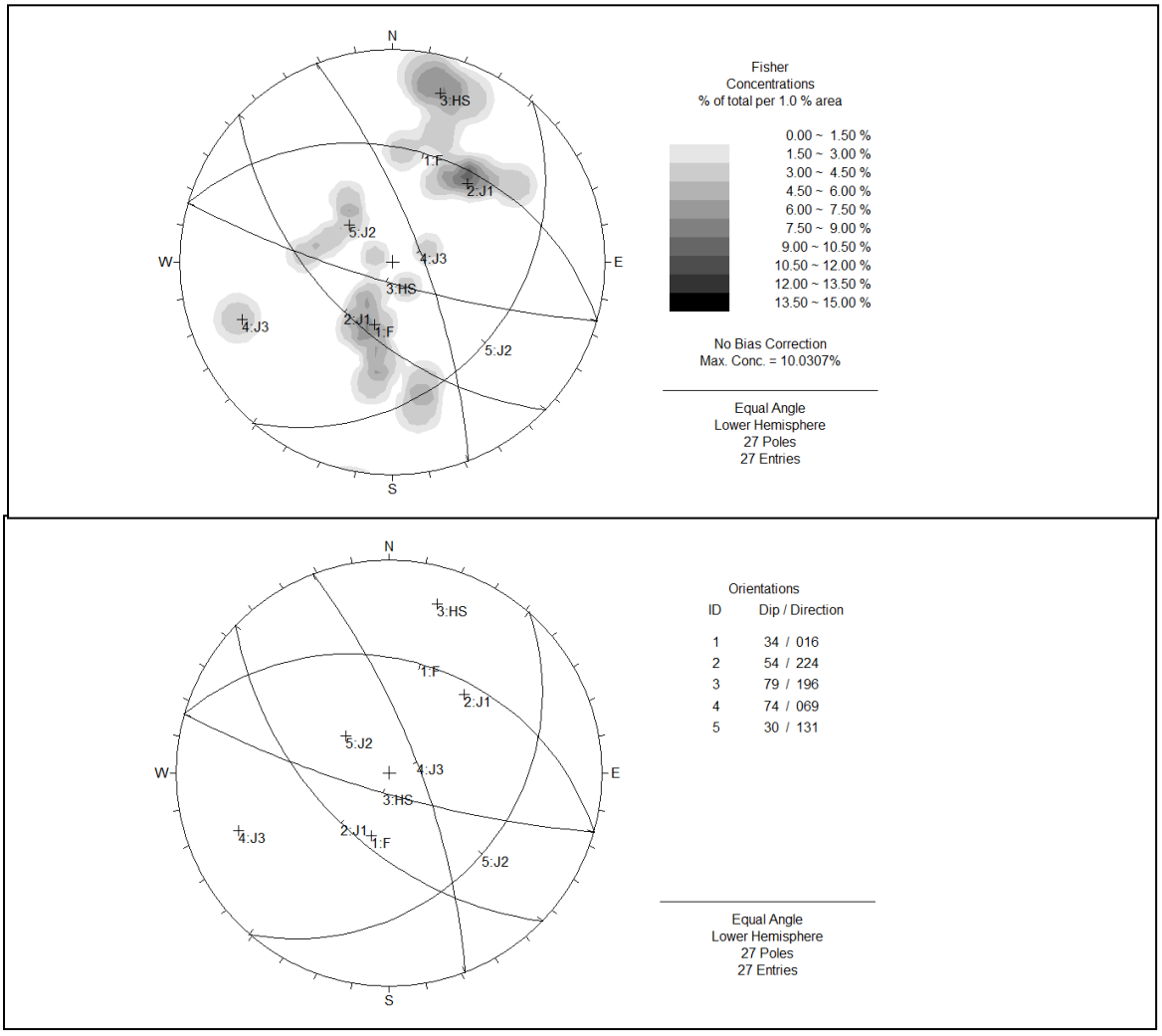

Fig. 4.7 Stereographic Projection of the rock mass exposed around the Intake and Weir Axis Area

4.3.3 Engineering Geological Conditions of the Approach Tunnel Alignment and Diversion Tunnel Alignment Area

Both the proposed approach tunnel alignment and diversion tunnel alignment lie in the right bank of the Bhote Koshi River. The approach tunnel passes through the bedrocks of quartzite and phyllite. The study shows the landslide representing colluvium is not active.

The diversion tunnel passes through the beds of quartzite and phyllite. It is about 500 m long. The topography is vertical in lower part but gentle slope in upper part.

4.3.3.1 Rock Classification

Rock mass classification for jointed rock mass of the approach tunnel and diversion tunnel alignment area using CSIR classification and Q-system was carried out on the detailed surface discontinuity. Most of the Rock Mass Rating (RMR) of the proposed area falls around 62. It indicates the rock mass of the area is Class III type i.e. Fair Rock (Table 4.5). The NGI Tunneling Index Q of the proposed area falls around 4.86. It indicates the rock mass of the area is Class III type i.e. Fair Rock (Table 4.6).

4.3.3.2 Weathering and Strength

The rocks along the river bank are fresh while at higher hill slope, they are slightly weathered (Annex-III). The quartzite is hard and competent in nature. The Uniaxial Compressive Strength of rock is 137.344 MPa.

4.3.3.3 Slope Stability Condition

Slope stability assessment analysis of the hill slope was carried out on the basis of geotechnical and geological observations. About 27 measurements of discontinuities including foliation planes are measured. An analysis of these discontinuities using Lower Hemisphere Projection in Schmidt's equal area net is shown in Fig. 4.7.

The attitude of foliation and joints in terms of dip direction and dip amount are: Foliation = 016°/34°, J_1 = 224°/54°, J_2 = 131°/30° and J_3 = 069°/74°. In general, the dipping of foliation plane is favorable for the proposed underground structures. But, some wedges formed by the intersection of the discontinuities F and J_1 and F and J_2 are unstable.

4.3.4 Engineering Geological Conditions of the Desander Basin and Portal Inlet Area

The 130 m long underground desander basin and portal inlet lie on the right bank of Bhote Koshi River. The area is composed of thick bedded, fine- to medium-grained quartzite intercalated with phyllite. Thin layers of colluvial deposit cover the rocks in some parts of the area. The topography is steep (85°) in lower part but gentle slope (55°) in upper part. Geomechanical properties of the area are given in Annex-III.

4.3.4.1 Rock Classification

Rock mass classification for jointed rock mass of the desander basin and portal inlet area using CSIR classification and Q-system was carried out on the detailed surface discontinuity. Most of the Rock Mass Rating (RMR) of the proposed area falls around 64. It indicates the rock mass of the area is Class III type i.e. Fair Rock (Table 4.5). The NGI Tunneling Index Q of the proposed area falls around 4.86. It indicates the rock mass of the area is Class III type i.e. Fair Rock (Table 4.6).

4.3.4.2 Weathering and Strength

The rocks are fresh to slightly weathered (Annex-III). The quartzite is hard and competent in nature. The Uniaxial Compressive Strength of rock is 137.344 MPa.

4.3.4.3 Slope Stability Condition

The stability of these underground structures is analyzed on the basis of geotechnical and geological observations on the surface of the hill slope. About 25 measurements of discontinuities including foliation planes are measured. An analysis of these discontinuities using Lower Hemisphere Projection in Schmidt's equal area net is shown in Fig. 4.8. The internal friction angle is assumed to be 30° for the stability condition.

The attitude of foliation and joints in terms of dip direction and dip amount are: Foliation = 036°/42°, J_1 = 248°/61°, J_2 = 148°/56° and J_3 = 194°/54°.

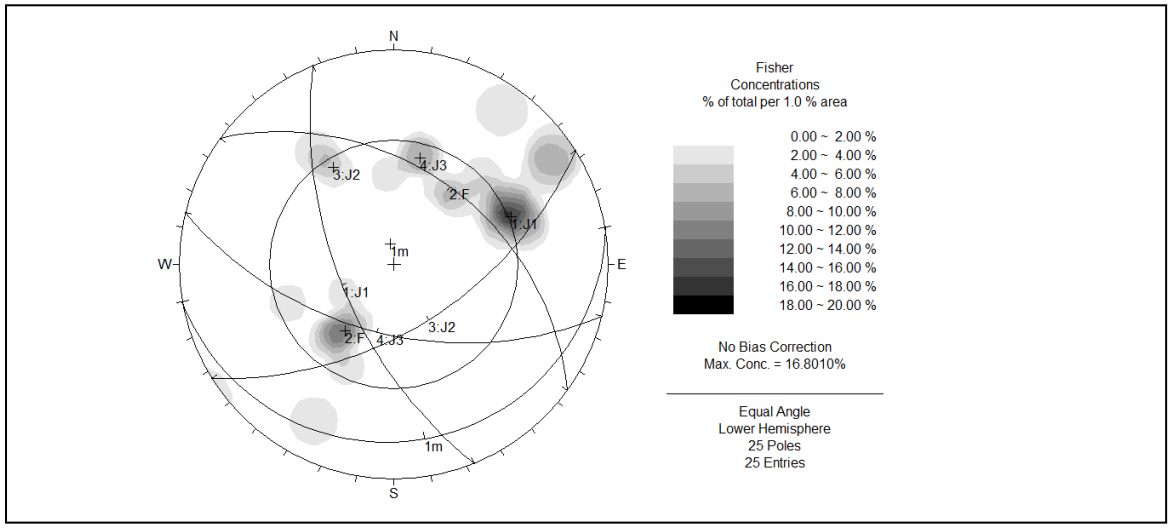

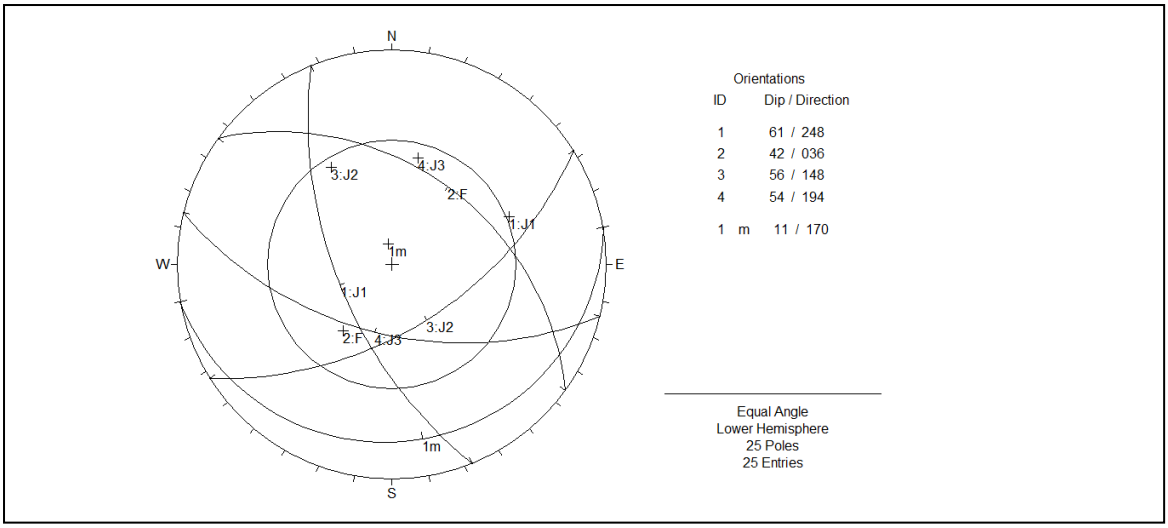

Fig. 4.8 Stereographic Projection of the rock mass exposed around the Desander Basin and Portal Inlet Area

Fig. 4.8 depicts four day lighting wedges i.e. wedges formed by the intersection of F and J_2, J_1 and J_2, J_2 and J_3 and J_3 and J_1 inside failure envelope. These wedges trigger failure during excavation. To minimize wedge failure, it is recommended to align the proposed structure in the direction of 045° - 225° from north.

4.3.5 Engineering Geological Conditions of the Headrace Tunnel Alignment Area

The horse shoe shaped proposed headrace tunnel is about 3,170 m long. It runs almost northeast to southwest direction on the right bank of Bhote Koshi River. The proposed alignment represents a shortest route considering geological structures, side cover, overburden and phreatic level in order to meet the requirements of the tunnel design.

The overall rock cover varies from 28 m to 146 m. Generally, there is good rock cover all over the tunnel alignment except Gre Khola and Tasangi Khola crossings. Though tunnel alignment passes through Syo Khola Fault and Gre Khola Fault, the study shows the faults are passive. A shallow depth landslide can be observed on the hill slope at Gre near the tunnel alignment, but no any deep landslide is found to intersect the tunnel. Generally, foliation is oblique to the proposed tunnel axis with dip against the drive which is favorable for the tunnel excavation. Engineering geological condition of the headrace tunnel is presented on the following paragraphs on different chainage.

Portal Inlet to Syo Khola (Ch. 0+411.46 m – Ch. 0+734.70 m)

The tunnel alignment from the inlet portal to Ch. 0+734.70 m runs at first with an azimuth of 260° and finally with 230°. Surface mapping reveals good rock cover (>100 m) with

thin layers (<1 m) of colluvial deposits on the hill slope. The rock mass is thick bedded, fine- to medium-grained quartzite intercalated with greenish grey, crenulated phyllite. The ratio of quartzite is greater than phyllite. Generally, there are three sets of joints which have moderately closed to very wide spacing, medium to very high persistence, rough, stepped surface with surface alteration (Annex-III). The joints are completely dry.

Syo Khola to Gre Khola (Ch. 0+734.70 m – Ch. 2+179.50 m)

The tunnel alignment from Ch. 0+734.7 m – Ch. 2+179.50 m runs with an azimuth of 230°. Topographic study shows that there is good rock cover (> 75 m) with thin layers (<1 m) of colluvial deposits on the hill slope. The area consists of intercalation of thick bedded, grey quartzite and greenish grey phyllite. The proportion of quartzite is greater than that of phyllite. A landslide is present in this section. Based on visual estimation, the landslide is not so deep to affect the tunnel alignment. Generally, there are three sets of joints which have moderately closed to very wide spacing, medium to very high persistence, rough, stepped surface with surface alteration (Annex-III). The joints are completely dry.

Gre Khola to Tasangi Khola (Ch. 2+179.50 m – Ch. 2+614.65 m)

The tunnel alignment from Ch. 2+179.50 m – Ch. 2+614.65 m runs with an azimuth of 230°. Surface mapping reveals that there is good rock cover (> 50 m) except in Tasangi Khola crossing (about 27 m). Thin layers (<1 m) of colluvial deposits cover the rocks on the hill slope. To be clear about subsurface condition two ERT lines have been conducted along Gre Khola and Tasangi Khola. The area consists of intercalation of thick bedded, grey quartzite and greenish grey phyllite. The ratio of quartzite is greater than that of phyllite. Generally, there are three sets of joints which have wide to very wide spacing, medium to very high persistence, rough, planar surface. The joints are completely dry.

Tasangi Khola to Khahare Khola (Ch. 2+614.65 m – Ch. 3+212.93 m)

The tunnel alignment from Ch. 2+614.65 m – Ch. 3+212.93 m runs with an azimuth of 215°. Surface mapping reveals that there is good rock cover (> 100 m) with thin layers (1 – 3 m) of colluvial deposits on the hill slope. The area consists of intercalation of thick bedded grey quartzite and greenish grey phyllite. The ratio of phyllite is greater than that of quartzite. Generally, there are three sets of joints which have wide to very wide spacing, medium to very high persistence, rough, planar surface (Annex-III). The joints are completely dry.

Khahare Khola to Surge Tank Area (Ch. 3+212.93 m – Ch. 3+580.87 m)

The tunnel alignment from Ch. 3+212.93 m – Ch. 3+580.87 m runs with an azimuth of 215°. Topographic study shows that there is good rock cover (>70 m) with thin to thick layers of colluvial deposits on the hill slope. To be clear about subsurface condition one ERT line has been conducted along Khahare Khola. The area consists of intercalation of thick bedded, grey quartzite and greenish grey, crenulated phyllite. The proportion of quartzite is greater than that of phyllite. Generally, there are three sets of joints which have wide to very wide spacing, medium to very high persistence, rough, stepped surface (Annex-III). The joints are completely dry.

4.3.5.1 Rock Classification

Rock mass classification for jointed rock mass of headrace tunnel alignment area using CSIR classification and Q-system was carried out on the detailed surface discontinuity. Most of the Rock Mass Rating (RMR) value of the sections Portal Inlet to Syo Khola (Ch. 0+411.46 m – Ch. 0+734.70 m); Syo Khola to Gre Khola (Ch. 0+734.7 m – Ch. 2+179.50 m); Gre Khola to Tasangi Khola (Ch. 2+179.50 m – Ch. 2+614.65 m); Tasangi Khola to Khahare Khola (Ch. 2+614.65 m – Ch. 3+212.93 m) and Khahare Khola to Surge Tank Area (Ch. 3+212.93 m – Ch. 3+580.87 m) falls around 62, 59, 62, 46 and 61. It indicates the rock mass of these sections are Class III type i.e. Fair Rock except that of section Tasangi Khola to Khahare Khola, whose rock is Class IV type i.e. Poor Rock.

Similarly, the Q value of these sections falls around 4.86, 3.86, 3.85, 1.68 and 8.66 respectively. It indicates the rock mass of these sections are Class III type i.e. Fair Rock except that of section Tasangi Khola to Khahare Khola, whose rock is Class IV type i.e. Poor Rock.

4.3.5.2 Weathering and Strength

The rocks are fresh to slightly weathered (Annex-III). The quartzite is hard and competent in nature. The Uniaxial Compressive Strength of rock ranges from 93.264 to 130.384 MPa.

4.3.5.3 Slope Stability Condition

The stability of these underground structures is analyzed on the basis of geotechnical and geological observations on the surface of the hill slope. About 175 measurements of discontinuities including foliation planes are measured. An analysis of these discontinuities using Lower Hemisphere Projection in Schmidt's equal area net is shown in Fig. 4.9, Fig. 4.10, Fig. 4.11, Fig. 4.12 and Fig. 4.13. The internal friction angle is assumed to be 30° for the stability condition.

Portal Inlet to Syo Khola (Ch. 0+411.46 m – Ch. 0+734.70 m)

The attitude of foliation and joints in terms of dip direction and dip amount are: Foliation = 036°/42°, J_1 = 248°/61°, J_2 = 148°/56° and J_3 = 194°/54°.

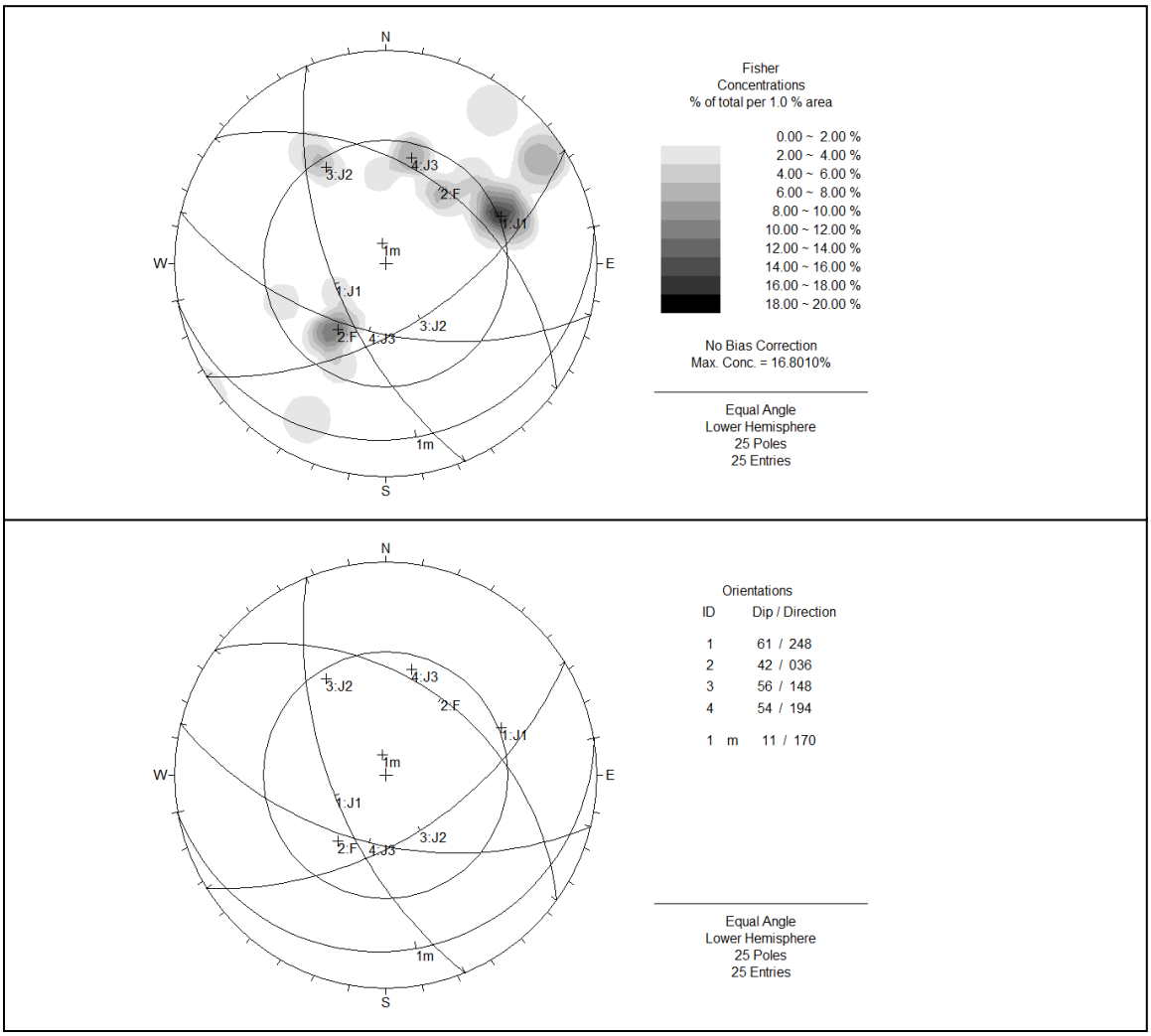

Fig. 4.9 Stereographic Projection of rock mass exposed between Portal Inlet and Syo Khola

Fig. 4.9 depicts four day lighting wedges i.e. wedges formed by the intersection of F and J_2, J_1 and J_2, J_2 and J_3 and J_3 and J_1 inside failure envelope. These wedges trigger failure during excavation.

Syo Khola to Gre Khola (Ch. 0+734.70 m – Ch. 2+179.50 m)

The attitude of foliation and joints in terms of dip direction and dip amount are: Foliation = 019°/39°, J_1 = 217°/59°, J_2 = 110°/76° and J_3 = 294°/47°.

Fig. 4.10 depicts four day lighting wedges i.e. wedges formed by the intersection of F and J_2, F and J_3, J_1 and J_2, and J_3 and J_1 inside failure envelope. These wedges trigger failure during excavation.

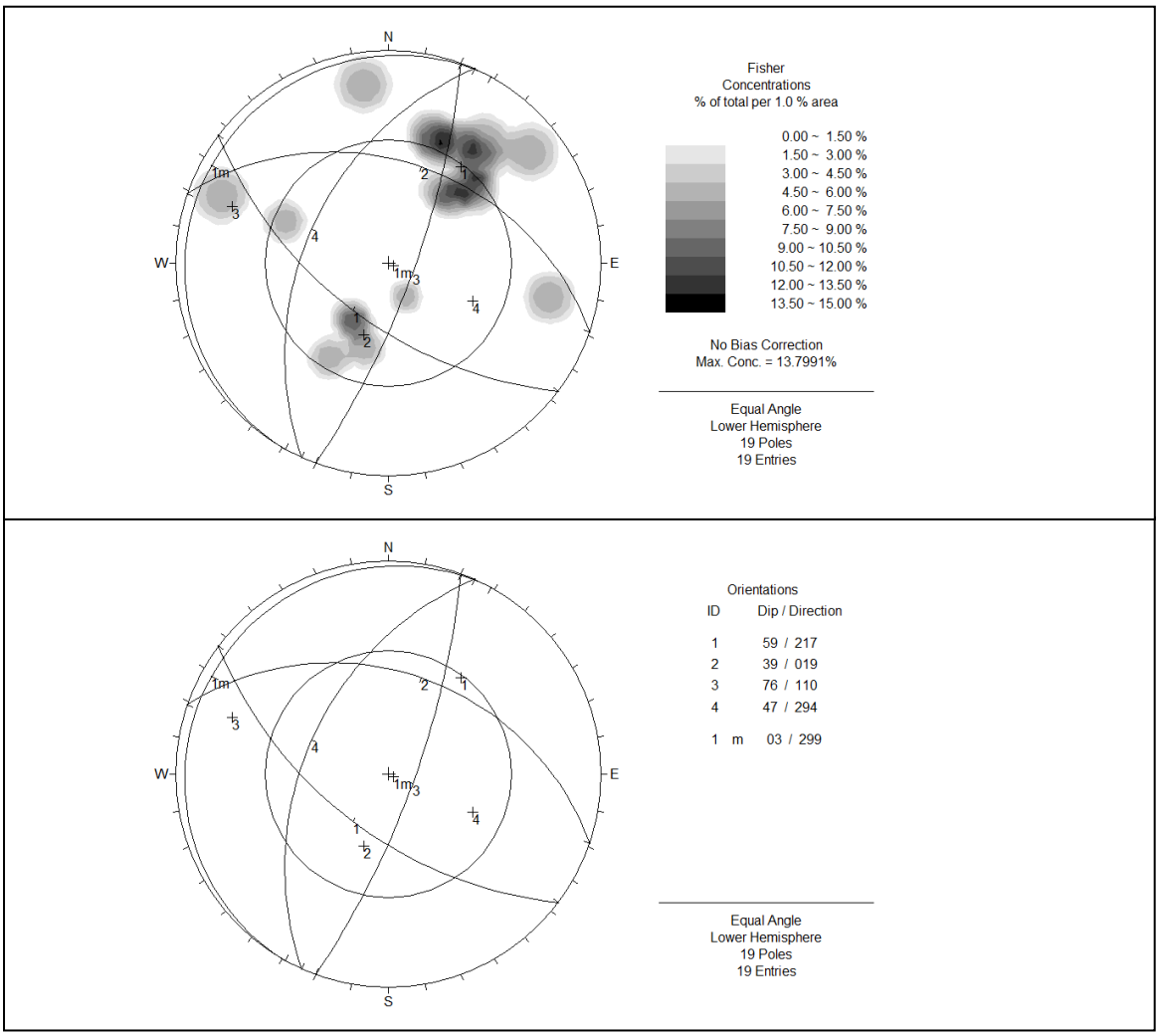

Fig. 4.10 Stereographic Projection of rock mass exposed between Syo Khola and Gre Khola

Gre Khola to Tasangi Khola (Ch. 2+179.50 m – Ch. 2+614.65 m)

The attitude of foliation and joints in terms of dip direction and dip amount are: Foliation = 021°/36°, J_1 = 232°/64°, J_2 = 124°/64° and J_3 = 316°/51°. Fig. 4.11 depicts four day lighting wedges i.e. wedges formed by the intersection of F and J_2, F and J_3, J_1 and J_2, and J_3 and J_1 inside failure envelope. These wedges trigger failure during excavation.

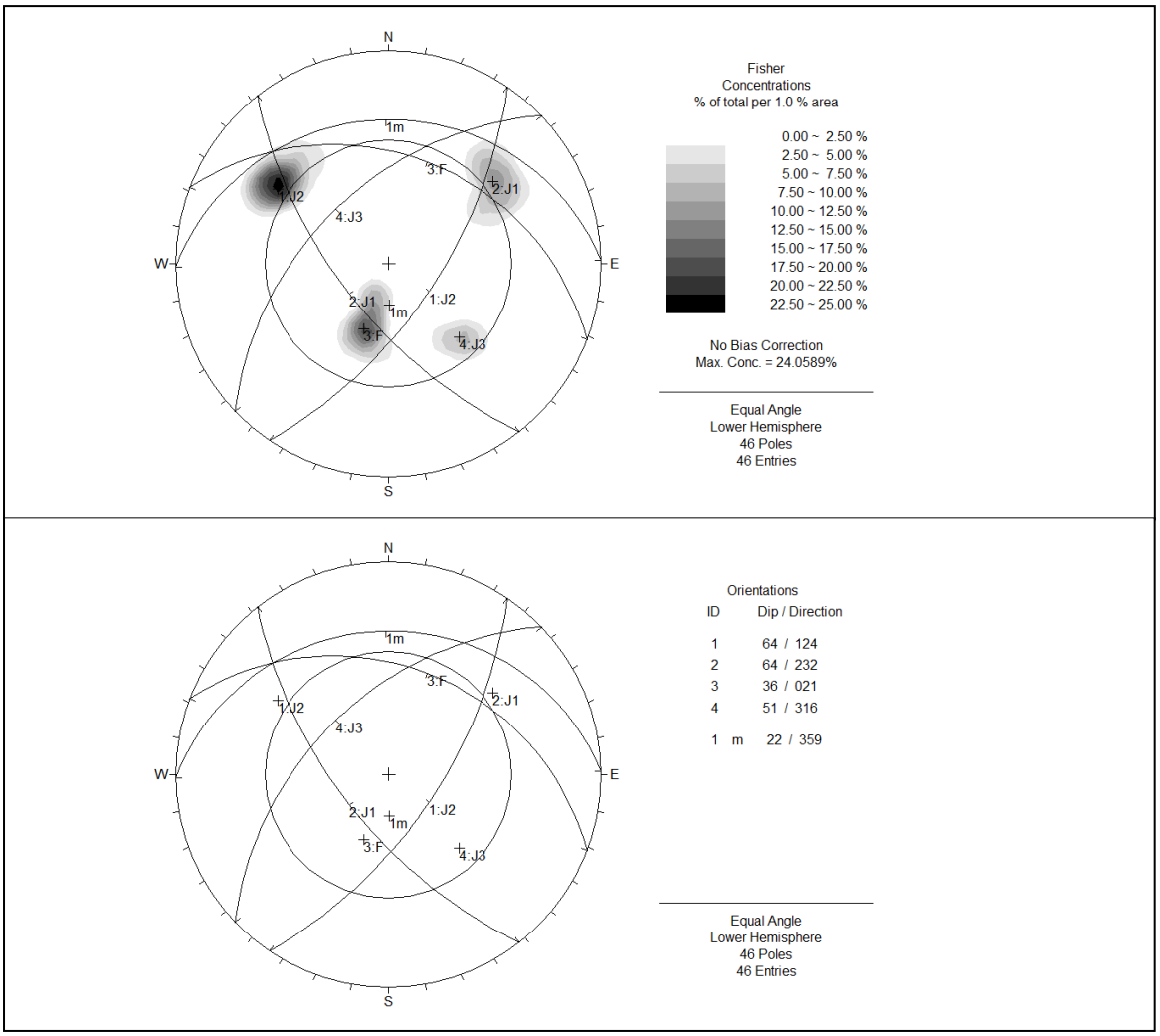

Fig. 4.11 Stereographic Projection of rock mass exposed between Gre Khola and Tasangi Khola

Tasangi Khola to Khahare Khola (Ch. 2+614.65 m – Ch. 3+212.93 m)

The attitude of foliation and joints in terms of dip direction and dip amount are: Foliation = 038°/35°, J_1 = 243°/34°, J_2 = 156°/67° and J_3 = 341°/38°. Fig. 4.12 depicts two day lighting wedges i.e. wedges formed by the intersection of F and J_3 and J_1 and J_2 inside failure envelope. These wedges trigger failure during excavation.

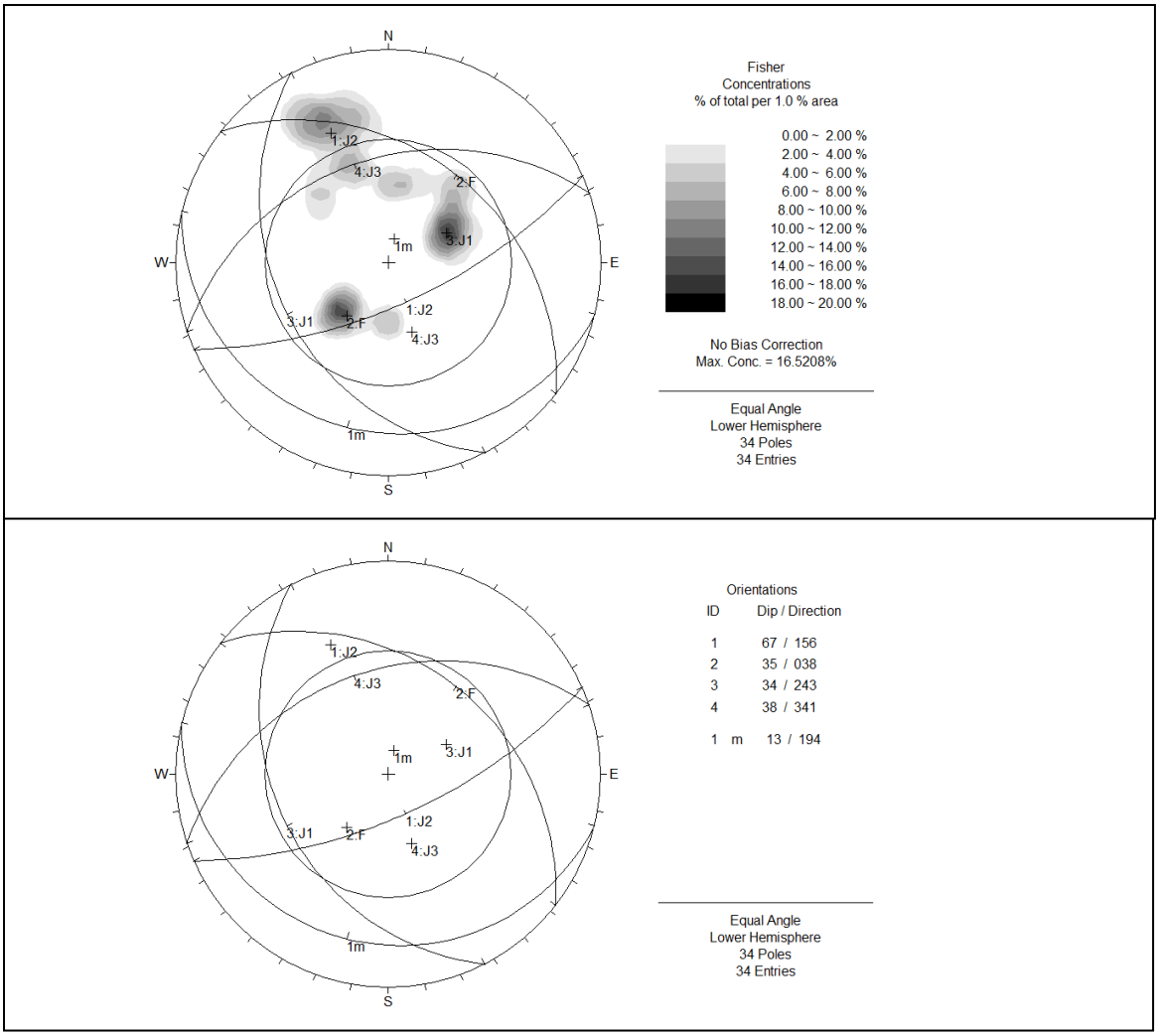

Fig. 4.12 Stereographic Projection of rock mass exposed between Tasangi Khola and Khahare Khola

Khahare Khola to Surge Tank Area (Ch. 3+212.93 m – Ch. 3+580.87 m)

The attitude of foliation and joints in terms of dip direction and dip amount are: Foliation = 009°/50°, J_1 = 216°/71°, J_2 = 152°/48° and J_3 = 268°/82°.

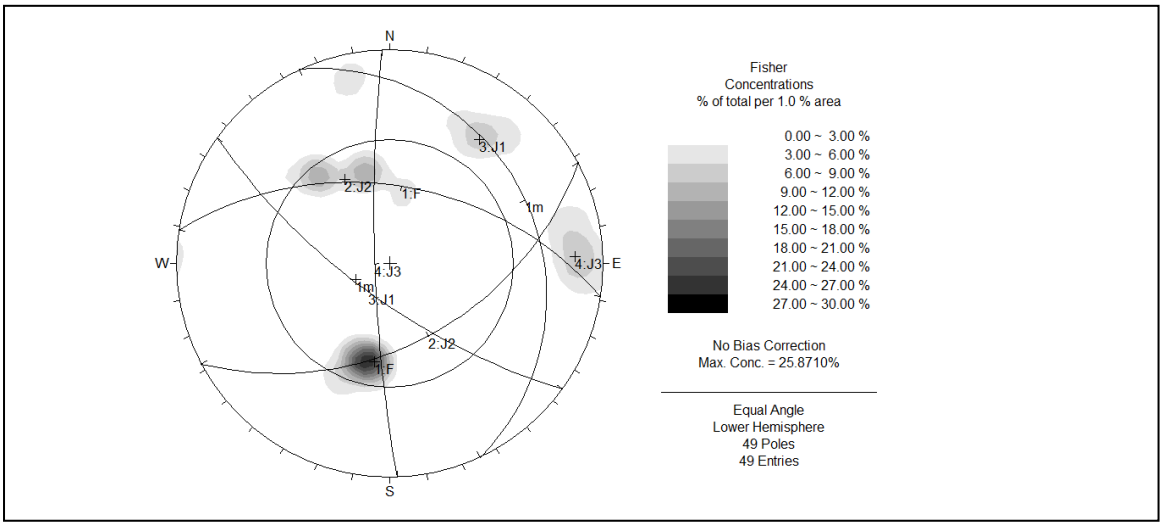

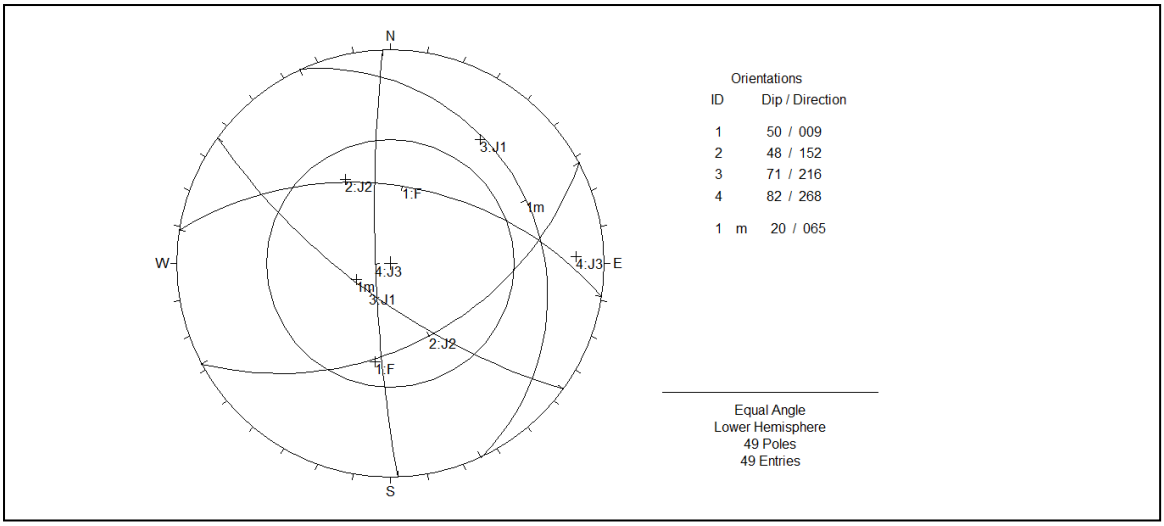

Fig. 4.13 Stereographic Projection of rock mass exposed between Khahare Khola and Surge Tank Area

Fig. 4.13 depicts four day lighting wedges i.e. wedges formed by the intersection of F and J_3, J_1 and J_2, J_2 and J_3 and J_3 and J_1 inside failure envelope. These wedges trigger failure during excavation.

4.3.6 Engineering Geological Conditions of the Surge Tank and Surge Shaft Area

The surge tank and surge shaft area is located on the right bank of the Bhote Koshi River. The surge tank is cylindrical restricted orifice, underground type which is about 300m uphill from the proposed powerhouse site. The area consists of intercalation of thick bedded, grey quartzite and greenish grey phyllite. The ratio of quartzite is greater than that of phyllite. Thin layers of colluvial deposit cover the rocks on the hill slope. Generally, there are three sets of joints which have moderately close to very wide spacing, medium to very high persistence, rough, planar surface. The joints are completely dry.

4.3.6.1 Rock Classification

Rock mass classification for jointed rock mass of the surge tank and vertical shaft area using CSIR classification and Q-system was carried out on the detailed surface discontinuity. Most of the Rock Mass Rating (RMR) of the proposed area falls around 57. It indicates the rock mass of the area is Class III type i.e. Fair Rock (Table 4.5). The NGI Tunneling Index Q of the proposed area falls around 8.66. It indicates the rock mass of the area is Class III type i.e. Fair Rock (Table 4.6).

4.2.6.2 Weathering and Strength

The rocks are fresh to slightly weathered (Annex-III). The quartzite is hard and competent in nature. The Uniaxial Compressive Strength of rock is 131.66 MPa.

4.3.6.3 Slope Stability Condition

The stability of these underground structures is analyzed on the basis of geotechnical and geological observations on the surface of the hill slope. About 59 measurements of discontinuities including foliation planes are measured. An analysis of these discontinuities using Lower Hemisphere Projection in Schmidt's equal area net is shown in Fig. 4.14. The internal friction angle is assumed to be 30° for the stability condition.

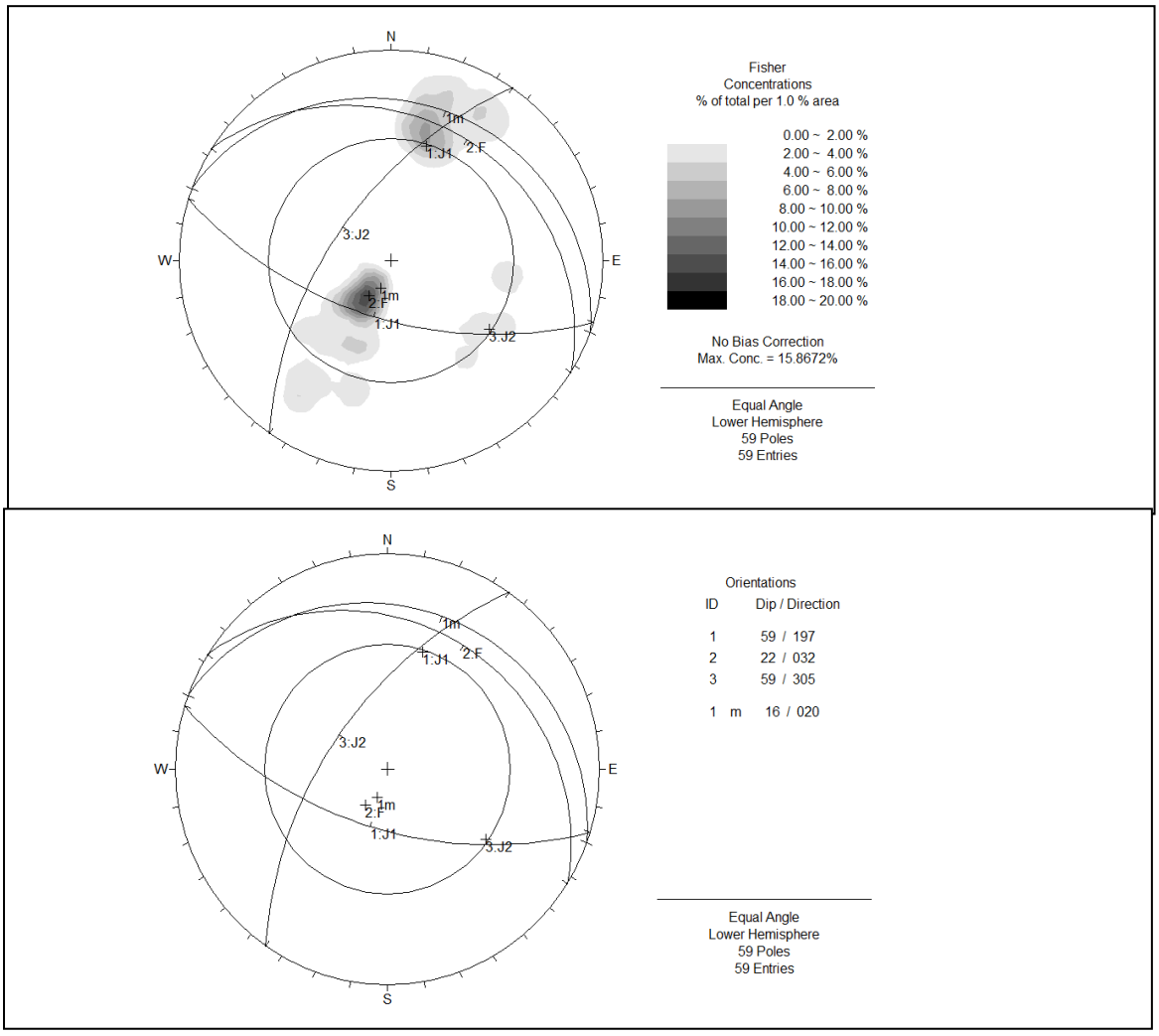

Fig. 4.14 Stereographic Projection of rock mass exposed around Surge Tank, Surge Shaft, Powerhouse and Tailrace Tunnel Alignment Area

The attitude of foliation and joints in terms of dip direction and dip amount are: F = 029°/38°, J_1 = 241°/70° and J_2 = 124°/65°. Fig. 4.14 depicts one day lighting wedge i.e. wedge formed by the intersection of J_1 and J_2 inside failure envelope. This wedge may trigger failure during excavation.

4.3.7 Engineering Geological Conditions of the Powerhouse and Tailrace Tunnel Alignment Area

The proposed powerhouse site and tailrace tunnel alignment are located at the right bank of the Bhote Koshi River. Downhill side of this structure has gentle slope made by old alluvial deposits. It consists of boulders (> 70%) and fine materials (< 30%). More than 80% of boulders are quartzite and gneiss while remaining are schist and phyllite. To be clear about subsurface condition, two ERT lines have been conducted. Uphill side of this structure comprises intercalation of quartzite and phyllite. The proportion of quartzite is greater than that of phyllite. Generally, there are three sets of joints which have moderately close to very wide spacing, medium to very high persistence, rough, planar surface (Annex-III). The joints are completely dry.

4.3.7.1 Rock Classification

Rock mass classification for jointed rock mass of the powerhouse and tailrace tunnel alignment area using CSIR classification and Q-system was carried out on the detailed surface discontinuity. Most of the Rock Mass Rating (RMR) of the proposed area falls around 57. It indicates the rock mass of the area is Class III type i.e. Fair Rock (Table 4.5). The NGI Tunneling Index Q of the proposed area falls around 8.66. It indicates the rock mass of the area is Class III type i.e. Fair Rock (Table 4.6).

4.3.7.2 Weathering and Strength

The rocks are fresh to slightly weathered (Annex-III). The quartzite is hard and competent in nature. The Uniaxial Compressive Strength of rock is 131.66 MPa.

4.3.7.3 Slope Stability Condition

The stability of these underground structures is analyzed on the basis of geotechnical and geological observations on the surface of the hill slope. About 59 measurements of discontinuities including foliation planes are measured. An analysis of these discontinuities using Lower Hemisphere Projection in Schmidt's equal area net is shown in Fig. 4.14. The internal friction angle is assumed to be 30° for the stability condition.

The attitude of foliation and joints in terms of dip direction and dip amount are: Foliation = 029°/38°, J_1 = 241°/70° and J_2 = 124°/65°. Fig. 4.14 depicts one day lighting wedge i.e. wedge formed by the intersection of J_1 and J_2 inside failure envelope. This wedge may trigger failure during excavation.

4.3.8 Engineering Geological Conditions of the Adit-1 Area

The proposed adit area lies on the right bank of Gre Khola (at chainage 2+203 m). The length of adit is about 300 m. The proposed site consists of intercalation of quartzite and phyllite. The ratio of quartzite is greater than that of phyllite. Downhill side of this structure consists of alluvial and colluvial deposits. Generally, there are three sets of joints which have moderately closed to very wide spacing, medium to very high persistence, rough, stepped surface with surface alteration (Annex-III). The joints are completely dry.

4.3.8.1 Rock Classification

Rock mass classification for jointed rock mass of the adit area using CSIR classification and Q-system was carried out on the detailed surface discontinuity. Most of the Rock Mass Rating (RMR) of the proposed area falls around 62. It indicates the rock mass of the area is Class III type i.e. Fair Rock (Table 4.5). The NGI Tunneling Index Q of the proposed area falls around 3.85. It indicates the rock mass of the area is Class III type i.e. Fair Rock (Table 4.6).

4.3.8.2 Weathering and Strength

The rock exposed in the area is fresh. The quartzite is hard and competent in nature. The Uniaxial Compressive Strength of rock is 115.536 MPa.

4.3.8.3 Slope Stability Condition

The stability of these underground structures is analyzed on the basis of geotechnical and geological observations on the surface of the hill slope. About 46 measurements of discontinuities including foliation planes are measured. An analysis of these discontinuities using Lower Hemisphere Projection in Schmidt's equal area net is shown in Fig. 4.11. The internal friction angle is assumed to be 30° for the stability condition.

The attitude of foliation and joints in terms of dip direction and dip amount are: F = 021°/36°, J_1 = 232°/64°, J_2 = 124°/64° and J_3 = 316°/51°. Fig. 4.11 depicts four day

lighting wedges i.e. wedges formed by the intersection of F and J_2, F and J_3, J_1 and J_2, and J_3 and J_1 inside failure envelope. These wedges trigger failure during excavation.

4.3.9 Engineering Geological Conditions of the Adit-2 and 3 Areas

The proposed adit-2 and 3 areas are located at about 300 m uphill of the powerhouse site. The area is characterized by the intercalation of quartzite and phyllite. The ratio of quartzite is greater than that of phyllite. Thick layers of colluvial deposits cover the rocks on the hill slope. Generally, there are three sets of joints which have wide to very wide spacing, medium to very high persistence, rough, stepped surface (Annex-III). The joints are completely dry.

4.3.9.1 Rock Classification

Rock mass classification for jointed rock mass of the surge tank and vertical shaft area using CSIR classification and Q-system was carried out on the detailed surface discontinuity. Most of the Rock Mass Rating (RMR) of the proposed area falls around 57. It indicates the rock mass of the area is Class III type i.e. Fair Rock (Table 4.5). The NGI Tunneling Index Q of the proposed area falls around 8.66. It indicates the rock mass of the area is Class III type i.e. Fair Rock (Table 4.6).

4.3.9.2 Weathering and Strength

The rocks exposed around the proposed area are fresh to slightly weathered. The quartzite is hard and competent in nature. The Uniaxial Compressive Strength of rock is 115.582 MPa.

4.3.9.3 Slope Stability Condition

The stability of these underground structures is analyzed on the basis of geotechnical and geological observations on the surface of the hill slope. About 27 measurements of discontinuities including foliation planes are measured. An analysis of these discontinuities using Lower Hemisphere Projection in Schmidt's equal area net is shown in Fig. 4.15. The internal friction angle is assumed to be 30° for the stability condition.

The attitude of foliation and joints in terms of dip direction and dip amount are: F = 029°/38°, J_1 = 241°/70° and J_2 = 124°/65°.

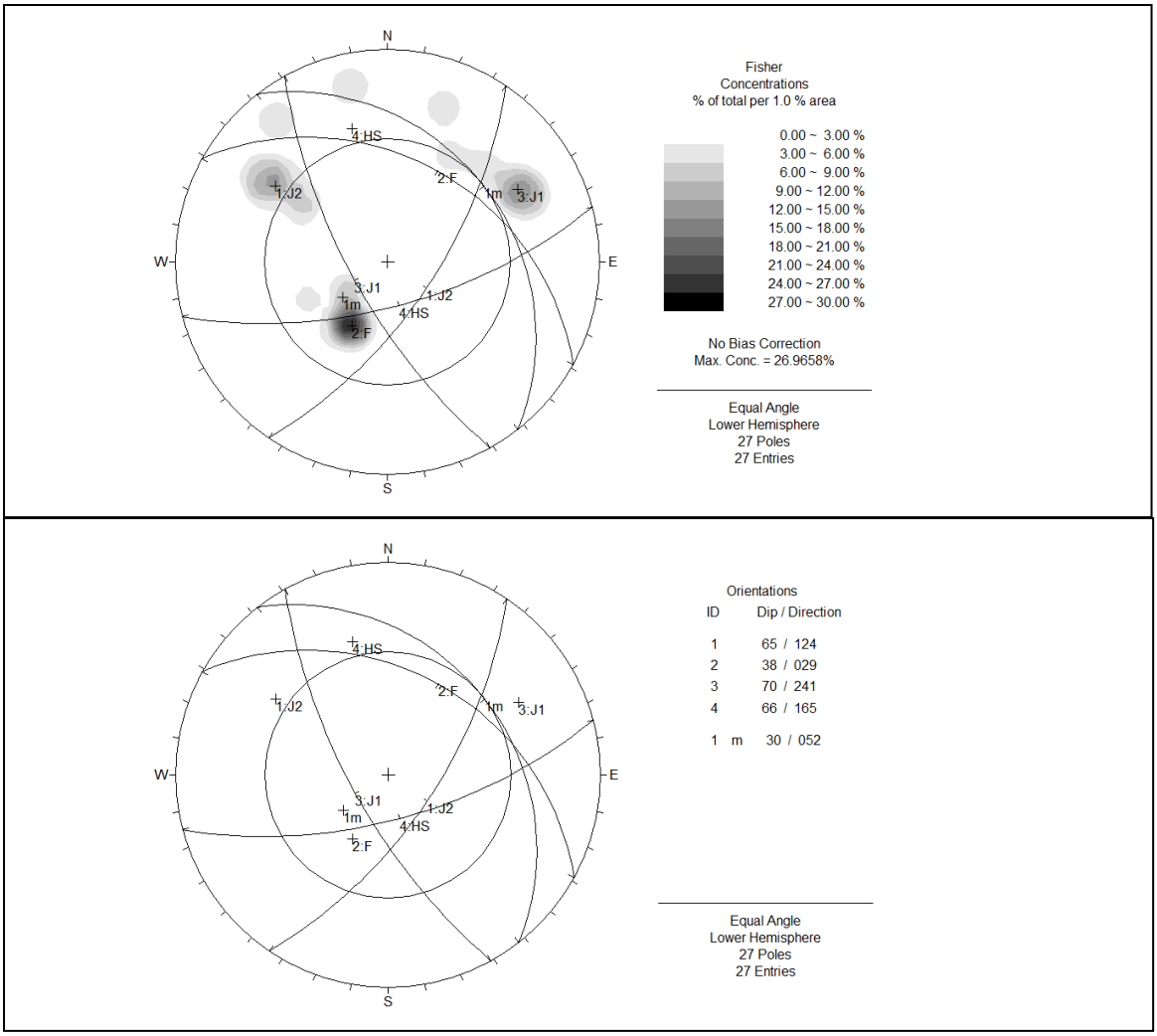

Fig. 4.15 Stereographic Projection of rock mass exposed around Adit-2 and 3 areas

Fig. 4.15 depicts two day lighting wedges i.e. wedges formed by the intersection of F and J_2 and J_1 and J_2 inside failure envelope. These wedges trigger failure during excavation.

CHAPTER 5

GEOTECHNICAL STUDIES OF THE UNDERGROUND STRUCTURES

Underground excavation is challenging job to geotechnical engineers since misjudgements in the design of support system can lead to very costly failure. In order to understand the issue involved in the process of designing support for a tunnel, it is necessary to examine how a rock mass surrounding a tunnel deforms and how the support system acts to control this deformation.

Geotechnical studies of the proposed underground structures in the Upper Trishuli-2 HEP include establishment of geotechnical parameters in order to know the interaction between the existing ground condition and the structure that will be built on it. Data required for the geotechnical studies of these structures are acquired from geological and engineering geological mapping, field test, laboratory test and empirical techniques. Since all the necessary parameters for geotechnical studies are not available at the present level of study, those parameters which are the most essence for the geotechnical studies are determined using empirical relationships. Geotechnical studies include preliminary stress analysis and rock excavation support design along the underground structures.

5.1 Stress analysis along the underground structures

The present study is focused on the analysis of stress condition produced by overburden rock body along the underground structures using RMR, GSI and Q which are extracted from the surface mapping and other values obtained from different empirical methods. This includes determination of in-situ stress deformation modulus (E_m), in-situ stress condition, elastic and plastic behavior and failure criteria. However, at this stage of study, all the data like in-situ stress and elastic and plastic parameters are difficult to acquire, therefore some assumptions are made for stress parameters. They are as follows:

- It is assumed that major principal stress (σ_1) is oriented along vertical direction, minor principal stress (σ_3) is oriented along horizontal direction and intermediate principal stress (σ_2) is oriented in longer axis of the underground opening.
- Elastic and plastic parameters are obtained from the empirical relation proposed by Hoek *et al.* (1995).

5.1.1 Estimation of in-situ deformation modulus

In-situ deformation modulus (E_m) of a rock mass is a significant parameter in any form of numerical analysis related to stability of rock masses, but this parameter is difficult and expensive to determine in the field. However, this parameter can be determined empirically using following relations.

$E_m = 2RMR - 100$ for $55 < RMR < 90$ (Bieniawski, 1978)…….. (5.1)

$E_m = 10^{(RMR - 10)/40}$ for $30 < RMR < 55$ (Serafim and Pereira, 1983)…….. (5.2)

$E_m = 25 \log_{10} Q$ for $Q > 1$ (Grimstad and Barton, 1993)……. (5.3)

Where, E_m = In-situ deformation modulus of rock mass in GPa

RMR = Rock Mass Rating System

Q = Tunneling Quality Index

In-situ deformation modulus (E_m) along the proposed headrace tunnel is calculated using RMR and Q value from the equations 5.1, 5.2 and 5.3. The calculated in-situ deformation modulus (E_m) is presented in Table 5.1.

Table 5.1 Estimation of in-situ deformation modulus of rock mass along the underground structures

Structures		**Rock Type**	**RMR**	**Q**	**E_m = 2RMR - 100**	**$E_m = 10^{(RMR - 10)/40}$**	**E_m = 25 $\log_{10}$ Q**	**Average E_m (GPa)**
Approach / Diversion Tunnel Alignment		Quartzite >> Phyllite	62	4.86	24		17.166	20.583
Portal Inlet / Desander Basin		Quartzite >> Phyllite	64	4.86	28		17.166	22.583
Headrace Tunnel	(Ch. 0+411.46m – 0+734.70 m)	Quartzite >> Phyllite	62	4.86	24		17.166	20.583
	(Ch. 0+734.70m – 2+179.50m)	Quartzite >> Phyllite	59	3.86	18		14.665	16.3325
	(Ch. 2+179.50m – 2+614.65m)	Quartzite >> Phyllite	62	3.85	24		14.636	19.318
	(Ch. 2+614.65m – 3+212.93m)	Quartzite << Phyllite	46	1.68		7.94	5.633	6.7865
	(Ch. 3+212.93m – 3+580.87m)	Quartzite >> Phyllite	61	8.66	22		23.438	22.719
Surge Tank and Powerhouse		Quartzite >> Phyllite	57	8.66	14		23.438	18.719

5.1.2 In-situ stress analysis

Basically, governing parameters for the stability of rock inside the tunnel are orientation of joints, their separation and pressure caused by overburden rock. In order to avoid hydraulic fracturing of rock with consequent opening of existing joints, the minor principal component of in-situ stresses should be higher than that of internal hydrostatic pressure in the tunnel. At this level of study, it is expensive to carry out the test required to measure in-situ stress. Therefore, an empirical method is used here for the evaluation of in-situ stress along the underground structures. Analysis using rock cover is a very simplified approximation and a more elaborate method to analyze in-situ stresses. Vertical stresses acting on the underground structures are estimated from a simple relationship.

$\sigma_v = \gamma z$ …….. (5.4)

Where, σ_v = Vertical stress

γ = Unit weight of overlying rock body (~0.027 MN/m^3)

z = Depth below a surface

Horizontal stress acting on the tunnel at a depth z below a surface can be estimated as,

$\sigma_h = k\sigma_{v,}$

Where, σ_h = Horizontal stress

k = Ratio of horizontal to vertical stress

Sheory (1994) has given an empirical equation to estimate the value of horizontal to vertical stress ratio (k) as,

$k = 0.25 + 7\ E_m\ (0.001 + 1/z)$ …….. (5.5)

Where, z = Depth below a surface in meter

E_m = Average deformation modulus of upper part of Earth crust measured in horizontal direction in GPa

Vertical and horizontal stress as well as horizontal to vertical ratio (k) along the underground structure stress is calculated and presented in Table 5.2. Their distribution along the structures is given in Fig. 5.1. The actual position of the bedrock below the surface is not ascertained on present study. Overburden from the crown of the tunnel to the surface level (Fig. 4.5) is used as the maximum rock cover (z) ignoring the depth of

residual/colluviums cover above the bedrock though residual/colluviums cover varied at different level along the tunnel alignment. Unit weight of the overlying rock (γ) is assumed to be 0.027 MN/m^3 and in-situ deformation modulus (E_m) is taken from Table 5.1.

Table 5.2 Estimation of in-situ vertical and horizontal stress along the underground structures

Structures			**Overburden z (m)**	**Specific gravity γ (MN/m^3)**	**Vertical stress σ_v (MPa)**	**Average deformation modulus E_m (GPa)**	**Horizontal to vertical stress ratio k**	**Horiz-ontal stress σ_h (MPa)**
Approach Tunnel Alignment			60	0.027	1.62	20.583	2.795	4.5279
Desander Basin			80	0.027	2.16	22.583	2.384	5.1494
Portal Inlet			130.27	0.027	3.51729	22.583	1.622	5.7050
Headrace Tunnel Alignment	Inlet portal to Syo Khola	0+411.46m - 0+538.70m	143.33	0.027	3.86991	20.583	1.399	5.4140
		0+538.70m - 0+629.598m	136.19	0.027	3.6773	20.583	1.452	5.3394
		0+629.598m - 0+685.684m	108.5	0.027	2.9295	20.583	1.722	5.0446
		0+685.684m - 0+700m	123	0.027	3.321	20.583	1.565	5.1974
		0+700m - 0+734.701m	101	0.027	2.727	20.583	1.821	4.9659
	Syo Khola to Gre Khola	0+734.701m - 0+807.214m	81.475	0.027	2.199	16.3325	1.767	3.8856
		0+807.214m - 0+940.711m	120.5	0.027	3.2549	16.3325	1.313	4.2737
		0+940.711m - 1+400m	65.404	0.027	1.766	16.3325	2.112	3.7298
		1+400m - 1+580m	78.404	0.027	2.117	16.3325	1.822	3.8572
		1+580m - 2+068m	65	0.027	1.755	16.3325	2.123	3.7259

Contd…

Structures			Overburden z (m)	Specific gravity γ (MN/m^3)	Vertical stress σ_v (MPa)	Average deformation modulus E_m (GPa)	Horizontal to vertical stress ratio K	Horizontal stress σ_h (MPa)
Headrace Tunnel Alignment		2+068m - 2+100m	57.786	0.027	1.56	16.3325	2.343	3.6551
		2+100m - 2+127m	56.286	0.027	1.5197	16.3325	2.395	3.6397
		2+127m - 2+179.50m	55	0.027	1.485	16.3325	2.443	3.6278
	Gre Khola to Tasangi Khola	2+179.50m - 2+186.06m	43.52	0.027	1.175	19.318	3.492	4.1031
		2+186.06m - 2+209.63m	44.5	0.027	1.2015	19.318	3.424	4.1139
		2+209.63m - 2+443.58m	61	0.027	1.647	19.318	2.602	4.2855
		2+443.58m - 2+614.65m	47	0.027	1.269	19.318	3.262	4.1395
	Tasangi Khola to Khahare Khola	2+614.65m - 2+800m	27.405	0.027	0.74	6.7865	2.031	1.5029
		2+800m - 3+055.82m	114.905	0.027	3.1024	6.7865	0.711	2.2058
		3+055.82m - 3+212.93m	145.905	0.027	3.9394	6.7865	0.623	2.4499
	Khahare Khola to Surge Tank	3+212.93m - 3+292.87m	82.405	0.027	2.225	22.719	2.339	5.2043
		3+292.87m - 3+500m	70.741	0.027	1.91	22.719	2.657	5.0748
		3+500m - 3+510.73m	73.241	0.027	1.9775	22.719	2.580	5.1019
		3+510.73m - 3+551.76m	61	0.027	1.647	22.719	3.016	4.9673
		3+551.76m - 3+580.87m	59.5	0.027	1.6065	22.719	3.082	4.9512
Surge Tank			68.91	0.027	1.8606	18.719	2.28	4.2422
Powerhouse/Tailrace Tunnel Alignment			54	0.027	1.458	18.719	2.807	4.0926

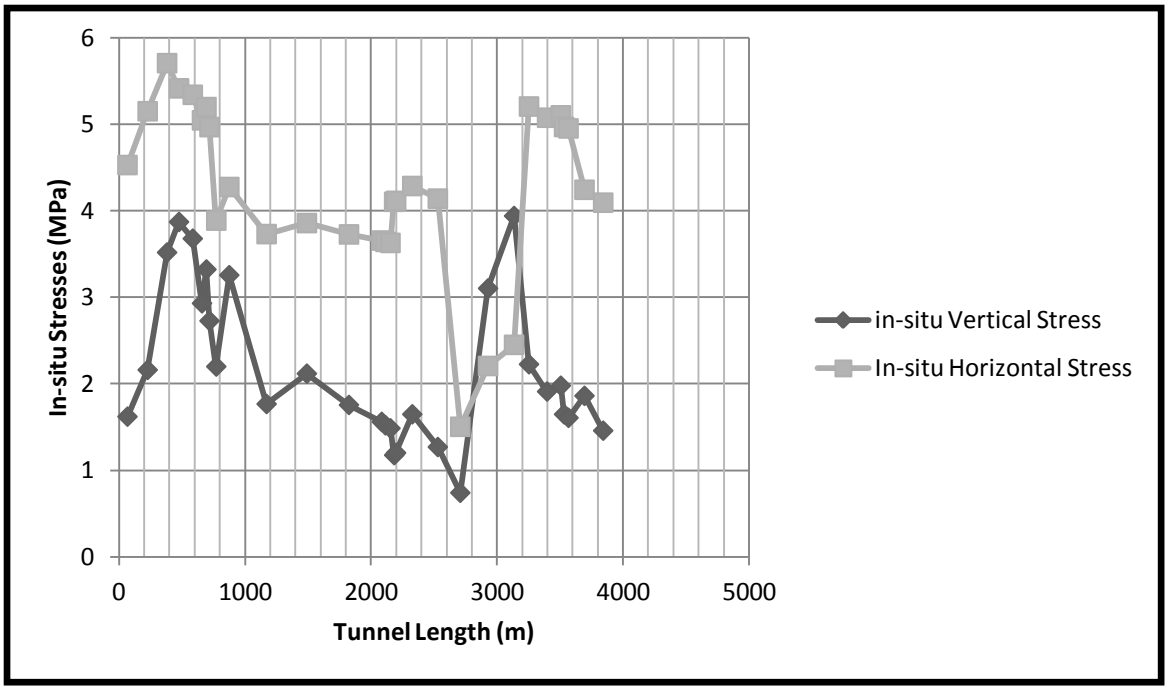

Fig. 5.1 Distribution of in-situ vertical and horzontal stresses along the underground structures

Normally, the value of k is les than 2 for the depth up to 1000 m but on the present study, its value reaches up to 5.7050. Since, the vertical stress is estimated from the product of the overburden and assumed unit weight of the rock and E_m is calculated from the RMR value and Q value which is sometime not reliable, hence the value of k sems anomalous. Thus, the evaluation of in-situ stress along the underground structures is needed for the detailed design.

5.1.3 Determination of elastic and/or plastic behavior of rock

Different stress parameters like vertical stress, maximum tangential boundary stress, in-situ deformation modulus and ratio of horizontal to vertical stress are used here to find out elastic and/or plastic behavior of rock along the underground structures. The ratio of maximum tangential boundary stress to unconfined compressive strength of rock mass is reffered as damage index (D_i). the damage index is thus given by,

$D_i = \sigma_{max}/\sigma_c$ …….. (5.6)

Where, σ_{max} = Maximum tangential boundary stress

σ_c = Unconfined compressive stress

If $D_i \leq 0.4$, rock behaves as elastic and if $D_i \geq 0.4$, rock behaves as plastic. Maximum tangential boundary stress (σ_{max}) is given by the Kirsch equation,

$\sigma_{max} = \sigma_v (3k - 1)$ …….. (5.7)

Where, k = Horizontal to vertical ratio

σ_v = vertical stress

Damage index for the underground structures is estimated and presented in Table 5.3. Vertical stress and horizontal to vertical stress ratio are taken from Table 5.2 and unconfined compressive strength (UCS) obtained by laboratory is used for determination of damage index.

Table 5.3 Damage index of rock mass along the underground structures

Structures			Vertical stress σ_v (MPa)	Horizontal to vertical stress ratio K	σ_c (MPa)	σ_{max} (MPa)	D_i
Approach Tunnel Alignment			1.62	2.795	137.344	11.9637	0.0871
Desander Basin			2.16	2.384	137.344	13.2883	0.0967
Portal Inlet			3.51729	1.622	137.344	13.5978	0.0990
Headrace Tunnel Alignment	Inlet portal to Syo Khola	0+411.46m - 0+538.70m	3.86991	1.399	130.384	12.3721	0.0949
		0+538.70m - 0+629.598m	3.6773	1.452	130.384	12.341	0.0946
		0+629.598m - 0+685.684m	2.9295	1.722	130.384	12.204	0.0936
		0+685.684m - 0+700m	3.321	1.565	130.384	12.271	0.0941
		0+700m - 0+734.701m	2.727	1.821	130.384	12.171	0.0933
	Syo Khola to Gre Khola	0+734.701m - 0+807.214m	2.199	1.767	115.536	9.4578	0.0819
		0+807.214m - 0+940.711m	3.2549	1.313	115.536	9.566	0.0828
		0+940.711m - 1+400m	1.766	2.112	115.536	9.4234	0.0816
		1+400m - 1+580m	2.117	1.822	115.536	9.454	0.0818
		1+580m - 2+068m	1.755	2.123	115.536	9.4225	0.0815

Contd…

Structures			Vertical stress σ_v (MPa)	Horizontal to vertical stress ratio K	σ_c (MPa)	σ_{max} (MPa)	D_i
Headrace Tunnel Alignment		2+068m - 2+100m	1.56	2.343	115.536	9.405	0.0814
		2+100m - 2+127m	1.5197	2.395	115.536	9.3993	0.0813
		2+127m - 2+179.50m	1.485	2.443	115.536	9.398	0.0813
	Gre Khola to Tasangi Khola	2+179.50m - 2+186.06m	1.175	3.492	121.522	11.134	0.0916
		2+186.06m - 2+209.63m	1.2015	3.424	121.522	11.1403	0.0917
		2+209.63m - 2+443.58m	1.647	2.602	121.522	11.2094	0.0922
		2+443.58m - 2+614.65m	1.269	3.262	121.522	11.149	0.0917
	Tasangi Khola to Khahare Khola	2+614.65m - 2+800m	0.74	2.031	93.264	3.768	0.0404
		2+800m - 3+055.82m	3.1024	0.711	93.264	3.515	0.0377
		3+055.82m - 3+212.93m	3.9394	0.623	93.264	3.4233	0.0367
	Khahare Khola to Surge Tank	3+212.93m - 3+292.87m	2.225	2.339	115.582	13.388	0.1158
		3+292.87m - 3+500m	1.91	2.657	115.582	13.3146	0.1152
		3+500m - 3+510.73m	1.9775	2.580	115.582	13.328	0.1153
		3+510.73m - 3+551.76m	1.647	3.016	115.582	13.255	0.1147
		3+551.76m - 3+580.87m	1.6065	3.082	115.582	13.247	0.1146
Surge Tank			1.8606	2.28	112.59	10.866	0.0965
Powerhouse/Tailrace Tunnel Alignment			1.458	2.807	112.59	10.819	0.0961

As mentioned earlier, for damage index $D_i \leq 0.4$, rock mass behaves as an elastic and no visible damage occurs. On the present study, all calculated value of D_i lies between 0.0367 and 0.1158. Hence, the rock mass behaves as elastic. It indicates no possibility of damage in the underground structures due to overburden rock body. Distribution of damage index along the underground structures is depicted on Fig. 5.2.

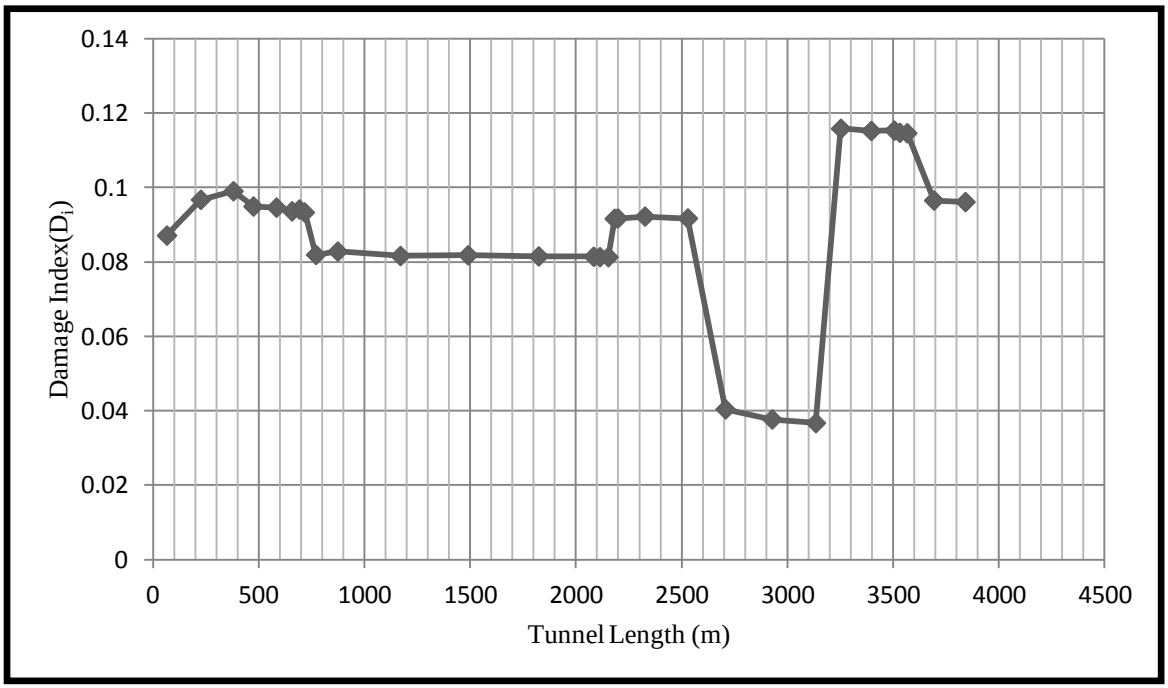

Fig. 5.2 Distribution of damage index along the underground structures

5.1.4 Determination of rock mass strength parameters

Rock mass properties are assumed to be adequately characterized by the biaxial failure criteria developed by Hoek and Brown (1980). Most generalized form of the Hoek-Brown criterion is given by the following empirical relationship for both the intact and fractured rock.

$$\sigma_1 = \sigma_3 + (m_b\sigma_c\sigma_3 + s\sigma_c^2)^{1/2} \quad \ldots\ldots\ldots\ldots\ldots\ldots \quad (5.8)$$

Where, σ_1 = Major Principal Stress at failure

σ_3 = Minor Principal Stresses applied to the specimen

σ_c = Uniaxial Compressive Strength of intact rock material in the specimen

m_b and s = material constants which depend upon properties of rock and an extent to which it has been broken before subjected to stresses σ_1 and σ_3.

Uniaxial compressive strength (σ_{cs}) of a specimen is given by substituting $\sigma_3 = 0$ in Eq. 5.8, giving,

$\sigma_{cs} = (s\sigma_c^2)^{1/2}$ …….. (5.9)

For the intact rock, $\sigma_{cs} = \sigma_c$ and s = 1, $m_b = m_i$. For the previously broken rocks, s < 1 and the strength at zero confining pressure is given by Eq. 5.9.

The uniaxial tensile strength (σ_t) of the specimen is given by substituting $\sigma_1 = 0$ in the Eq. 5.8 and by solving the resulting quadratic equation for σ_3.

$\sigma_t = ½ \sigma_c (m_b – (m_b^2 + 4s)^{½})$ …….. (5.10)

The strength parameters, m and s for the intact rock and the fractured rocks are as follows.

Intact rock, s =1

Very fractured rock, s = 0

Good quality rock, $m_i = 25$

Weak rock, $m_i = 0$

Values of m and s used in analysis are determined from the following equation and RMR is determined according to Bieniawski (1989).

For GSI > 25 (undisturbed rock masses)

$m_b/m_i = \exp^{(GSI-100)/28}$ …….. (5.11)

$s = \exp^{(GSI-100)/9}$ …….. (5.12)

Where, GSI = Geological Strength Index

The relation between GSI and RMR is given by an equation,

$GSI = RMR_{89} – 5$ …….. (5.13)

Where, RMR_{89} = Rock mass classification proposed by Bieniawski (1989)

Values of constant m_i for the intact rock are given in Table 5.4.

In order to determine rock mass strength parameters, m_b and s, GSI calculated and tabulated on Table 4.5 is taken. The value of m_i is taken from Table 5.4. Thus determined strength parameter is tabulated on Table 5.5.

By using rock mass strength parameters tabulated in Table 5.5 and the standard set up on software itself, Hoek-Brown classification, Hoek-Brown criterion, failure envelope range, Mohr-Coulomb fit and rock mass parameters are obtained using the RocLab software developed by Rocscience. Input parameters used for stress analysis on the software are intact uniaxial compressive strength (σ_c), m_i, GSI and disturbance factor (D), modulus ratio (m_r), unit weight of the rock (γ) and tunnel depth (z). Among these parameters, intact uniaxial compressive strength, m_i, GSI and tunnel depth are taken from Table 5.5. Disturbance factor is considered as zero considering blasting results minimal disturbance to surrounding rock mass. Modulus ratio (m_r) for different rocks is used from the table given in the software. Modulus ratio is used to calculate intact modulus ($E_i = m_r\sigma_c$). Unit weight of rock is considered as 0.027 MN/m^3. Thus obtained rock mass strength parameters for the underground structures are given in Fig. 5.3.

Table 5.4: Values of constant m_i for intact rock (after Marinos and Hoek, 2001)

Rock type	**Class**	**Group**	**Texture**			
			Coarse	**Medium**	**Fine**	**Very Fine**
SEDIMENTARY	Clastic		Conglomerate (21±3) Breccias (19±5)	Sandstone (17±4)	Siltstone (7±2) Greywacke (18±3)	Claystone (4±2) Shale (6±2) Marls(7±2)
	Non-clastic	Carbonate	Crystalline limestone (12±3)	Sparitic Limestone (10±2)	Micritic Limestone (9±2)	Dolomite (9±3)
		Evaporite		Gypsum (8±2)	Anhydrite (12±2)	
		Organic				Chalk (7±2)
METAMORPHIC	Non foliated		Marble (9±3)	Hornfels (19±4) Metasandstone (19±3)	Quartzite (20±3)	
	Slightly foliated		Migmatite (29±3)	Amphibolite (26±6)	Gneiss (28±5)	
	Foliated			Schist (12±3)	Phyllite (7±3)	Slate (7±4)
IGNEOUS	Plutonic	Light	Granite (32±3) Granodiorite (29±3)	Diorite (25±35		
		Dark	Gabbro (29±3) Norite (29±3)	Dolerite (29±3)		
	Hypabyssal		Porphyrite (20±5)		Diabase (15±5)	Peridotite (25±5)
	Volcanic	Lava		Rhyolite (25±5) Andesite (25±5)	Dacite (25±3) Basalt (25±5)	
		Pyroclastic	Agglomerate (19±3)	Volcanic breccias (19±5)	Tuff (13±5)	

Table 5.5: Determination of rock mass strength parameters, m_b and s

Structures			Max. rock cover (z) m	GSI	σ_c (MPa)	m_i	m_b	s
Approach Tunnel Alignment			60	57	137.344	17	3.660	0.00841
Desander Basin			80	59	137.344	17	3.931	0.01051
Portal Inlet			130.27	59	137.344	17	3.931	0.01051
Headrace Tunnel Alignment	Inlet portal to Syo Khola	0+411.46m - 0+538.70m	143.33	57	130.384	17	3.660	0.00841
		0+538.70m - 0+629.598m	136.195	57	130.384	17	3.660	0.00841
		0+629.598m - 0+685.684m	108.5	57	130.384	17	3.660	0.00841
		0+685.684m - 0+700m	123	57	130.384	17	3.660	0.00841
		0+700m - 0+734.701m	101	57	130.384	17	3.660	0.00841
	Syo Khola to Gre Khola	0+734.701m - 0+807.214m	81.475	54	115.536	17	3.288	0.00603
		0+807.214m - 0+940.711m	120.5	54	115.536	17	3.288	0.00603
		0+940.711m - 1+400m	65.404	54	115.536	17	3.288	0.00603
		1+400m - 1+580m	78.404	54	115.536	17	3.288	0.00603
		1+580m - 2+068m	65	54	115.536	17	3.288	0.00603
		2+068m - 2+100m	57.786	54	115.536	17	3.288	0.00603
		2+100m - 2+127m	56.286	54	115.536	17	3.288	0.00603
		2+127m - 2+179.50m	55	54	115.536	17	3.288	0.00603
	Gre Khola to Tasangi Khola	2+179.50m - 2+186.06m	43.52	57	121.522	17	3.660	0.00841
		2+186.06m - 2+209.63m	44.5	57	121.522	17	3.660	0.00841

Contd…

Structures			Max. rock cover (z) m	GSI	σ_c (MPa)	m_i	m_b	s
Headrace Tunnel Alignment		2+209.63m - 2+443.58m	61	57	121.522	17	3.660	0.00841
		2+443.58m - 2+614.65m	47	57	121.522	17	3.660	0.00841
	Tasangi Khola to Khahare Khola	2+614.65m - 2+800m	27.405	41	93.264	10	1.216	0.00142
		2+800m - 3+055.82m	114.905	41	93.264	10	1.216	0.00142
		3+055.82m - 3+212.93m	145.905	41	93.264	10	1.216	0.00142
	Khahare Khola to Surge Tank	3+212.93m - 3+292.87m	82.405	56	115.582	17	3.532	0.00753
		3+292.87m - 3+500m	70.741	56	115.582	17	3.532	0.00753
		3+500m - 3+510.73m	73.241	56	115.582	17	3.532	0.00753
		3+510.73m - 3+551.76m	61	56	115.582	17	3.532	0.00753
		3+551.76m - 3+580.87m	59.5	56	115.582	17	3.532	0.00753
Surge Tank			68.91	52	112.59	17	3.062	0.00483
Powerhouse/Tailrace Tunnel Alignment			54	52	112.59	17	3.062	0.00483

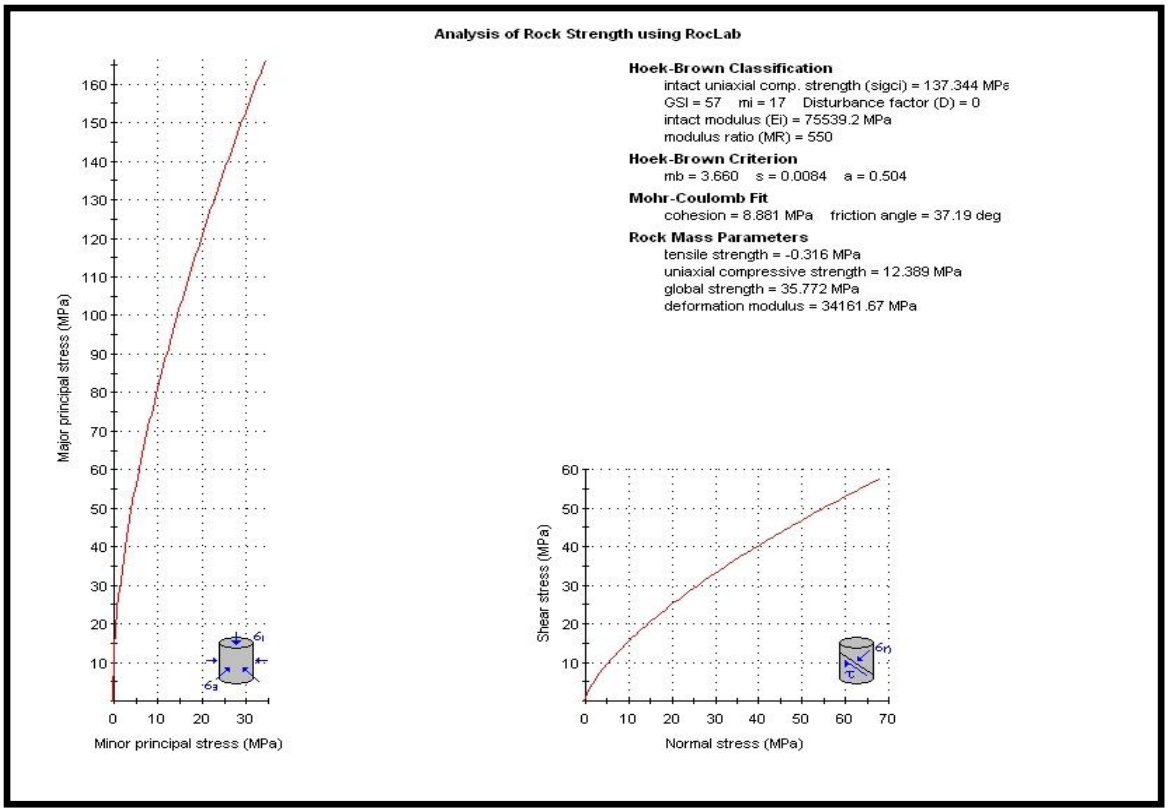

Fig. 5.3 (a) Graphical representation of stress condition for failure criteria of the rock (quartzite >> phyllite) of Approach Tunnel Alignment Area

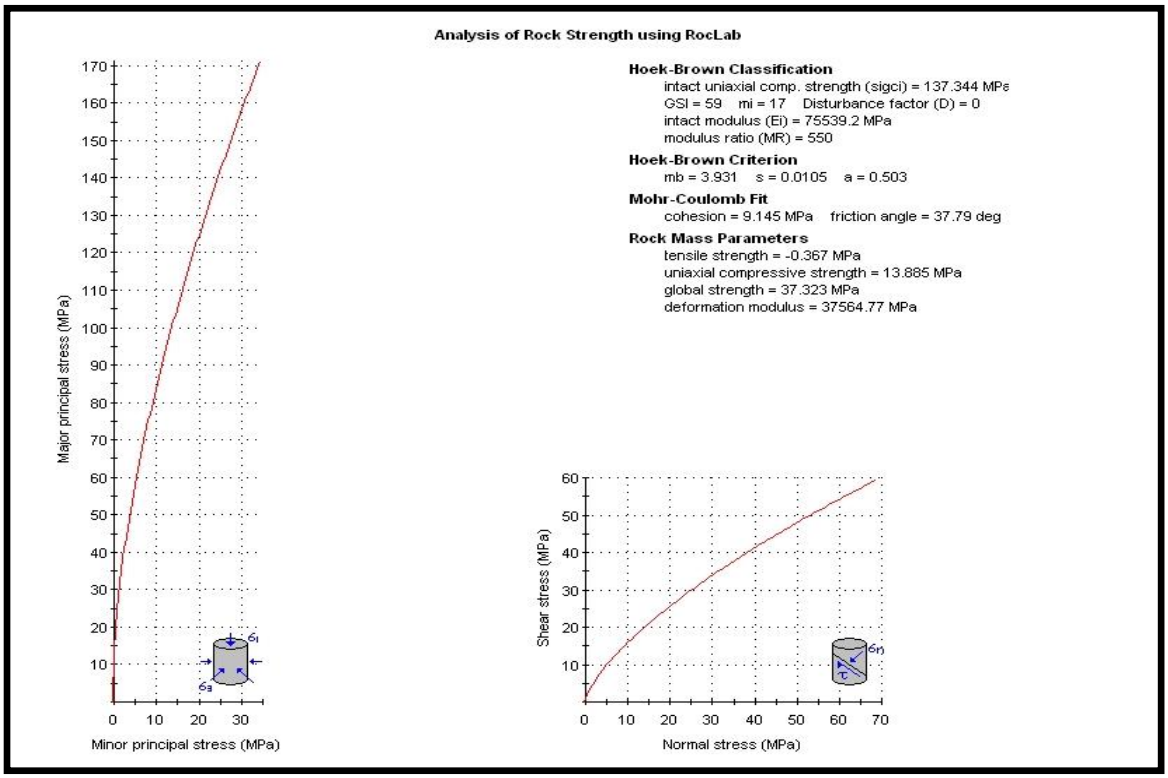

Fig. 5.3 (b) Graphical representation of stress condition for failure criteria of the rock (quartzite >> phyllite) of Desander Basin and Portal Inlet Area

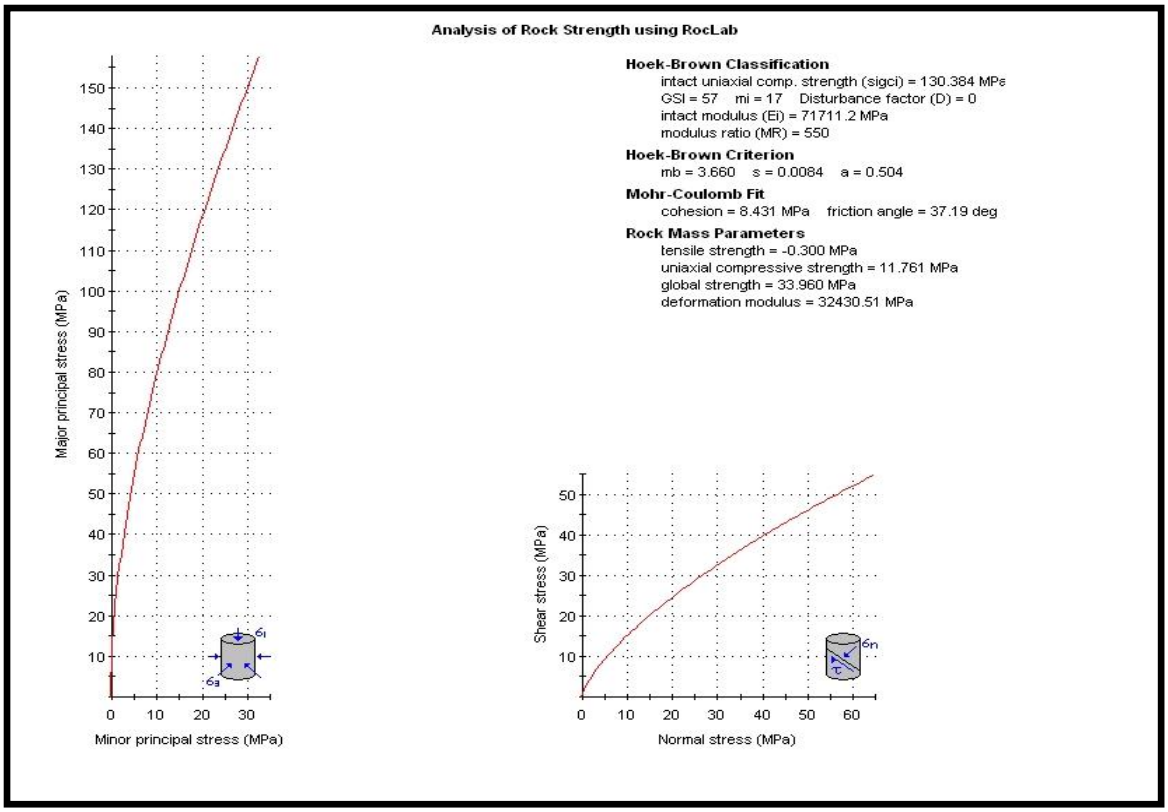

Fig. 5.3 (c) Graphical representation of stress condition for failure criteria of the rock (quartzite >> phyllite) of Headrace Tunnel Alignment (0+411.46m – 0+734.701m)

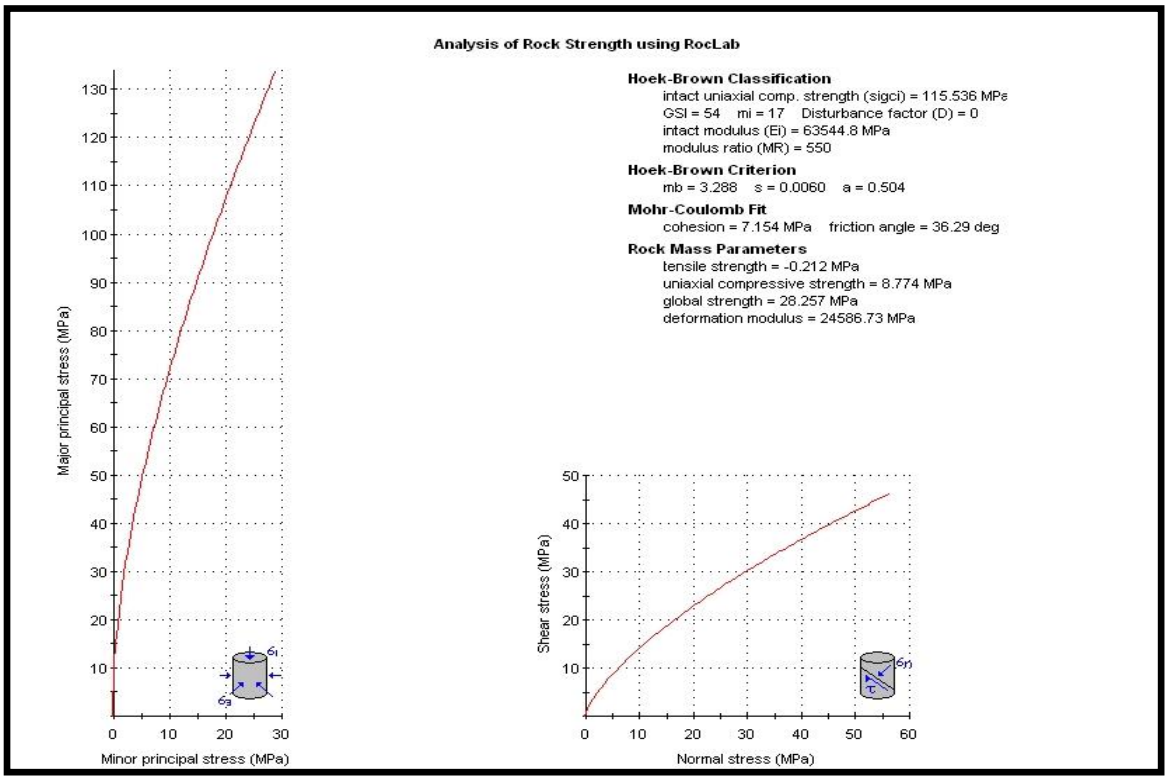

Fig. 5.3 (d) Graphical representation of stress condition for failure criteria of the rock (quartzite >> phyllite) of Headrace Tunnel Alignment (0+734.701m - 2+179.50m)

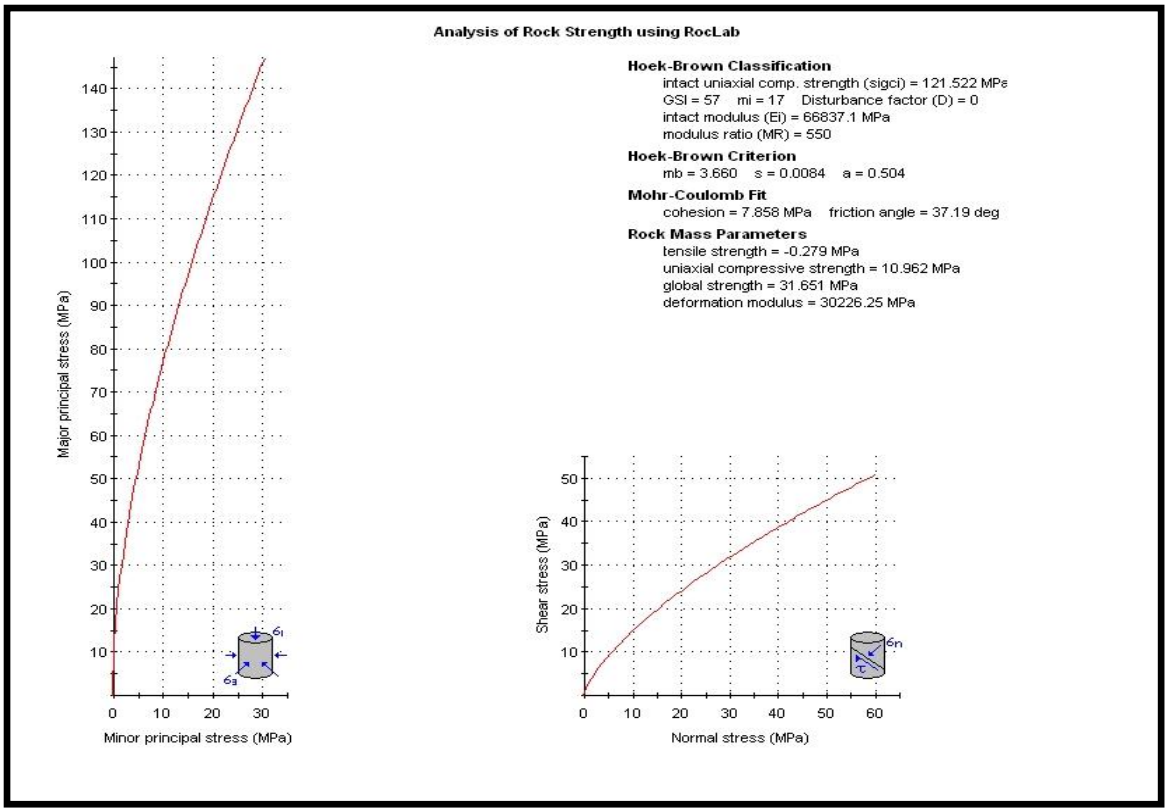

Fig. 5.3 (e) Graphical representation of stress condition for failure criteria of the rock (quartzite >> phyllite) of Headrace Tunnel Alignment (2+179.50m - 2+614.65m)

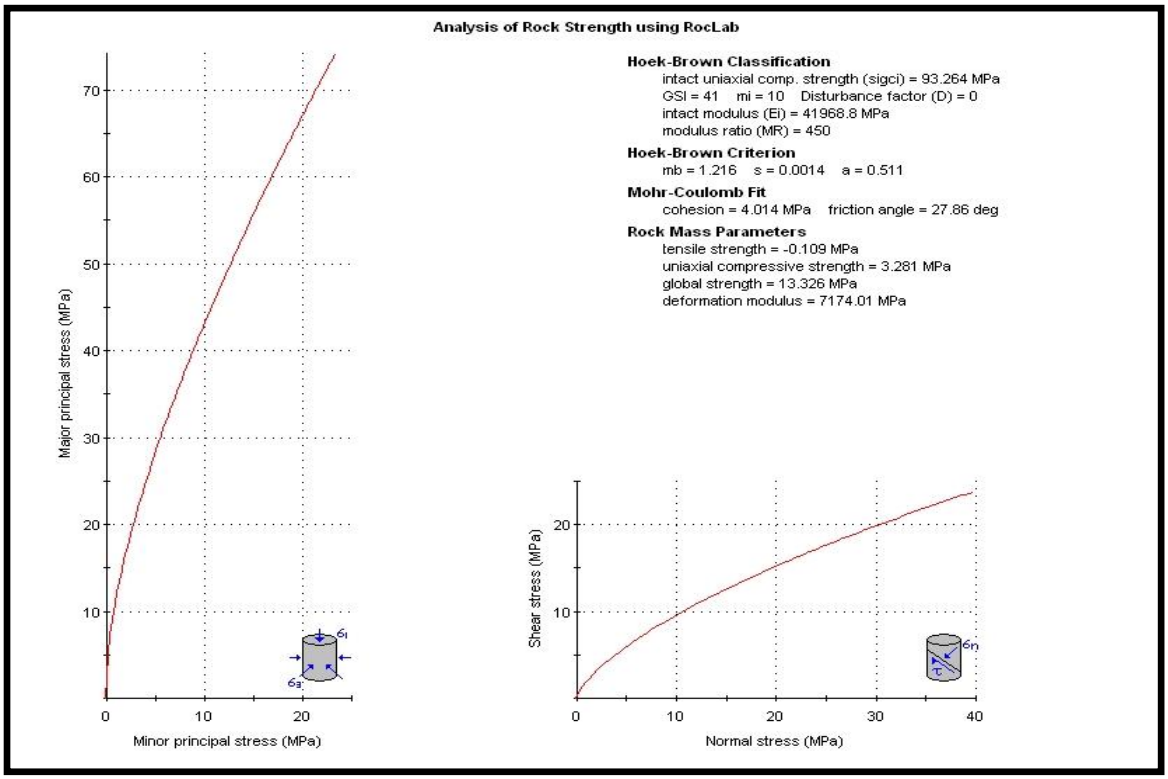

Fig. 5.3 (f) Graphical representation of stress condition for failure criteria of the rock (quartzite << phyllite) of Headrace Tunnel Alignment (2+614.65m - 3+212.93m)

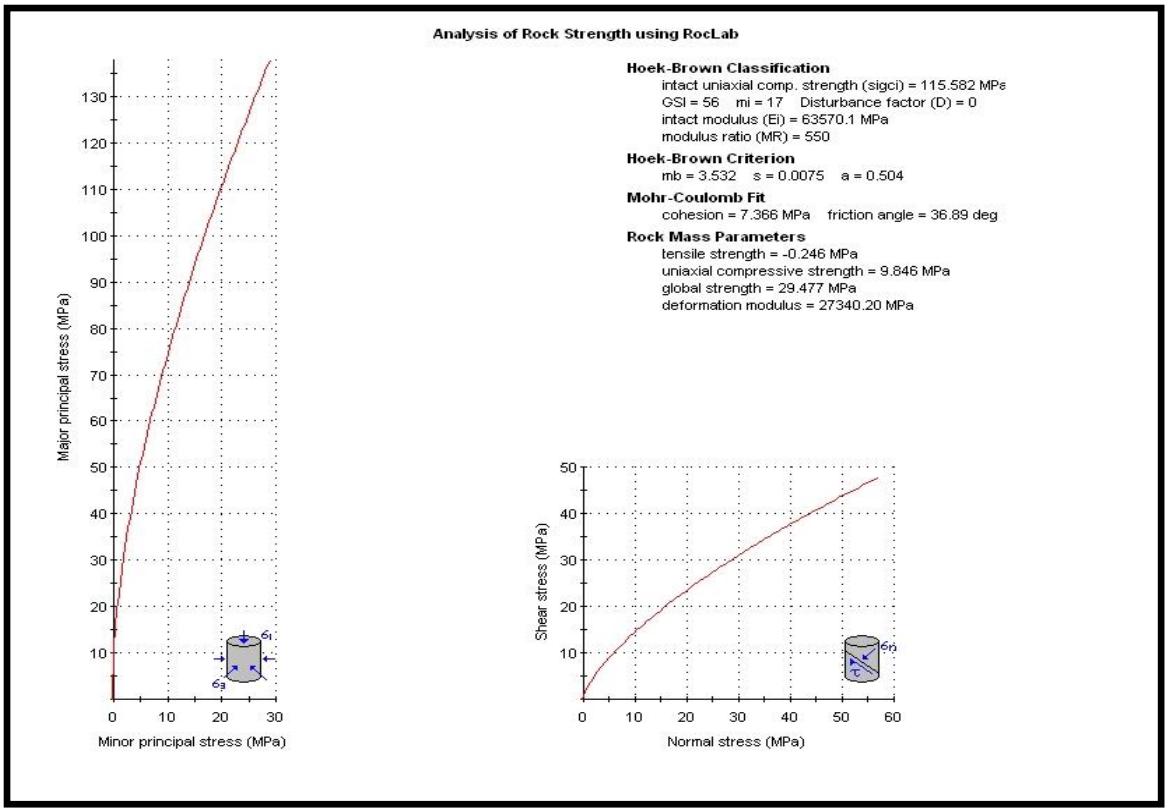

Fig. 5.3 (g) Graphical representation of stress condition for failure criteria of the rock (quartzite >> phyllite) of Headrace Tunnel Alignment (3+212.93m - 3+580.87m)

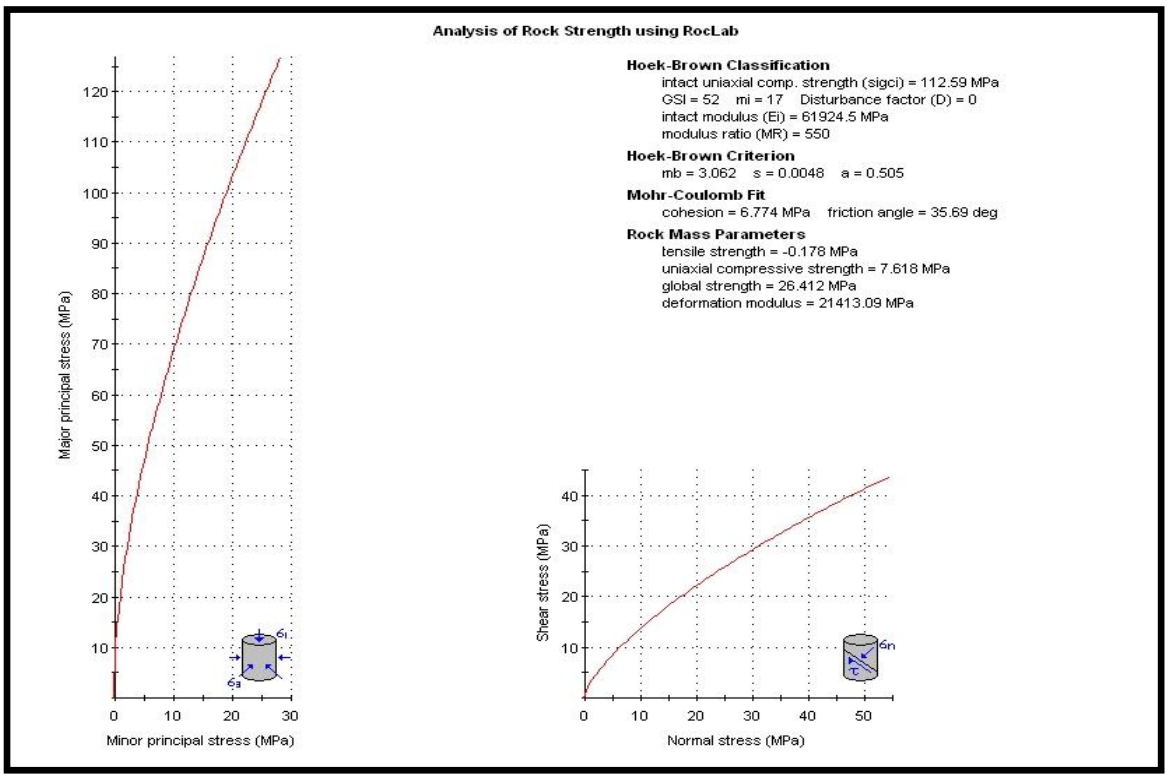

Fig. 5.3 (g) Graphical representation of stress condition for failure criteria of the rock (quartzite >> phyllite) of Surge Tank, Powerhouse and Tailrace Tunnel Alignment Area

5.2 Rock excavation support design

The proposed rock excavation process along the underground structures is a conventional drilling and blasting. The rock support along these excavated underground structures strengthens the rock mass by preventing the detachment of loose blocks as well as interlocking individual blocks. A basic principle is to design the support system so as to make use do the strength of the rock, if possible diverting the imposed loads away from the perimeter of the excavation and into the interior of the surrounding walls. Another basic principle is to try to improve the engineering strength of the earth material by means of some form of reinforcement, possibly changing it from an incompetent to withstand the imposed loads without failure.

Empirical assessment of rock enforcement requirement for the underground structures is empirically based on the rock mass classification and slope stability analysis. Once the excavation begins, the parameters used to determine the rock mass quality must be re-evaluated continuously. These parameters include:

- Number of joints per unit volume and their orientations.
- Joint conditions such as tightness, openings and in-fill materials.
- Joint water surface conditions such as roughness, degree of weathering and coatings.
- Presence and orientation of shear zones, clay seams or loose open joints crossing the tunnel excavation or the presence of squeezing of swelling rocks.
- The rock strength with ratio to the major principal rock stress expected at the tunnel periphery.

The best way to achieve flexible rock support is the use of rock bolts, steel fiber shotcrete, pre-injection grouting and the steel ribs. Generally, rock support in the tunnel is carried out in two main stages:

1. The **initial support** is installed immediately after the excavation of the tunnel to secure safe working conditions to the tunneling crew working at the tunnel face. In this stage, the type and methods of rock support should be decided in accordance to the quality of rock mass. More importantly, the initial support should be designed in such a way so that it can be converted as a part of the permanent rock support.

2. The **permanent support** is installed to meet long term stability requirements of the tunnel opening that guarantees satisfactory functioning of the opening during its life time operation. The extent of permanent rock support depends on the purpose and type of tunnels.

5.2.1 Rock support design based on RQD

Deere *et al.* (1970) presented support recommendations for the tunnels excavated conventionally based on RQD (Table 5.6). On the present study, an attempt is made to design the rock support based on RQD. Estimation of rock support based on RQD is presented on Table 5.7.

Table 5.6: Support recommended for tunnel in rock (6 m to 12 m diameter) based on RQD (after Deere et al., 1970)

Rock quality	**Alternative support systems**		
	Steel sets[3]	**Rockbolts[3]**	**Shotcrete**
Excellent[1] (RQD>90)	None to occasional light set	None to occasional	None to occasional local application 2 to 3 in.
Good (75<RQD<90)	Light sets on 5 to 6ft centre	Pattern, 5 to 6ft centre	Occasional local application 2 to 3 in.
Fair (50<RQD<75)	Light to medium sets on 4 to 5ft centre	Pattern, 3 to 5ft centre	4in. or more crown and sides
Poor[2] (25<RQD<50)	Medium to heavy circular sets on 2 to 4ft centre	Pattern, 2 to 4ft centre	6 in. or more on crown and sides, combine with bolts
Very poor[3] (RQD<25), Excluding squeezing or swelling ground)	Heavy circular sets on 2ft centre	Pattern, 3ft centre	6 in. or more on whole section, combine with medium sets
Very poor 3 (Squeezing or swelling)	Very heavy circular sets on 2ft centre	Pattern, 2 to 3ft centre	6 in. or more on whole section, combine with heavy sets

Notes:

- In good and excellent rock, the support requirement will be, in general, minimal but will be dependent upon joint geometry, tunnel diameter, and relative orientations of joints and tunnel.
- Lagging requirements will usually be zero in excellent rock and will range from up to 25 percent in good rock to 100 percent in very poor rock.

- Mesh requirements usually will be zero in excellent rock and will range from occasional mesh (or strips) in good rock to 100 percent.

Table 5.7: Estimation of rock support based on RQD

Structures		Rock type	RQD (%)	Rock Class	Support Estimated		
					Steel sets	Rock bolts	shotcrete
Desander basin / Approach / Diversion Tunnel Alignment Area		Quartzite >> Phyllite	62.2	Fair	Light to medium sets on 4 to 5ft centre	Pattern, 3 to 5ft centre	4in. or more crown and sides
Headrace Tunnel Alignment Area	Ch. 0+411.46m – 0+734.70 m	Quartzite >> Phyllite	62.2	Fair	Light to medium sets on 4 to 5ft centre	Pattern, 3 to 5ft centre	4in. or more crown and sides
	Ch. 0+734.70m – 2+179.50m	Quartzite >> Phyllite	55.6	Fair	Light to medium sets on 4 to 5ft centre	Pattern, 3 to 5ft centre	4in. or more crown and sides
	Ch. 2+179.50m – 2+614.65m	Quartzite >> Phyllite	42.4	Fair	Light to medium sets on 4 to 5ft centre	Pattern, 3 to 5ft centre	4in. or more crown and sides
	Ch. 2+614.65m – 3+212.93m	Quartzite << Phyllite	29.2	Poor	Medium to heavy circular sets on 2 to 4ft centre	Pattern, 2 to 4ft centre	6 in. or more on crown and sides, combine with bolts
	Ch. 3+212.93m – 3+580.87m	Quartzite >> Phyllite	58.9	Fair	Light to medium sets on 4 to 5ft centre	Pattern, 3 to 5ft centre	4in. or more crown and sides
Surge Tank / Powerhouse /Tailrace Tunnel Alignment Area		Quartzite >> Phyllite	58.9	Fair	Light to medium sets on 4 to 5ft centre	Pattern, 3 to 5ft centre	4in. or more crown and sides

5.2.2 Rock support design based on RMR

Bieniawski (1989) has proposed a guide for the choice of support for underground excavation based on RMR (Table 5.8). These guide lines depend on factors as the depth below surfaces, in-situ stress, tunnel size and shape and the method of excavation. The support estimated for the underground structures based on RMR is given in Table 5.9.

Table 5.8: Geomechanics classification for excavation and support in rock tunnel in accordance with the RMR system (after Bieniawski, 1989)

Rock Mass	**Rock Class**	**Rock Support Class**	**Assigned Rock Support Measures**
Very Good to Excellent	Class I	RS I	Generally no support required except for occasional spot bolting
Good	Class II	RS II	Fully grouted 25 mm diameter and 2 m long rock bolts spaced at 4.5 m circumferentially and 4.5 m longitudinally plus 100 mm thick shotcrete with single layer of wire mesh reinforcement (4 mm diameter welded in mesh size 100 mm x 100 mm) or steel fibercrete.
Fair	Class III	RS III	25 mm diameter 2 m long systematic grouted rock bolts at a spacing of 1.5 m x 1.5 m and 10cm thick steel fiber shotcrete in all tunnels and 25 mm diameter 4 m long systematic grouted rock bolts at a spacing of 1.5 m x 1.5 m 15 cm thick steel fiber shotcrete at the settling basin cavern.
Poor	Class IV	RS IV	25 mm diameter 3 m long systematic grouted rock bolts at a spacing of 1.3 m x 1.5 m and 20 cm thick steel fiber shotcrete. Advance pre-injection grouting to control water inflow into the tunnel.
Very Poor	Class V	RS V	25 mm diameter 3 m long systematic grouted rock bolts at a spacing of 1.3 m x 1.3 m and 20 cm thick steel fiber shotcrete.
Extremely Poor	Class VI	RS VI	25mm diameter 2 m long systematic grouted rock bolts at a spacing of 1.2 m x 1.2 m and 20 cm thick steel fiber shotcrete. Steel ribs at a spacing of 1 meter to control plastic deformation. Advance pre-injection grouting is provisioned to control water inflow into the tunnel.
Exceptionally Poor	Class VII	RS VII	25 mm diameter 3 m long systematic grouted rock bolts at a spacing of 1.1 m x 1.1 m and 20 cm thick steel fiber shotcrete. Steel ribs at a spacing of 1 meter to control plastic deformation.

Table 5.9 Estimation of rock support based on RMR

Structures		RMR	Rock Class	Rock Support Class	Assigned Rock Support Measures
Approach / Diversion Tunnel Alignment Area		62	Class III	RS III	25 mm diameter 2 m long systematic grouted rock bolts at a spacing of 1.5 m x 1.5 m and 10cm thick steel fiber shotcrete
Portal Inlet and Desander Basin Area		64	Class III	RS III	25 mm diameter 2 m long systematic grouted rock bolts at a spacing of 1.5 m x 1.5 m and 10cm thick steel fiber shotcrete in tunnel and 25 mm diameter 4 m long systematic grouted rock bolts at a spacing of 1.5 m x 1.5 m 15 cm thick steel fiber shotcrete at the settling basin cavern.
Headrace Tunnel Alignment Area	Portal Inlet to Syo Khola	62	Class III	RS III	25 mm diameter 2 m long systematic grouted rock bolts at a spacing of 1.5 m x 1.5 m and 10cm thick steel fiber shotcrete
	Syo Khola to Gre Khola	59	Class III	RS III	25 mm diameter 2 m long systematic grouted rock bolts at a spacing of 1.5 m x 1.5 m and 10cm thick steel fiber shotcrete
	Gre Khola to Tasangi Khola	62	Class III	RS III	25 mm diameter 2 m long systematic grouted rock bolts at a spacing of 1.5 m x 1.5 m and 10cm thick steel fiber shotcrete
	Tasangi Khola to Khahare Khola	46	Class IV	RS IV	25 mm diameter 3 m long systematic grouted rock bolts at a spacing of 1.3 m x 1.5 m and 20 cm thick steel fiber shotcrete. Advance pre-injection grouting to control water inflow into the tunnel.
	Khahare Khola to Surge Tank Area	61	Class III	RS III	25 mm diameter 2 m long systematic grouted rock bolts at a spacing of 1.5 m x 1.5 m and 10cm thick steel fiber shotcrete
Surge Tank / Powerhouse/Tailrace Tunnel Alignment Area		57	Class III	RS III	25 mm diameter 2 m long systematic grouted rock bolts at a spacing of 1.5 m x 1.5 m and 10cm thick steel fiber shotcrete

5.2.3 Rock support design based on Rock Quality Index (Q)

In order to relate Tunneling Quality Index (Q) to the behavior and support requirements of an underground excavation, Barton et al. (1974), defined an additional parameter, which is denoted by equivalent dimension (D_e) of the excavation. This dimension is obtained by dividing the span, diameter or wall height of the excavation by a parameter called the excavation support ratio (ESR).

Hence:

$$D_e = \frac{\text{Excavation span, diameter or height (m)}}{\text{Excavation Support Ratio}}$$

The excavation support ratio is related to the use for which the excavation is intended and extent to which some degree of instability is acceptable. ESR value for different types of tunnels after Barton et al. (1974) is given in Table 5.10.

Table 5.10: Excavation category and ESR (after Barton et al., 1974)

Class	Excavation category	ESR
A	Temporary mine opening	3-5
B	Permanent mine opening, water tunnels for hydropower (excluding high pressure penstock) pilot tunnels, drafts and headings for large excavation.	1.6
C	Storage rooms, water treatment plants, minor road and railway tunnels, surge chambers, access tunnels.	1.3
D	Power stations, major road and railway tunnels, civil defence chambers, portals, intersection.	1.0
E	Underground nuclear power stations, railway stations, sports and publics facilities, factories	0.8

The equivalent dimension (D_e) is plotted against the value of Q to define a number of support categories in a chart. This chart has been updated by Grimstad and Barton (1993) and has been reproduced as Fig. 5.4.

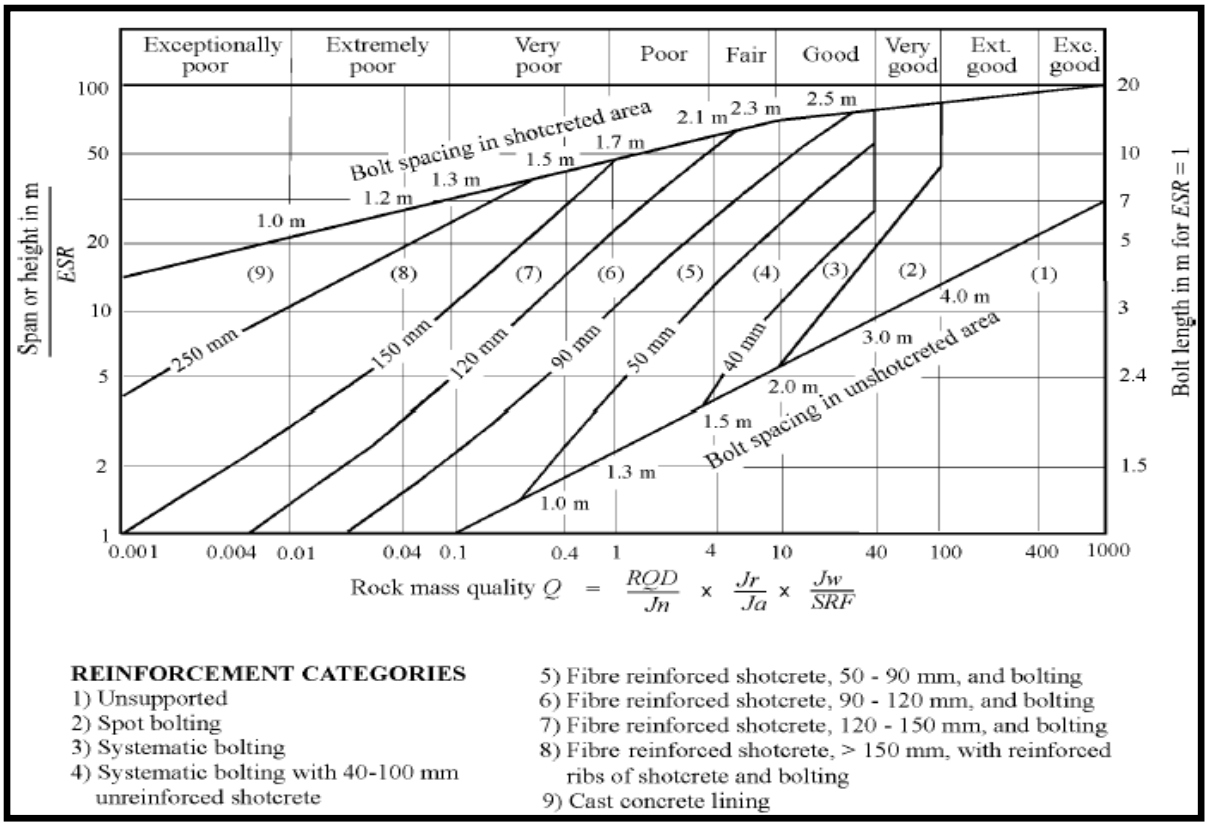

Fig. 5.4 Estimated support categories based on the tunneling quality index (Q)

The head race tunnel falls into a category water tunnel for hydropower and assigned ESR of 1.6 from Table 5.10. Hence, for an excavation span (B) of 7 m of approach tunnel, diversion tunnel and headrace tunnel, equivalent dimension (D_e) is calculated as 4.375. Similarly, D_e for desander basin, powerhouse and tailrace tunnel alignment is calculated as 6.437, 28 and 2.815 respectively. Estimation of rock support based on Q is presented on Table 5.11. Beside these support requirements, design values of excavation width, excavation support ratio and Q can be used to determine rock bolt length and maximum unsupported span for excavation using empirical relations.

Length of rock bolt (L) can be estimated from excavation width (B) and excavation support ratio (ESR) by the relation given below:

$$L = \frac{\qquad}{\qquad}$$

For desander basin, B = 10.3 m; minimum length of the rock bolt required, L = 2.216 m

For diversion tunnel, approach tunnel and headrace tunnel, B = 7 m; minimum length of the rock bolt required, L = 1.906 m

For powerhouse, B = 44.8 m; minimum length of the rock bolt required, L = 5.45 m.

For tailrace tunnel, B = 4.5 m; minimum length of the rock bolt required, L = 1.672 m.

Maximum unsupported span for excavation can be estimated from Q and excavation support ratio (ESR) by the relation given below:

Maximum unsupported span = 2 ESR $Q^{0.4}$

Estimation of maximum unsupported span for the underground structures is given in Table 5.11.

Table 5.11: Estimation of rock support based on Q

Structures		Rock Mass	Q	Maximum Unsupported Span	Support Categories	Supported Estimated	
						Rock Bolts	Shotcrete
Approach Tunnel Alignment		Fair	4.86	6.023	3	Systematic bolting	-
Desander Basin		Fair	4.86	6.023	4	Systematic bolting	40-100 mm unreinforced shotcrete
Diversion Tunnel Alignment		Fair	4.86	6.023	3	Systematic bolting	-
Headrace Tunnel Alignment	Portal Inlet to Syo Khola	Fair	4.86	6.023	3	Systematic bolting	-
	Syo Khola to Gre Khola	Fair	3.86	5.493	4	Systematic bolting	40-100 mm unreinforced shotcrete
	Gre Khola to Tasangi Khola	Fair	3.85	5.487	4	Systematic bolting	40-100 mm unreinforced shotcrete
	Tasangi Khola to Khahare Khola	Poor	1.68	3.938	4	Systematic bolting	40-100 mm unreinforced shotcrete
	Khahare Khola to Surge Tank Area	Fair	8.66	7.588	1	Unsupported	
Powerhouse		Fair	8.66	7.588	5	Bolting	50-90 mm fibre reinforced shotcrete
Tailrace Tunnel Alignment		Fair	8.66	7.588	1	Unsupported	

CHAPTER 6

SUB-SURFACE INVESTIGATION

The purpose of characterizing subsurface conditions is to determine if the soils beneath a facility exhibit properties that ensure the facility will remain stable under static and seismic conditions during construction and operation and after it is closed. In sub-surface investigation, geo-physical investigations enable precise identification of rock anomalies like fractures and faults, the Modulii of Elasticity in Shear and Compression etc., overburden thickness, rippability (excavability) of rock and almost any physical property of the sub-surface strata. These techniques optimize the scope of site investigations and eliminate the unexpected by virtue of continuous information provided, rather than discrete information obtained by conventional boreholes.

In present study, sub-surface investigation is conducted with the help of 2D – Electrical Resistivity.

6.1 2D – Electrical Resistivity Tomogram (ERT)

Electrical Resistivity Tomography is an earth resistance technique conducted along a series of single lines or profiles, rather than area surveys. It is of two types: 2D - ERT and 3D - ERT. A small electrical current is applied to series of probes laid out across a site, producing the cross-section of data indicating a broad stratigraphy of deeper features. The electrical resistivity tomography can then be combined with topographical data to provide an accurate representation of underlying soils.

2D-ERT is a two dimensional data acquisition method that maps vertical as well as lateral changes in Electrical Resistivity. It can be done using following arrays.

- Schlumberger Electrode Array
- Wenner Electrode Array
- Dipole-Dipole Array
- Two electrodes, Three electrodes etc.

In the present study, 14 lines of 2D Resistivity survey have been done using Dipole-Dipole Array. Out of them, nine profile lines are conducted at the headworks site, two profile lines at the powerhouse site and three profile lines across the three Kholsies at

the right bank of Bhote Koshi River between intake and powerhouse. It covers about 4 km in the project area.

6.1.1 Principle of Resistivity Survey

The resistivity survey is carried out by injecting DC current into the ground through two current electrodes and measuring the resulting voltage difference at two potential electrodes. For, the current value (I) and the observed voltage difference value (V), an apparent value (ρ_a) is calculated as,

$\rho_a = k\ V/I$

Where, k = Geometrical factor which depends on the arrangement of the four electrodes

The calculated value ρ_a is not the true resistivity of the subsurface materials. An apparent resistivity value of a homogeneous ground will give the same resistance value for the same electrode arrangement. The relationship between the apparent resistivity and the true resistivity is a complex relationship. In fact, an inversion of the measured apparent resistivity values using a computer program is necessary to determine the true subsurface resistivity.

The resistivity value of some common rocks and important geological materials is given in Table 6.1.

Table 6.1 Resistivity value of some common rocks and important geological materials

Rocks and Soil Materials	**Resistivity (Ωm)**
Gneiss (various)	6.8×10^4 (wet) – 3×10^6 (dry)
Quartzite (various)	$10 – 2 \times 10^8$
Normal quartzite	>1,000
Schist	$20 - 10^4$
Graphitic schist and Black phyllite	10 - 300
Unconsolidated wet clay	20
clays	1 - 100

Rocks and Soil Materials	Resistivity (Ωm)
Conglomerate	2×10^3 - 10^4
Sands	10 – 800
alluvium	10 – 800
Groundwater bearing Formation	10 – 200

Considering the phyllite, schist, quartzite etc. as the bedrock, and the alluvial/colluvial materials/big boulders as the overburden materials, the likely resistivity value range of the different geological materials is assumed as shown in the Table 6.2 in order to interpret the 2D Inverse Model Resistivity Sections obtained from the project area in terms of the lithology or the geological materials.

Table 6.2 adopted criteria for Resistivity – Lithology Conversion

True Resistivity range (Ωm)	Probable Rock Type / Geological Materials
< 200	Clay/ sandy clay/ wet sand/ Materials with some metallic minerals/ black phyllite and schist with graphite, ground water bearing formations, etc.
200 – 800	Highly weathered and saturated rocks or graphite bearing rocks/ wet overburden materials
500 – 1,000	Weathered to Semi weathered and partially saturated bedrock / coarse sand and pebbles/ Fracture and fault zones
800 – 2,000	Semi-weathered to Moderately fresh bedrock or sometime the higher resistivity materials at the surface are the dislodged rocks transported from the upper part of the cliff
2,000 – 4,000	Moderately fresh normal bedrock/sometime dry overburden
>4,000	Fresh and hard normal bedrocks

6.1.2 The Dipole-Dipole Array

The Dipole-Dipole array, sometimes called the double dipole, has the two current electrodes (A and B) and the two potential electrodes (M and N) aligned and exterior to

each other. The Dipole-Dipole (Fig. 6.1) is defined by the following lengths: a = AB, a = MN and L = PQ, P and Q being the centers of AB and MN respectively.

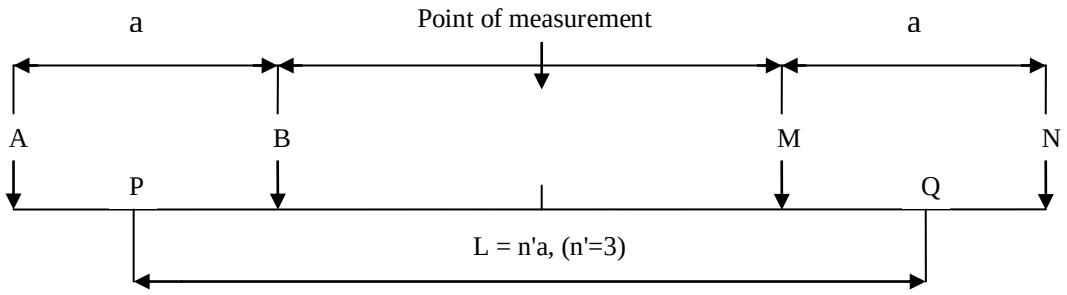

Fig. 6.1 Dipole-Dipole Array

In practice, geophysicists always use a symmetrical Dipole-Dipole, where BM = PQ – a = L – a = na, where n is a whole number equal to or greater than 1. Fig. 6.1 shows the location of electrodes for n = 2. Some authors define Dipole-dipole by PQ = L = n'a, n' = n+1.

Since the array is symmetrical, one considers the point of measurement as being the center of segment PQ (mid-point of BM) which is the center of symmetry of the configuration. The depth of investigation increase with the spacing, L = a (n+1) = n'a; i.e. with n of n' when the length a = AB = MN is fixed.

Table 6.3 Details of profile lines of 2D Electrical Resistivity Tomogram

Line No.		**Location**	**Direction**	**First Electrode at Station No.**	**Last Electrode at Station No.**	**Surface Coverage (m)**
L 1	L 1.1	Reservoir area	NE-SW	0	9	135
	L 1.2	Reservoir area	NE-SW	0	35	525
	L 1.3	Reservoir area	NE-SW	0	32	480
L 1s		Reservoir area	SE-NW	0	10	150
L 2s		Reservoir area	SE-NW	0	11	165
L 3s		Reservoir area	SE-NW	0	9	135
L 2	L 2.1	Access Road	NE-SW	0	20	300
	L 2.2	Access Road	NE-SW	0	20	300
L 4s		Middle Dam site	SE-NW	0	13	195

Contd…

Line No.	Location	Direction	First Electrode at Station No.	Last Electrode at Station No.	Surface Coverage (m)
L 5s	Middle Dam site	SE-NW	0	13	195
L 6s	Lower Dam site	SE-NW	0	14	210
L 3.0	Lower Dam site	NE-SW	0	20	300
L 9	Powerhouse	W-E	0	8	120
L 10	Powerhouse	NW-SE	0	9	135
L 11	Khahare Kholsi	NE-SW	0	16	240
L 12	Tasangi kholsi	NE-SW	0	15	225
L 13	Gre Kholsi	NE-SW	0	15	225
Total coverage (m)					4035

6.2 Headworks Area

Among nine profile lines, three lines are conducted parallel to the Bhote Koshi River namely profile L-1, L-2 and L-3.

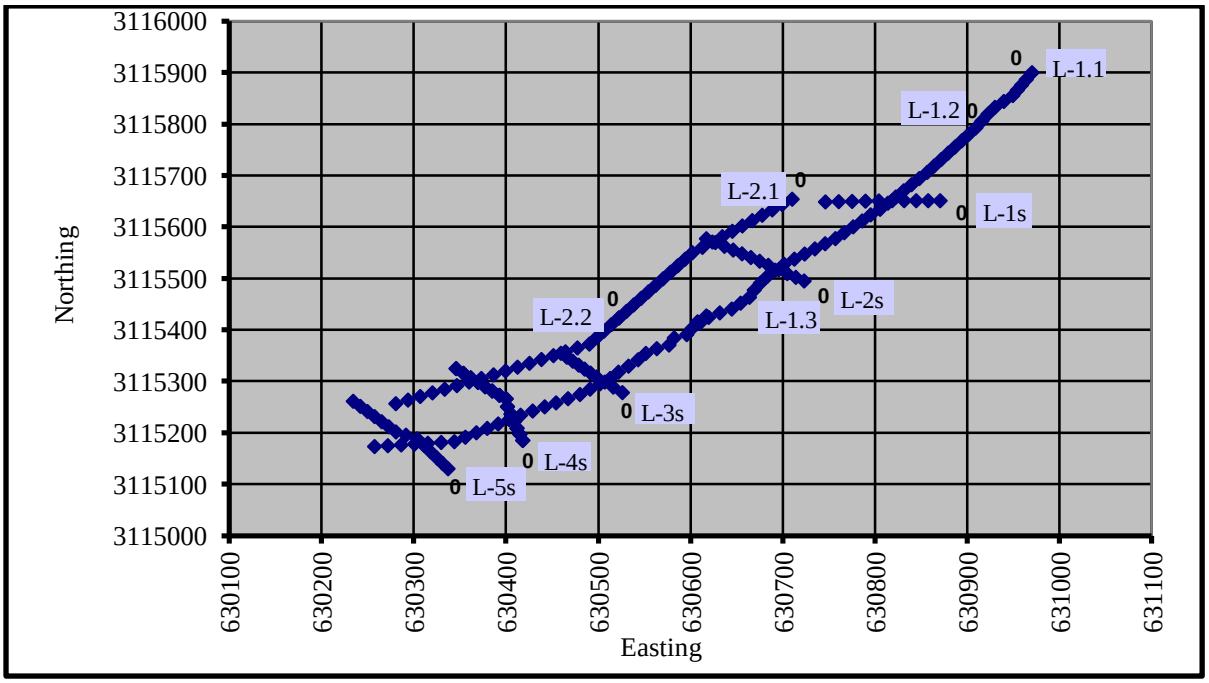

Fig. 6.2(a) Location chart for profile lines of headworks site (Reservoir and Middle Dam site)

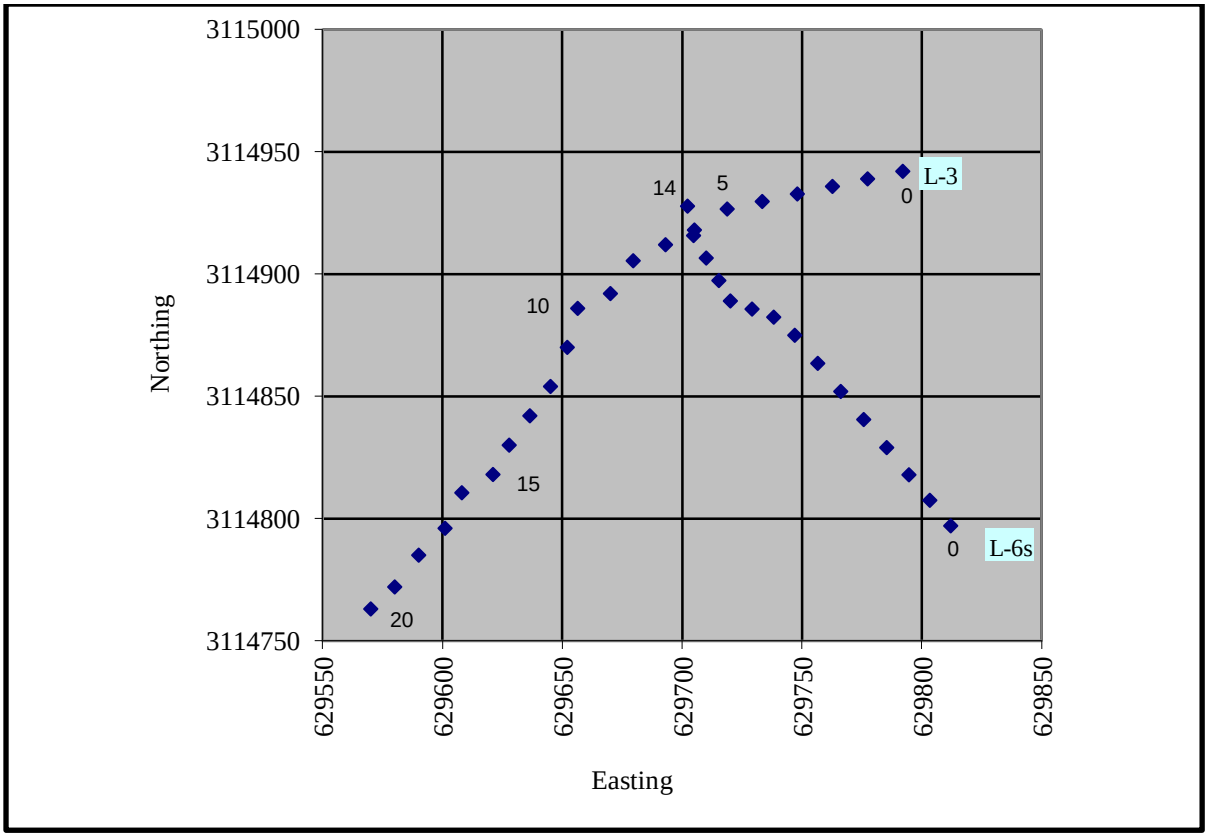

Fig. 6.2(b) Location chart for profile lines of headworks site (Lower Dam site)

Profile L-1 is divided into three parts namely profile L-1.1, L-1.2 and L-1.3. Similarly, profile L-2 is also divided into L-2.1 and L-2.2. The remaining six profile lines are conducted along the hill slope starting from the uphill to the end at the left bank of the Bhote Koshi River. They are named as Profile L-1s to L-6s. The location of these lines is given in Fig. 6.2(a) and Fig. 6.2(b).

6.2.1 Reservoir Area

The 2D resistivity survey was performed along the four profile lines. They are profile L-1, L-1s, L-2s and L-3s.

6.2.1.1 Profile Line L-1.1

This line (Fig. 6.3) starts from a point on the road 100 m SW from the Bhote Koshi Bridge at Syaphrubesi. It is about 135 m long.

The 2D resistivity survey indicates a very thick layer of overburden is present at the top layer of the area. The overburden seems to be cliff debris or old alluvial deposits. Its

thickness varies from few meters to more than 40 m from the ground surface. Below overburden, fresh rocks are expected to be present.

6.2.1.2 Profile Line L-1.2

This line (Fig. 6.4) starts from the end point of the profile L-1.1. It covers 525 m of the total length of L-1.

The 2D resistivity survey reveals the presence of very thick overburden having resistivity value ranging from 100 Ωm to more than 3,000 Ωm. It indicates the overburden comprising fine sand to very big boulders of old alluvial deposits and dry cliff debris. The thickness varies from few meters (chainage point 180 m) to more than 30 m (chainage point 360 m) from the ground surface.

The very low resistivity values observed below the chainage point 250 m, in-between the chainage points 320 m and 400 m and 435 m and 455 m may be generated by the presence of sand and clay. Below this thick overburden, fresh to highly weathered bedrocks are expected. Around the chainage point 150 m, formation of vertical zone of low resistivity value in-between the moderately fresh bedrocks may be due to some vertical crack zone. The normal bedrocks are expected to be present at about 25 m depth from the surface in the middle part of profile.

6.2.1.3 Profile Line L-1.3

This line (Fig. 6.5) starts form the end point of the profile L-1.2. It is about 480 m long. It crosses the road between the chainage points 0 m and 15 m and runs below the road in the direction to Dhunche.

The 2D resistivity survey shows the presence of bedrocks between chainage points 120 m and 270 m at the depth of 20 m to 45 m from the surface. The rocks are expected to be slightly weathered to fresh. A vertical zone of low resistivity value ranging from 250Ωm to 850Ωm is observed around the chainage point 300 m. It reveals to be crack zone.

A thick layer of overburdens are expected all along the profile line. Some places exhibit more than 30 m thick layer of overburden.

6.2.1.4 Profile Line L-1s

This profile line (Fig. 6.6) starts from a point, 60 m uphill slope from the road to Syaphrubesi that runs along NW direction to the left end of the river.

The resistivity survey indicates the presence of sound rocks from the beginning of the profile line to the chainage point 30 m. Between chainage points 30 m to 70 m, high resistivity value (> 1000Ωm) are observed. The resistivity value is high enough to interpret the formations as bedrocks, however being the nature of the resistivity value distribution irregular and unsymmetrical the formations are possible to be dry old alluvial deposits.

At the middle of the section, between chainage points 70 m and 100 m, a low resistivity zone is observed. The area is just below the road. Hence, the area may be composed of some road disposals. The bedrocks are supposed to be present at the depth of about 40 m.

At the end part of the profile line, irregular high resistivity values indicate the dislodged rocks transported from higher altitudes.

6.2.1.5 Profile Line L-2s

This profile line (Fig. 6.7) starts from a point near the cliff and follows the hill slope to reach the left bank of the Bhote Koshi River. It crosses the road between the chainage points 45 m and 60 m.

The resistivity survey shows the possibility of very thick overburden in this section. The thickness of overburden varies up to 45 m. The irregularly distributed resistivity values are present along the whole section. It may be due to the rocks dislodged from the higher cliffs. Between chainage points 85 m to 120 m, moderately fresh rocks can be expected.

6.2.1.6 Profile Line L-3s

The profile line (Fig. 6.8) starts from a point in the road and ends at the left bank of the Bhote Koshi River. It crosses the line L-1.3 at the chainage point 30 m.

The resistivity survey shows the presence of moderately fresh to fresh bedrocks along the whole section except the end part of the profile. In the beginning, the rocks are present in the depth of about 15 m but the depth goes on increasing as the line move towards the river. On the top of bedrocks, thick layers of overburden comprising boulders, cobbles, pebbles etc are expected.

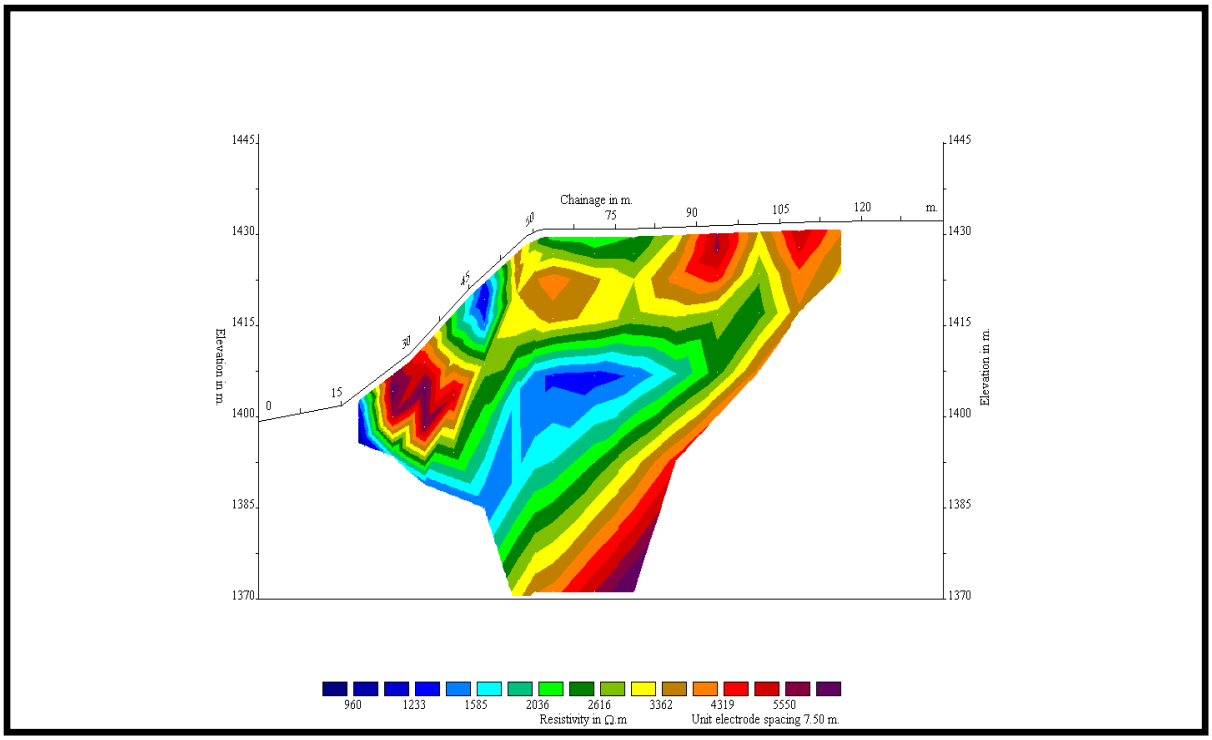

Fig. 6.3 Resistivity survey along profile line L-1.1

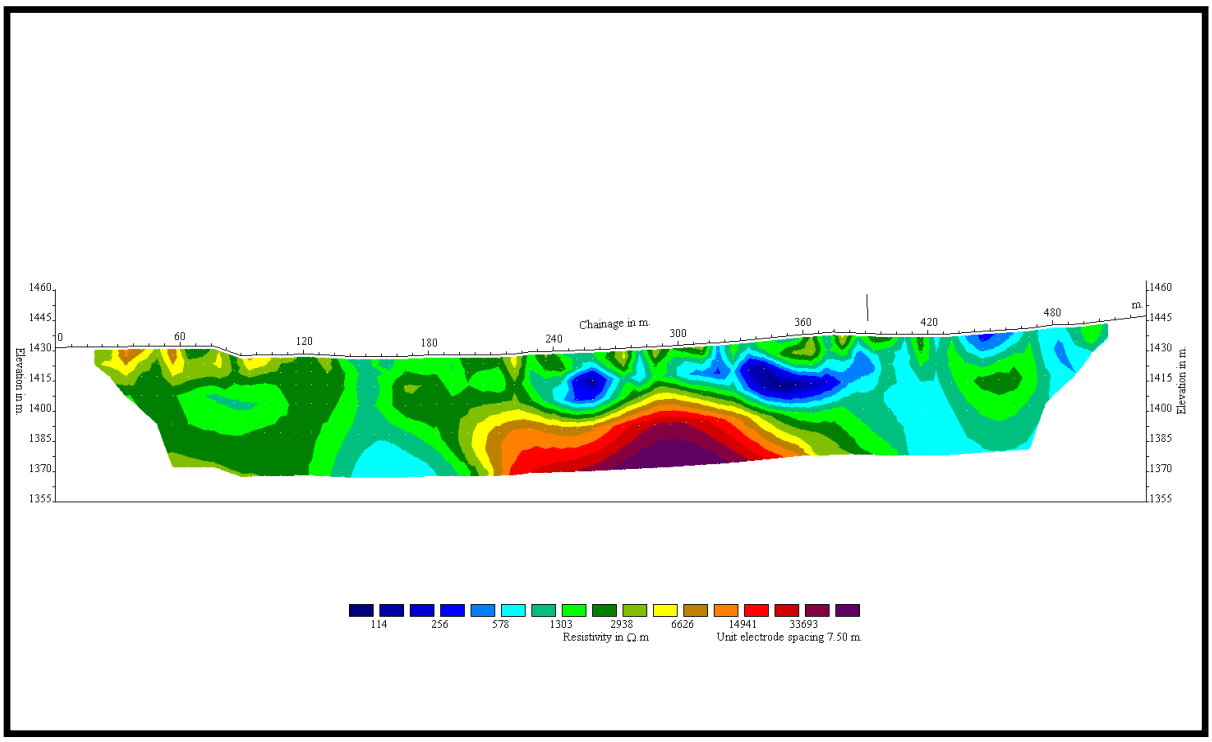

Fig. 6.4 Resistivity survey along profile line L-1.2

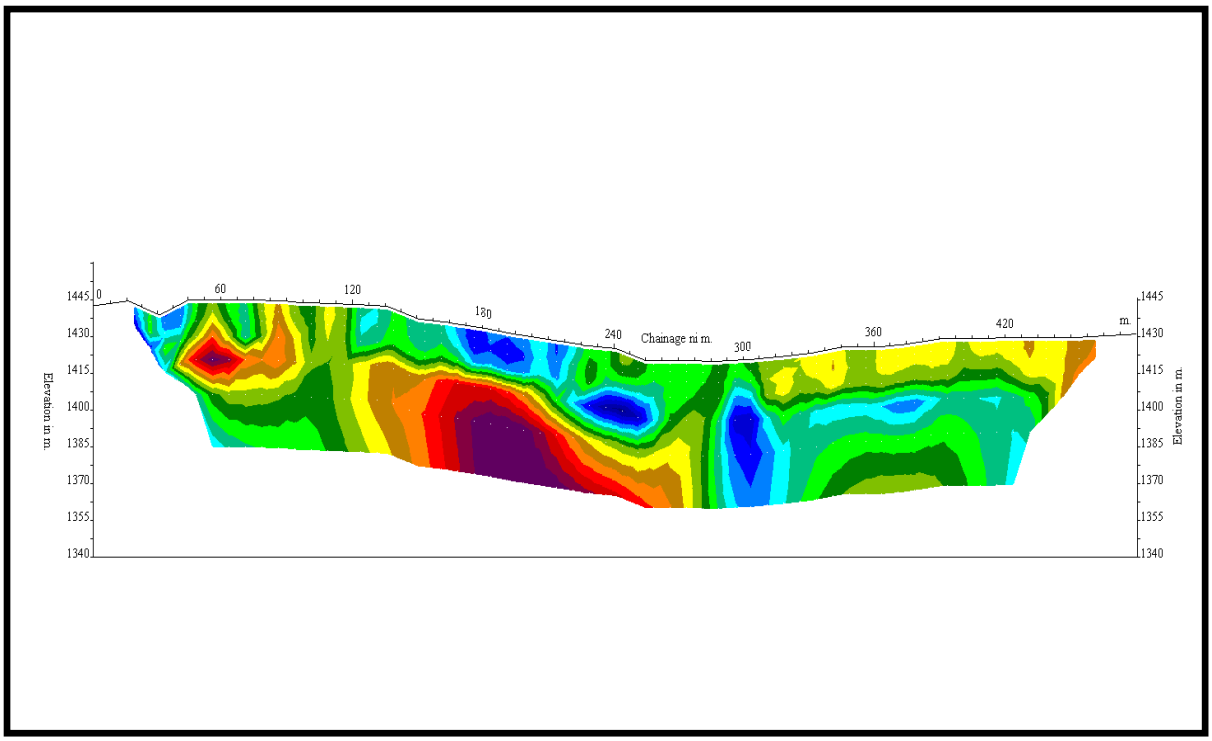

Fig. 6.5 Resistivity survey along profile line L-1.3

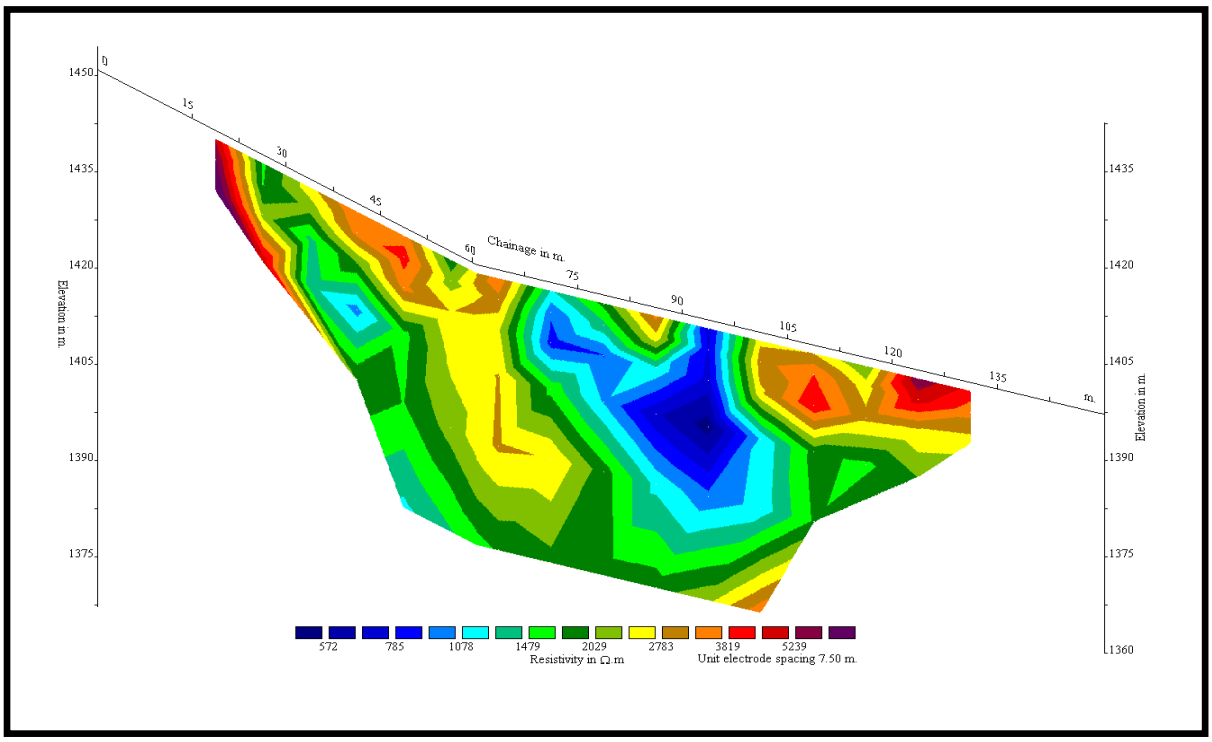

Fig. 6.6 Resistivity survey along profile line L-1s

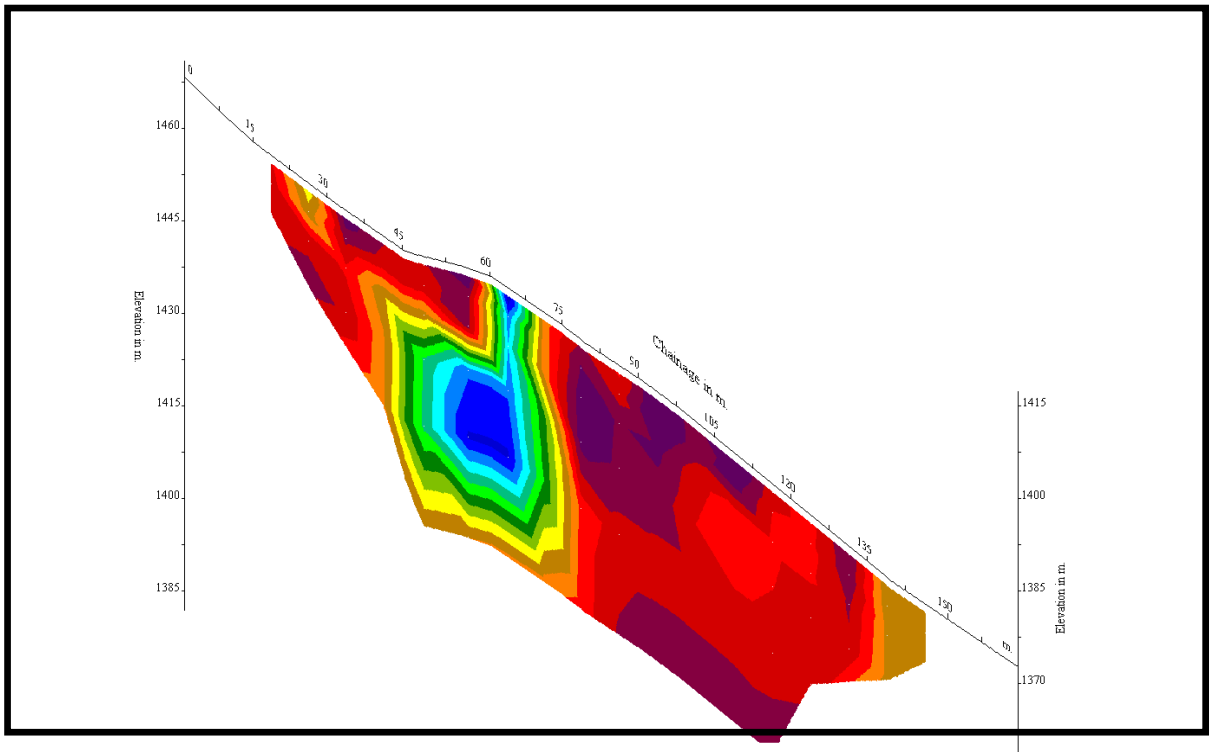

Fig. 6.7 Resistivity survey along profile line L-2s

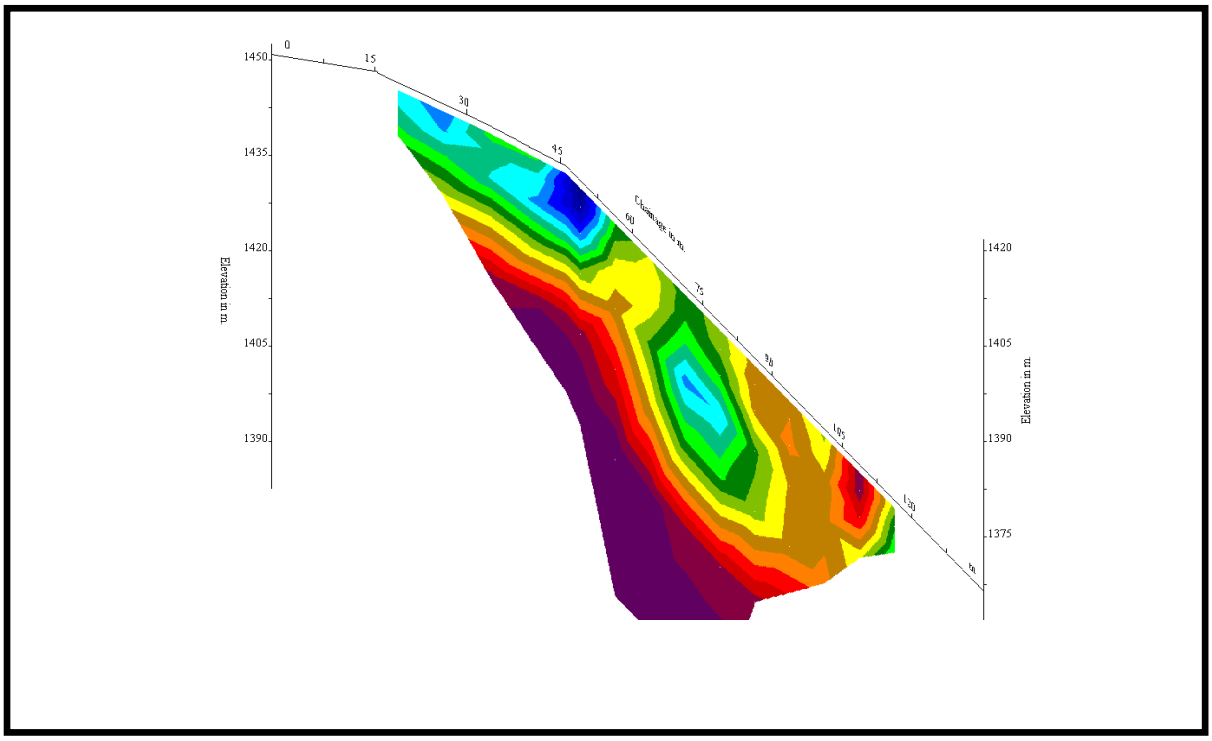

Fig. 6.8 Resistivity survey along profile line L-3s

6.2.2 Middle Dam Site

The 2D resistivity survey is accomplished by two profile lines. They are profile no.L-4s and L-5s.

6.2.2.1 Profile Line L-4s

The line (Fig. 6.9) starts from a point on the road and ends at the left bank of the Bhote Koshi River. It crosses the line L-1.3 at chainage point 295m.

The resistivity survey indicates 80% of the profile has high resistivity value (>1000Ωm) which is enough to interpret the formation as bedrocks. But, the irregular and unsymmetrical resistivity pattern reveals the formation as detached bedrocks or coarse sands. At 30 m depth below the chainage point 45 m, the geological formations comprise very low resistivity values (100 to 500 Ωm). Such low resistivity values may be generated by highly fractured and saturated rocks or groundwater bearing formations. Sound bedrocks are expected to present at the depth of about 30 m between chainage points 75 m and 145 m.

6.2.2.2 Profile Line L-5s

The line (Fig. 6.10) starts from a point on the road and ends at the left bank of the Bhote Koshi River. It is nearly parallel to line L-4s.

The resistivity survey indicates 80% of the profile has high resistivity value (>1000Ωm) which is enough to interpret the formation as bedrocks. But, the irregular and unsymmetrical resistivity pattern reveals the formation as detached bedrocks or coarse sands. At the end of the profile, low resistivity value formations are observed between chainage points 135 m and 180 m. These materials are possible to be either highly fractured and saturated rocks or old alluvial deposits comprising sand, pebbles etc.

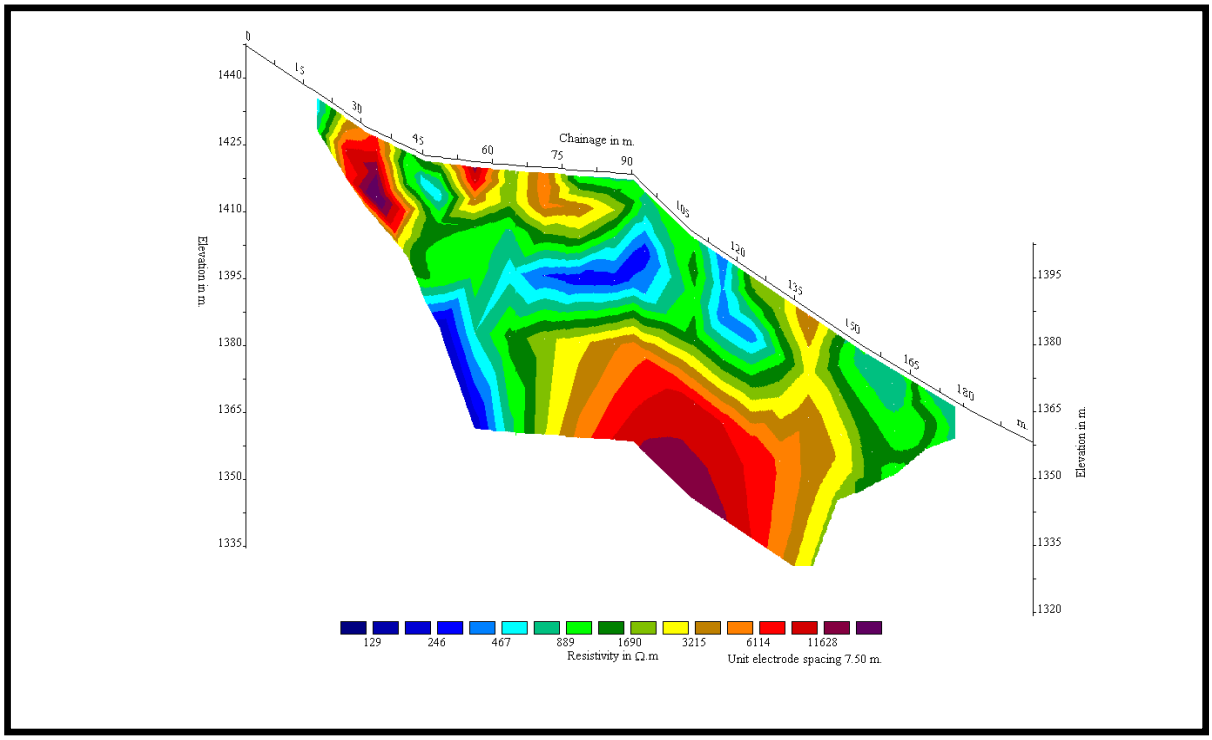

Fig. 6.9 Resistivity survey along profile line L-4s

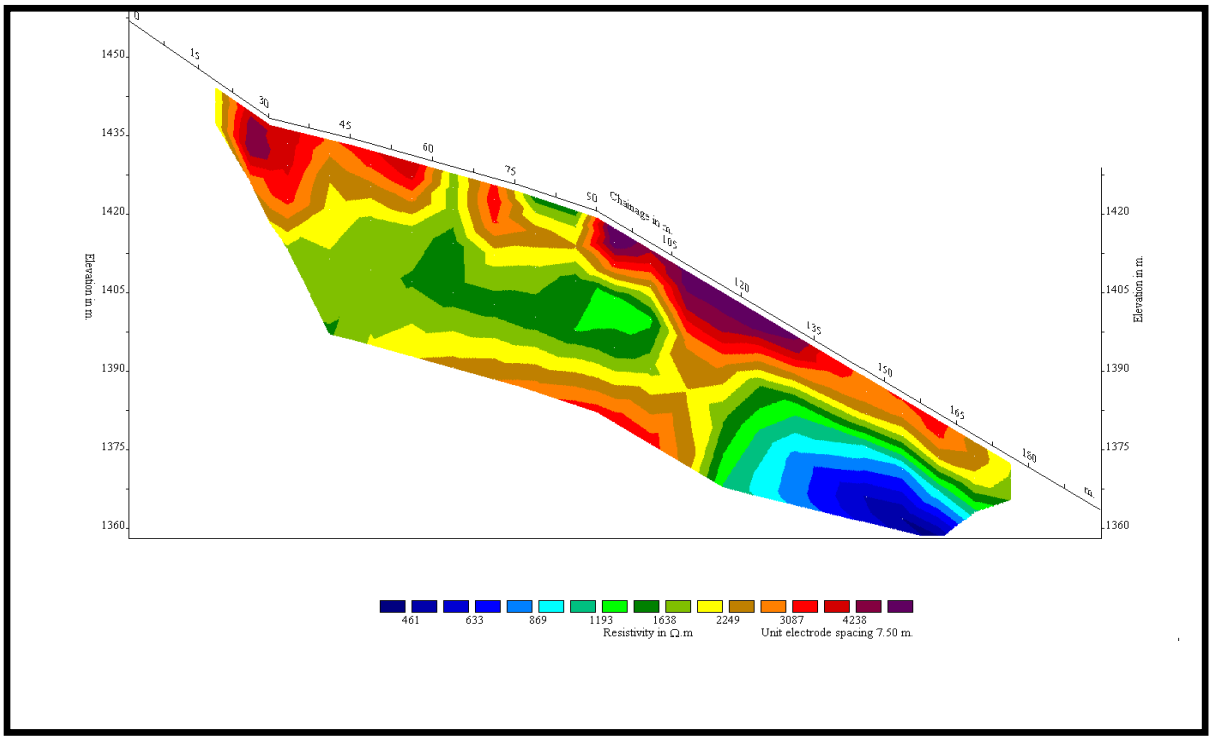

Fig. 6.10 Resistivity survey along profile line L-5s

6.2.3 Lower Dam Site

The 2D resistivity survey is accomplished by two profile lines. They are profile no.L-3 and L-6s.

6.2.3.1 Profile Line L-3

The line (Fig. 6.11) lies on the left bank of Bhote Koshi River where the lower dam site is proposed. It crosses profile line L-6s at the chainage point 195 m.

The resistivity survey reveals irregular distribution of resistivity value ranging from 20Ωm to more than 6000Ωm. This phenomenon indicates either a thrust zone is passing nearby this line or the presence of very thick old alluvial deposits along this line. Very low resistivity values are present in two places. The first one lies between chainage points 40 m and 85 m at about 20 m depth while the second one lies between chainage points 150 m and 240 m in bowl shape. The low resistivity formations are supposed to be either highly crushed or fractured and saturated rock mass or wet sandy clay with pebbles. Similarly, high resistivity values representing sound bedrocks are observed in two places. They are present at the depth ranging from 25 m to 30 m.

Between chainage points 45 m and 120 m and 170 m and 195 m, thick layer of dislodged rock mass are observed.

6.2.3.2 Profile Line L-6s

The line (Fig. 6.12) starts from a point in the hill slope and ends in the left bank of the Bhote Koshi River.

The resistivity survey indicates the presence of normal bedrocks between the chainage points 60 m to 150 m. The bedrocks are found at the depth of about 20 m at chainage point 75 m while at the depth of about 35 m at the steep slopes. The bedrocks are supposed to be covered by thick layer of overburden comprising alluvial deposits and dislodged rock mass.

Between chainage points 15 m to 60 m, thick vertical zone of low resistivity value is present. The low resistivity value formation may be formed due to some crack zone.

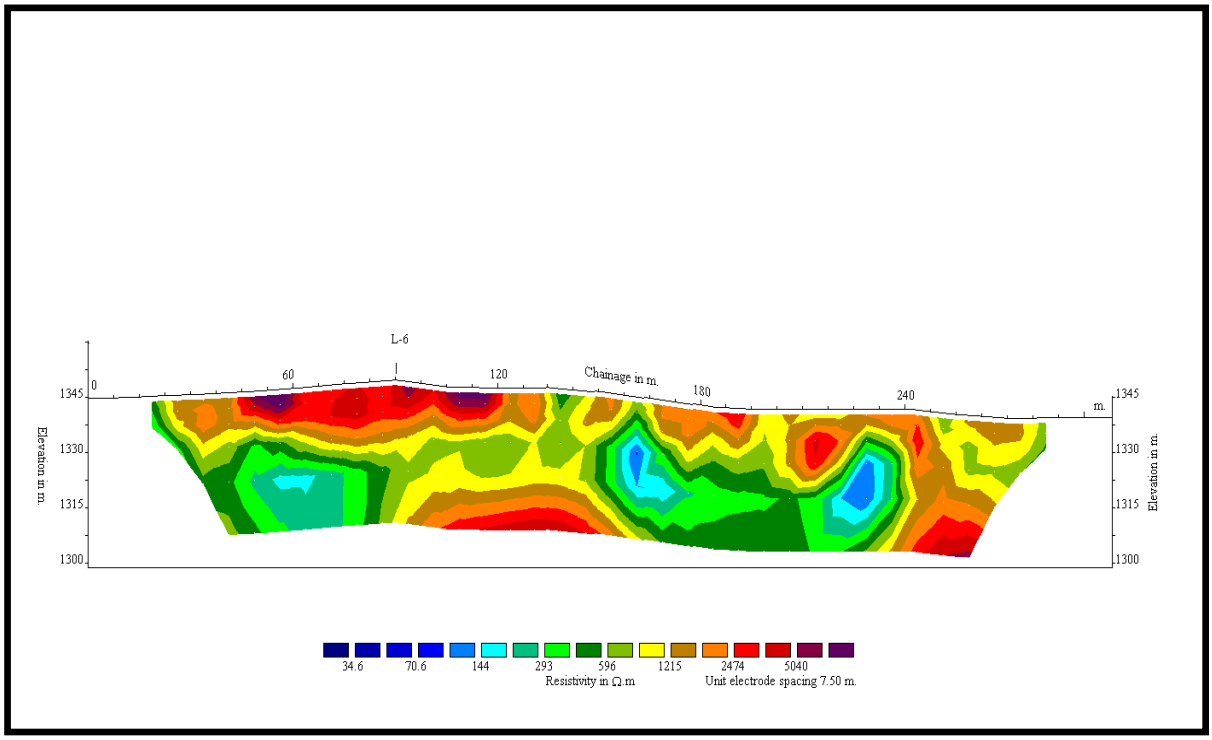

Fig. 6.11 Resistivity survey along profile line L-3

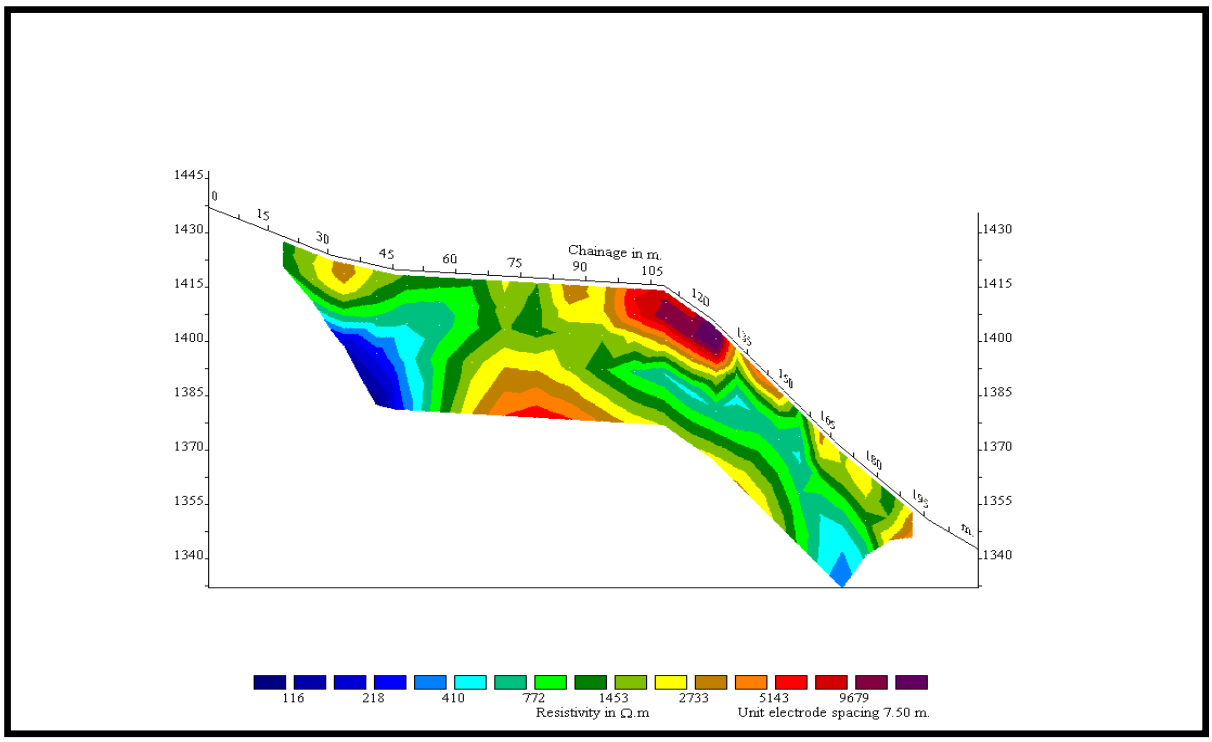

Fig. 6.12 Resistivity survey along profile line L-6s

6.2.4 Access Road Site

The 2D resistivity survey is accomplished by the profile line L-2. The length of this line is 600 m. It is divided into two parts i.e. L-2.1 and L-2.2 each having 300 m length. The line L-2.1 lies at reservoir area while line L-2.2 lies at the middle dam site area.

6.2.4.1 Profile Line L-2.1

The line (Fig. 6.13) lies on the left bank of the Bhote Koshi River. It is about 300 m long.

The resistivity survey indicates the presence of very thick layer of overburden whose thickness varies up to 45 m. Most of the overburden seems to be river sediments or cliff debris containing big boulders. The low resistivity values observed in the survey may be due to the presence of wet sand or some water bearing formations. In the chainage point 175 m, bedrocks are expected at the depth of 10 m.

6.2.4.2 Profile Line L-2.2

The line (Fig. 6.14) lies on the left bank of the Bhote Koshi River. It is about 300 m long. It starts from the last point of line L-2.1.

The resistivity survey indicates the presence of very thick overburden along the whole section. The thickness of overburden varies up to the depth of 60 m. Most of the overburden seems to be river sediments or cliff debris containing big boulders. No bedrocks are expected in this line up to the depth of investigation. The low resistivity value observed between the chainage points 90 m and 150 m and 215 m and 247 m may be due to the presence of saturated fine sand.

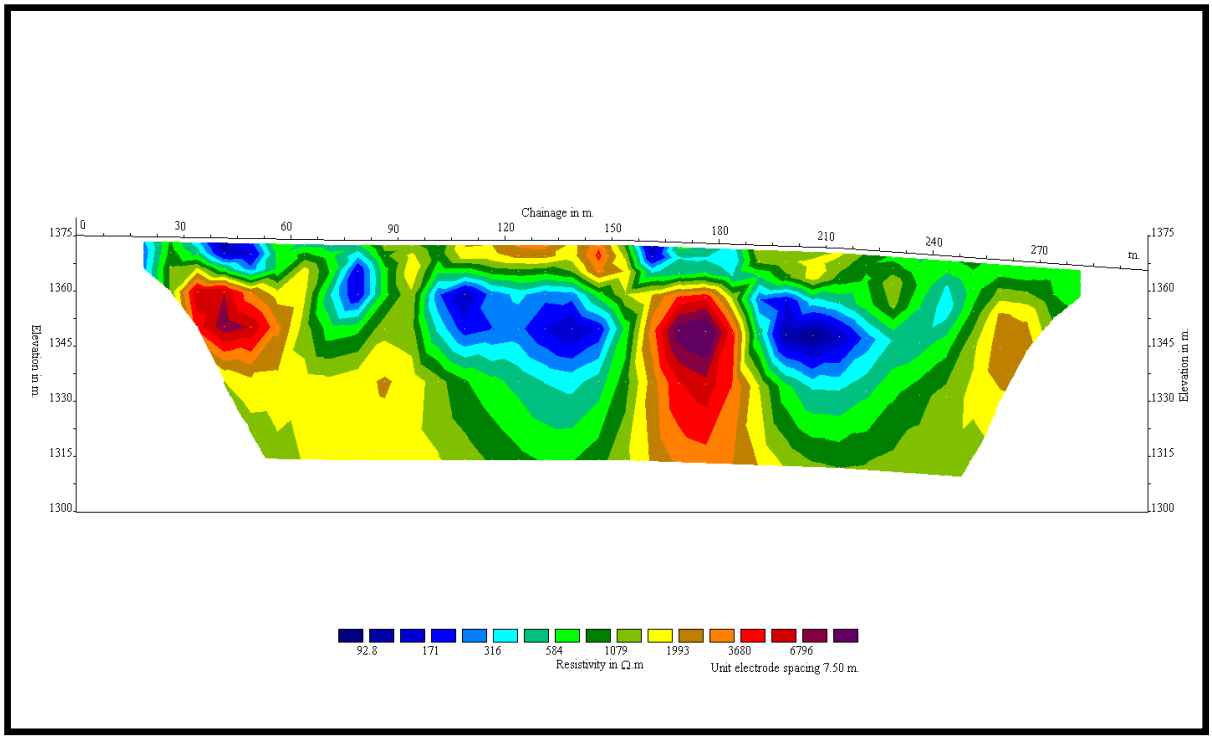

Fig. 6.13 Resistivity survey along profile line L-2.1

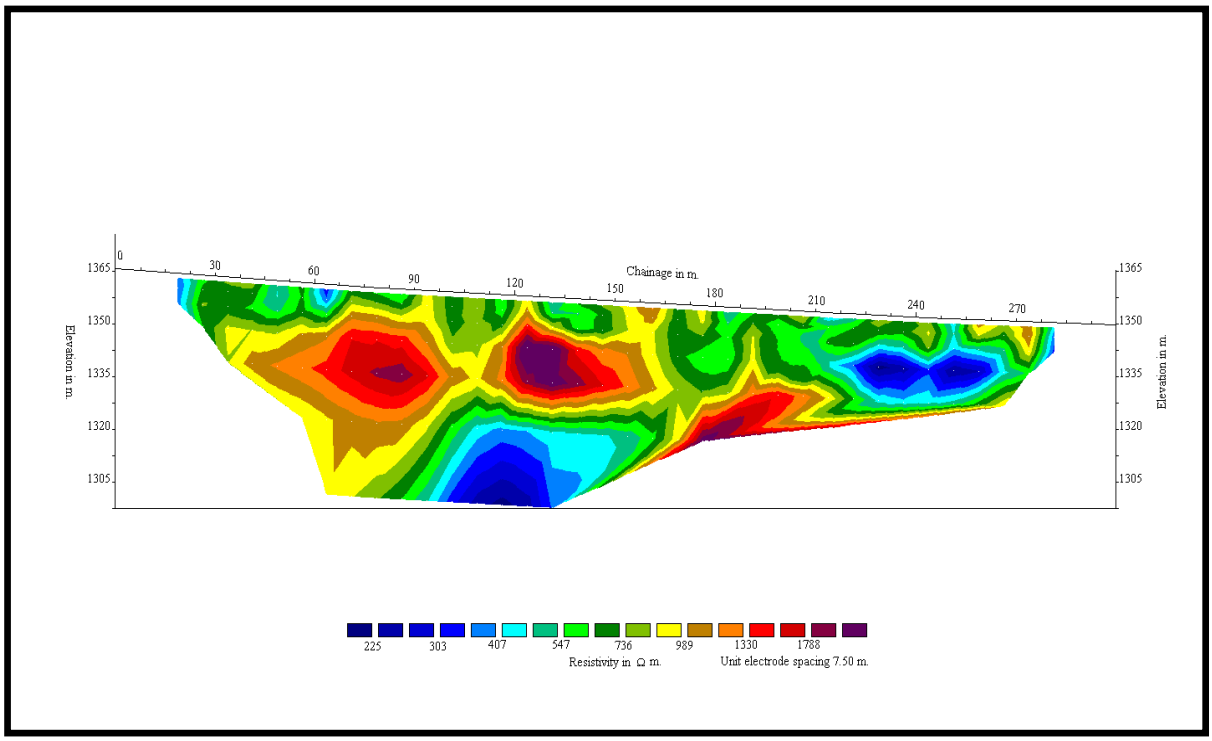

Fig. 6.14 Resistivity survey along profile line L-2.2

6.3 Powerhouse Site

Out of 14 profile lines, two lines namely L-9 and L-10 are conducted in the powerhouse area. The location of these lines is given in Fig. 6.15.

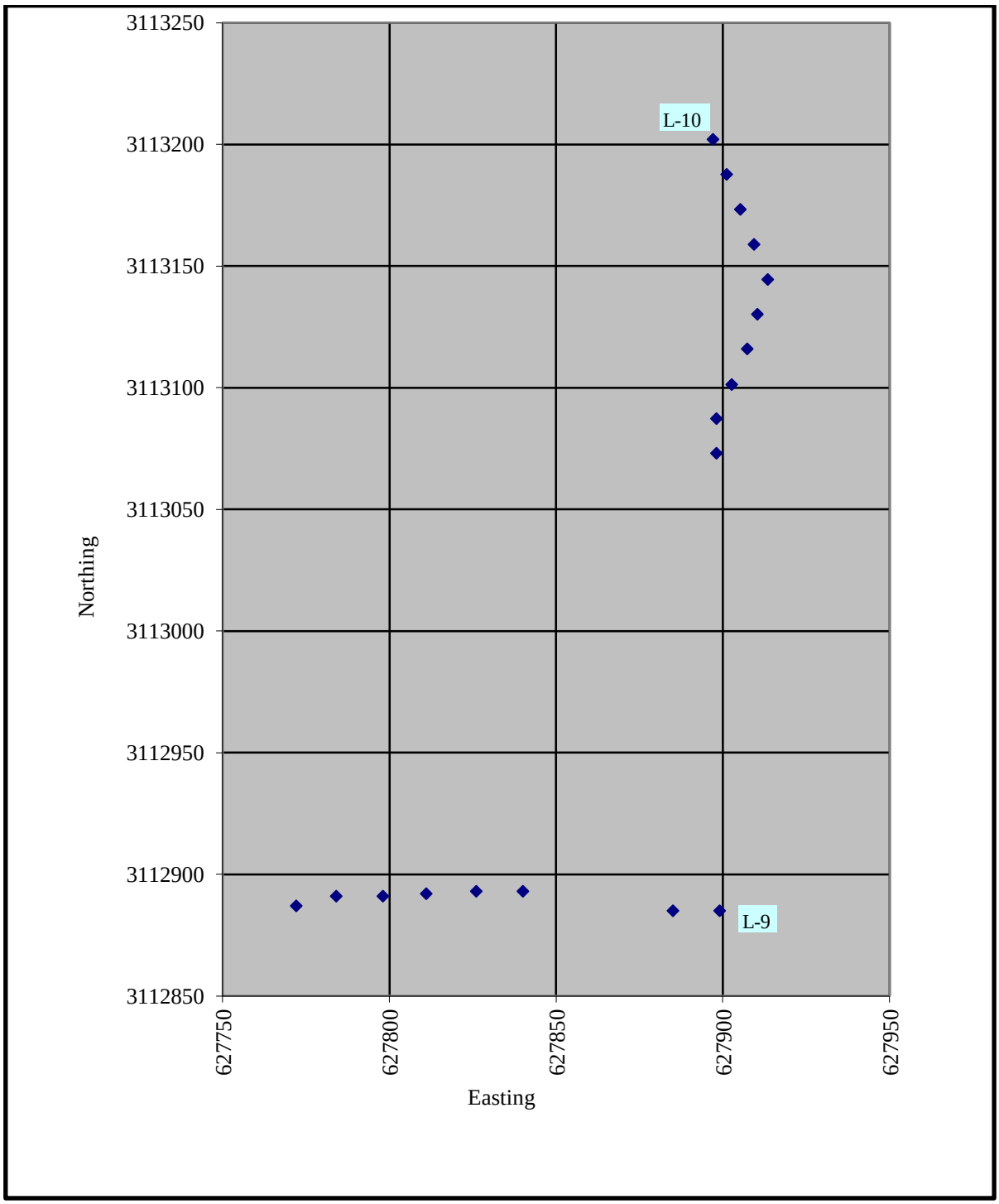

Fig. 6.15 Location chart for profile lines of powerhouse site

6.3.1 Profile Line L-9

The line (Fig. 6.16) is located at the southern part of the proposed powerhouse site. It starts from a point in the hill slope and ends at the right bank of the Bhote Koshi River.

The resistivity survey indicates the presence of regular and symmetrically distributed resistivity values towards depth. But, the resistivity values are decreasing in relation to depth. It reveals the presence of better quality rocks or compact dry overburden (old alluvium) at the top layer. Such moderately fresh rock mass are observed from the beginning of the line to the chainage point 85 m. The formations below the elevation of 1315 m have low resistivity value (<700Ωm). It is not enough to interpret the formations as sound bedrocks. So, it can be expected the zone being crack zone or thrust zone.

6.3.2 Profile Line L-10

The line (Fig. 6.17) is conducted in the north of line L-9. The study is conducted in the landslide along NW-SE direction.

The resistivity survey indicates the pattern of resistivity value is more or less similar to that of line L-9. As in the line L-9, high resistivity value are found sitting above the low resistivity value. The low resistivity value formations are occurring below the elevation of 1320 m. The presence of low resistivity value below the high resistivity value may be due to the formation of crack zone or fault zone.

The 10 m thick, high resistivity value formations are supposed to be moderately fresh rock mass that got detached from its parent rocks. Below this layer, semi weathered rock mass or alluvial deposits are expected.

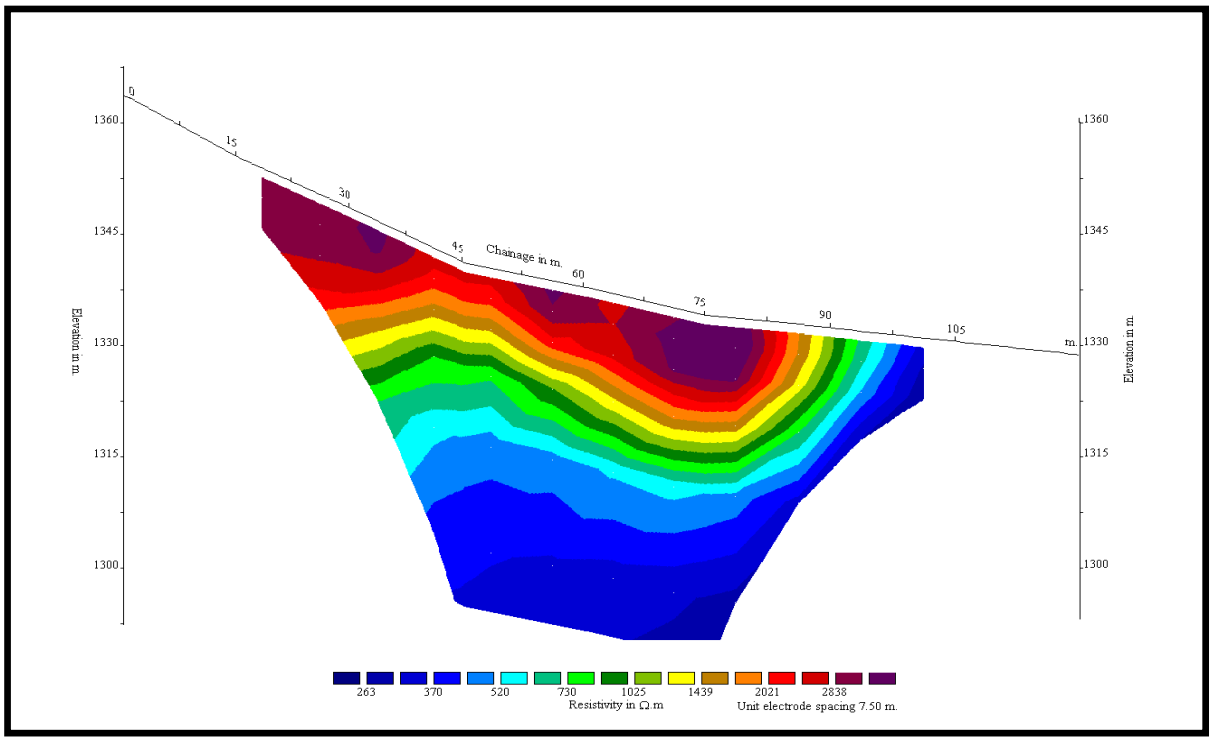

Fig. 6.16 Resistivity survey along profile line L-9

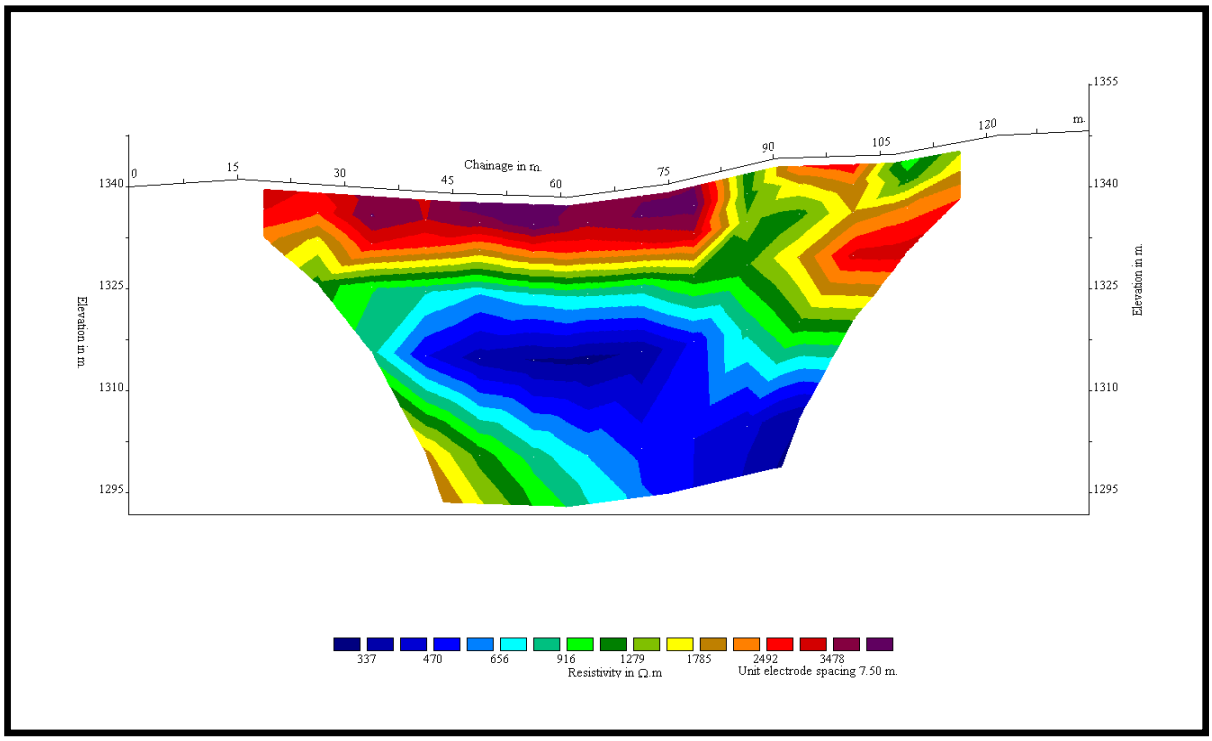

Fig. 6.17 Resistivity survey along profile line L-10

6.4 Kholsi Area

Out of 14 profile lines, three lines namely L-11, L-12 and L-13 are conducted across the three kholsies. The location of these lines is given in Fig. 6.18.

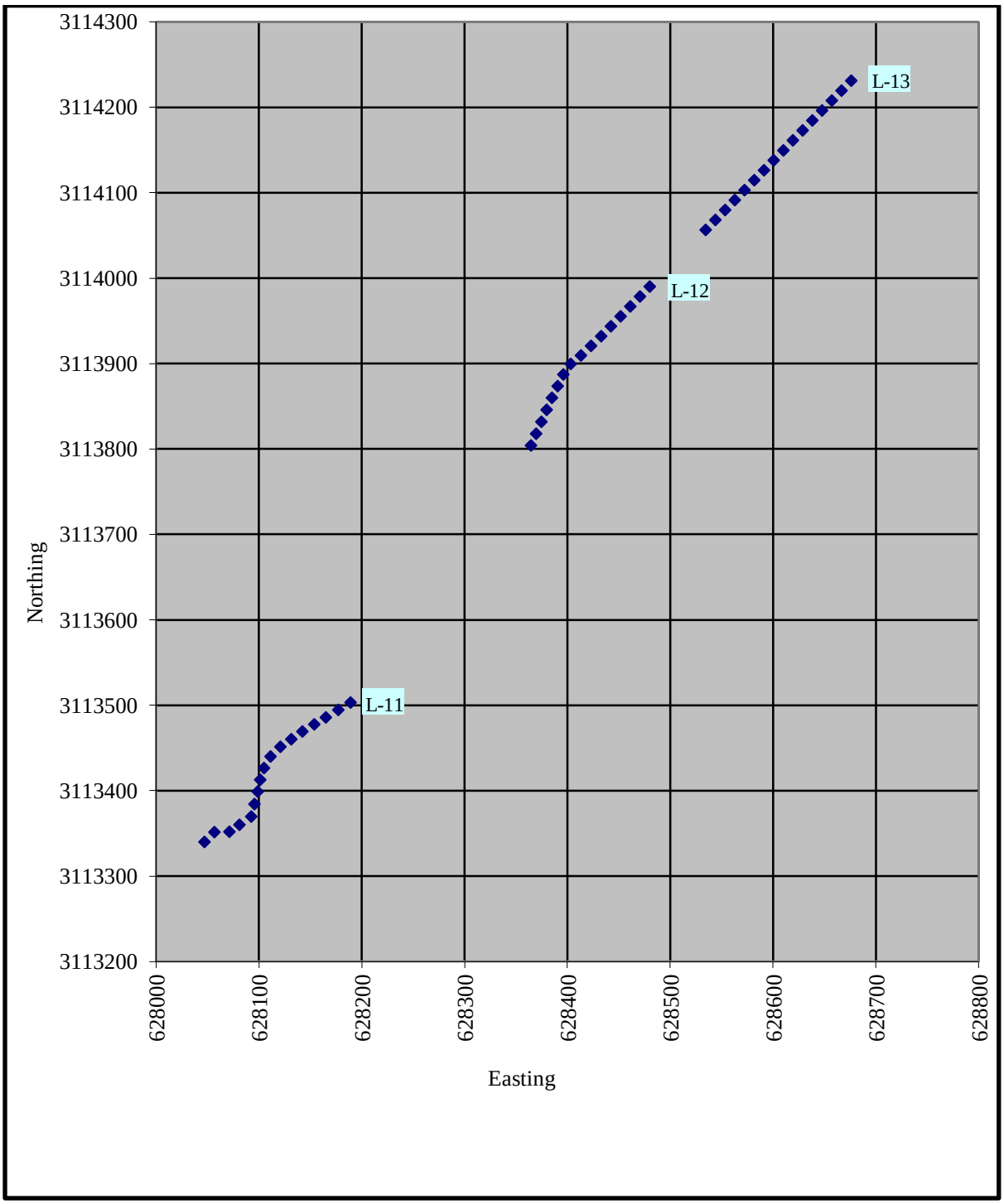

Fig. 6.18 Location chart for profile lines along three kholsies

6.4.1 Profile Line L-11

The line (Fig. 6.19) is conducted across the Khahare Kholsi at the right bank of the Bhote Koshi River. The purpose of the line is to study whether any fault zone or crack zone along the kholsi is present or not.

The resistivity survey reveals the presence of more than 80% formations having resistivity value greater than 2000Ωm. It means 80% of the formations are moderately fresh to fresh bedrocks. However, the irregular and unsymmetrical distribution of resistivity value indicates the presence of fractures and cracks within these bedrocks.

There are three low resistivity value formations along this section. The low resistivity value observed between chainage points 30 m and 45 m may be due to partially saturated rocks with minor cracks. But, the low resistivity value observed between chainage points 105m and 135m may be due to highly fractured or saturated materials with major cracks. The formations with high resistivity value over these low resistivity value formations are expected to be moderately fresh bedrocks or dry colluviums containing big fragments of rocks.

At the end of this line, the low resistivity value formation found between chainage points 170 m and 200 m are expected to be river sediments.

6.4.2 Profile Line L-12

The line (Fig. 6.20) is conducted across the Tasangi Kholsi at the right bank of the Bhote Koshi River. It starts from a point at the right bank of Bhote Koshi River and ends near a suspension bridge connecting Thulobharkhu and Gre village.

The resistivity survey reveals the first half comprising low resistivity value and the other half comprising high resistivity value. The low resistivity value formations (< 700Ωm) are expected to be either highly fractured and saturated rocks or river sediments comprising sand and pebbles. But, the formations with highly fractured and saturated rocks with recent alluvium on the top layer indicate the presence of crack zone.

The high resistivity value observed in second half of the section represents the presence of sound bedrocks. It is found in between chainage points 120 m and 210 m.

6.4.3 Profile Line L-13

The line (Fig. 6.21) is conducted across the Gre Kholsi at the right bank of the Bhote Koshi River.

The resistivity survey reveals the presence of low resistivity value formations along the whole section. So, the area is expected to be either a thick basin of river sediments or a thrust zone.

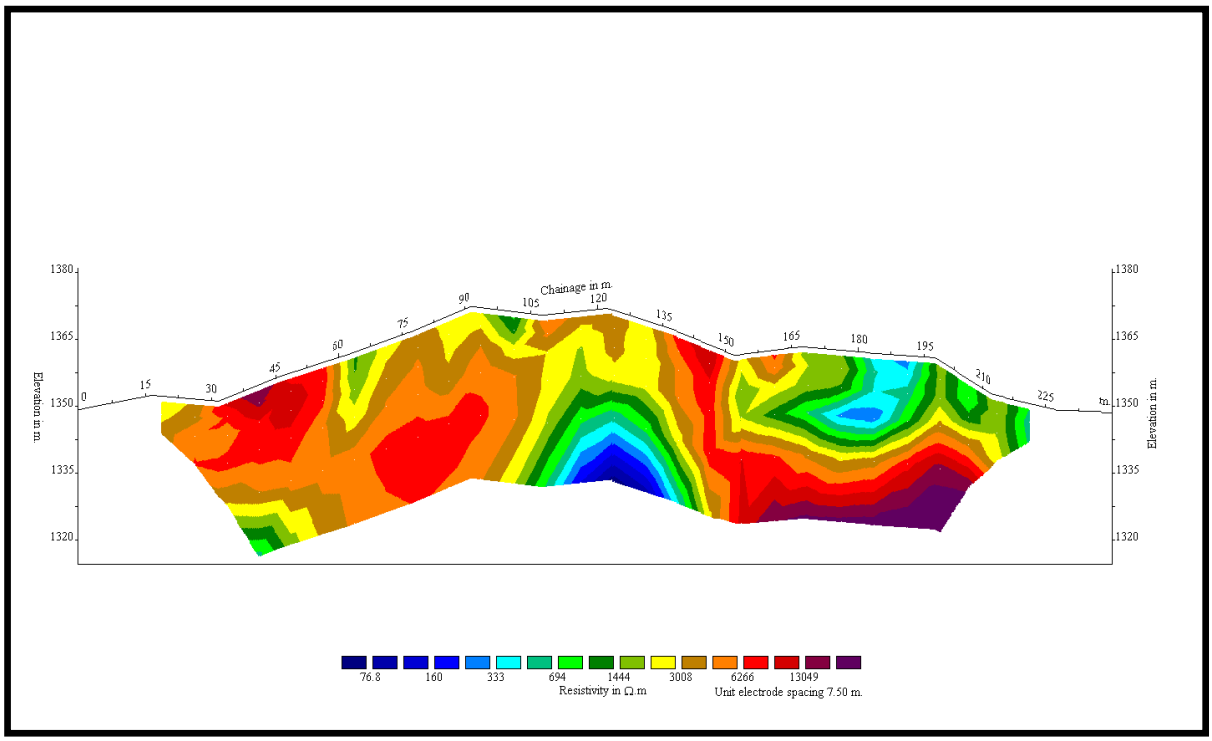

Fig. 6.19 Resistivity survey along profile line L-11

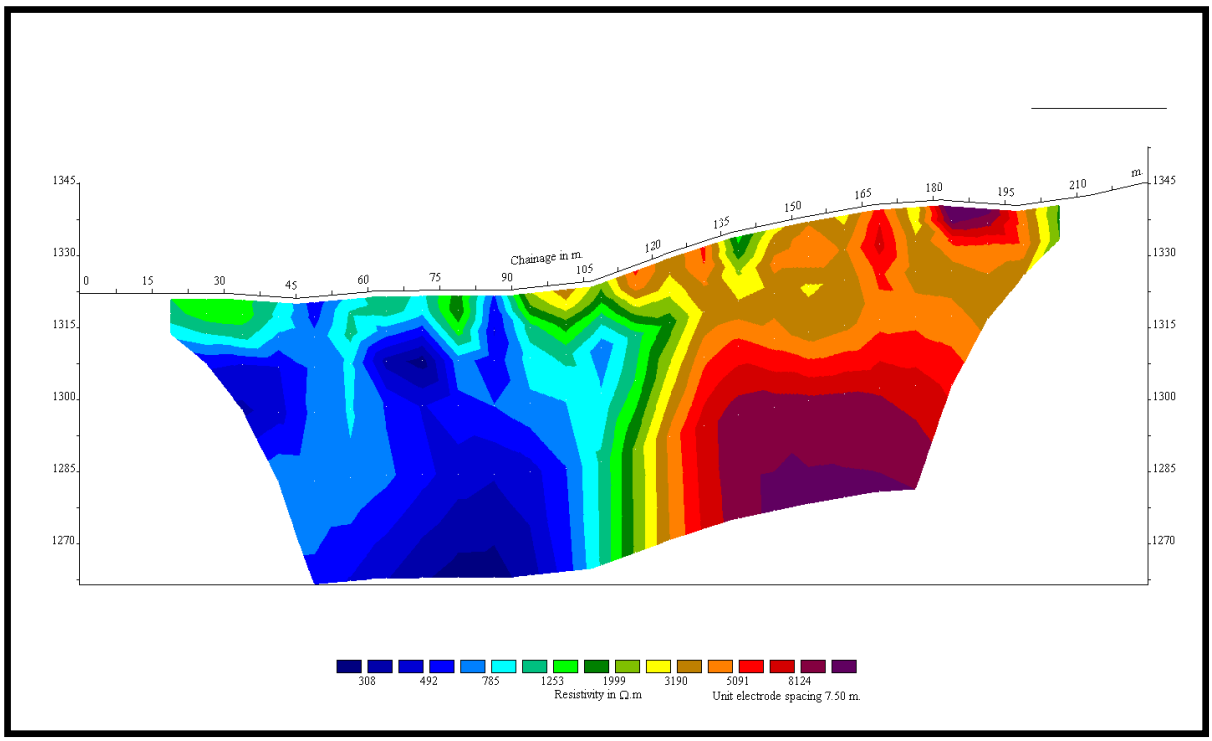

Fig. 6.20 Resistivity survey along profile line L-12

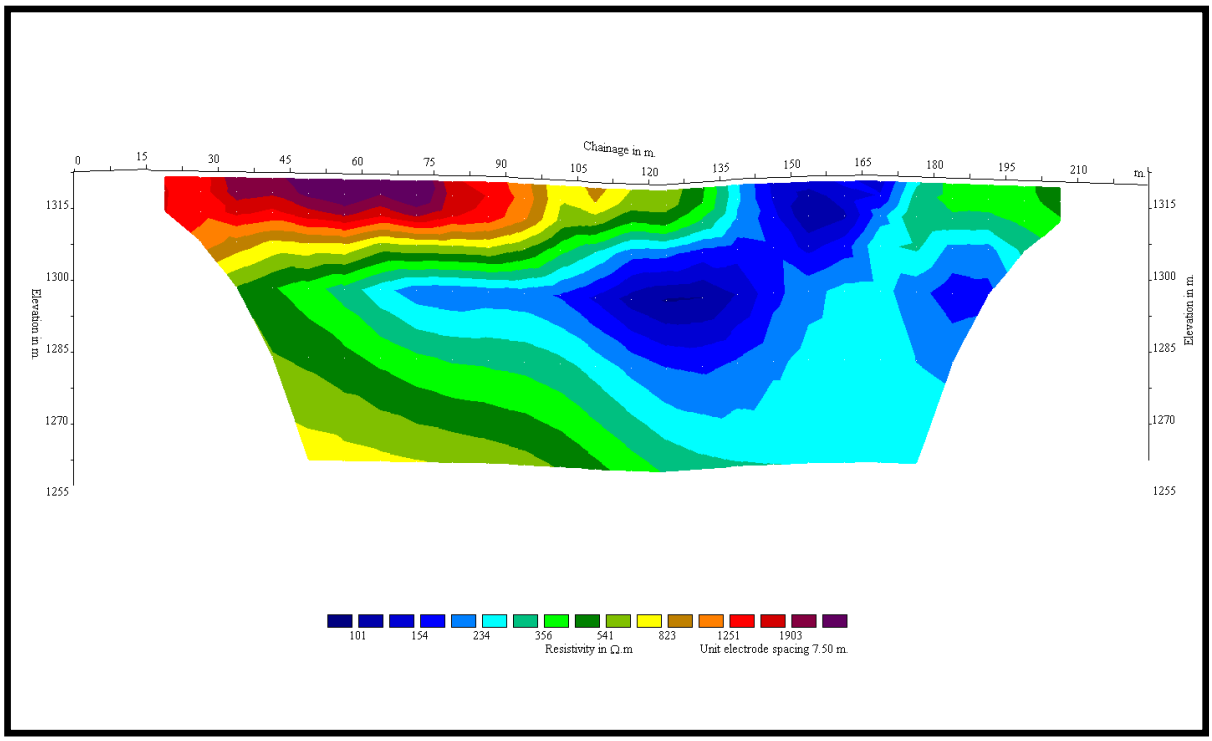

Fig. 6.21 Resistivity survey along profile line L-13

Note:

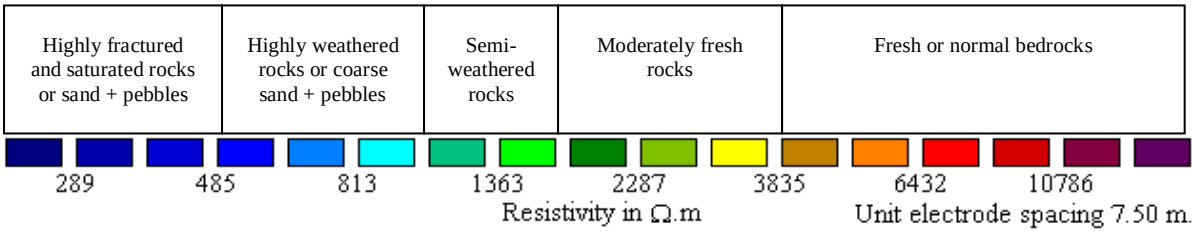

CHAPTER 7

CONSTRUCTION MATERIAL SURVEY

Construction material survey encompasses the identification of burrow areas by visual estimation in the field. The investigation is conducted in the vicinity of the headwork and powerhouse areas. It is focused on locating prospective burrow areas of non-cohesive materials which are to be used mainly as an ingredient of concrete. The prospective burrow sites are identified as sources of coarse aggregates.

7.1 Burrow Sites

The requisite quantities of construction material like boulders, cobble, gravel and sand are generally available in and around the project area. Point bar deposits of the Bhote Koshi River and excavated materials from the tunnel alignment area are the main source of construction material. The location and volume of construction materials are given in Fig. 7.1 and Table 7.1.

Table 7.1 Details of construction materials

SN	Location	Percentage of clasts	Volume (m^3)	Composition	Stability condition	Source of sediments	Land use	Distance from project structure
C1	Confluence of Syo Khola and Bhote Koshi River	Boulder-30% Cobble and pebble-50% Sand-20%	200×10×5	Gneiss-60% Quartzite-30% Schist-10%	Stable	River bed	Barren	850 m from intake and 3 km from powerhouse
C2	Confluence of Gre Khola and Bhote Koshi River	Boulder-30% Cobble and pebble-50% Sand-20%	200×15×5	Gneiss-60% Quartzite-30% Schist-10%	Stable	River bed	Barren	2.2 km from intake and 1.5 km from powerhouse
C3	Gum Area	Boulder-30% Cobble and pebble-50% Sand-20%	250×20×4	Gneiss-70% Quartzite-20% Schist-10%	Stable	River bed	Barren	2 km from intake and 1.7 km from powerhouse
C4	Chhokal Area	Boulder-30% Cobble and pebble-40% Sand-30%	500×100×25	Gneiss-40% Quartzite-40% Others-20%	Stable	River bed	Barren	1.8 km from intake and 1.9 km from powerhouse

Contd…

SN	Location	Percentage of clasts	Volume (m^3)	Composition	Stability condition	Source of sediments	Land use	Distance from project structure
C5	Betrawati	Red clay	Unlimited	Clay-100%	Stable	Quarry along the road	Barren	20 km from the project area
C6	Battar	Red clay	Unlimited	Clay-100%	Stable	Quarry along the road	Barren	30 km from the project area
TK03	On the left bank of Bhote Koshi River between ZK03 and ZK04	Boulder-50% Cobble and pebble-30% Sand-20%	Unlimited	Gneiss-60% Quartzite-20% Others-20%	Stable	River bed	Cultivated	400 m SE from the intake
TK04	On the left bank of Bhote Koshi River at about 100 m upstream from the proposed weir axis area	Boulder-50% Cobble and pebble-40% Sand-10%	300×10×3	Gneiss-70% Quartzite-20% Others-10%	Stable	River bed	Barren	300 m from intake and 3.4 km from powerhouse
TK07	On the left bank of Bhote Koshi River at about 250 m upstream from the weir axis	Boulder-40% Cobble and pebble-50% Sand-10%	500×10×3	Gneiss-40% Quartzite-40% Others-20%	Stable	River bed	Barren	500 m NE from intake
TK08	On the left bank of Bhote Koshi River in front of Syo Khola	Boulder-30% Cobble and pebble-50% Sand-20%	Unlimited	Gneiss-50% Quartzite-30% Others-20%	Stable	River bed	Barren	1 km downstream from intake
TK09	On the left bank of Bhote Koshi River at about 300 m SW of TK08	Boulder-50% Cobble and pebble-40% Sand-10%	Unlimited	Gneiss-60% Quartzite-30% Others-10%	Stable	River bed	Barren	1.6 km from intake and 2.1 km form powerhouse

Contd…

SN	Location	Percentage of clasts	Volume (m^3)	Composition	Stability condition	Source of sediments	Land use	Distance from project structure
TK11	On the left bank of Bhote Koshi River at about 70 m NE of TK03	Boulder-60% Cobble and pebble-30% Sand-10%	200×15×10	Gneiss-40% Quartzite-40% Others-20%	Stable	River bed	Barren	0.6 km NE from intake
TK12	On the right bank of Bhote Koshi River at about 250 m upstream from Chilime Powerhouse	Boulder-50% Cobble and pebble-40% Sand-10%	Unlimited	Gneiss-70% Quartzite-20% Others-10%	Stable	River bed	Barren	1 km NE from intake
TK13	On the left bank of Bhote Koshi River at about 250 m upstream from Chilime Powerhouse	Boulder-60% Cobble and pebble-30% Sand-10%	Unlimited	Gneiss-50% Quartzite-40% Others-10%	Stable	River bed	Barren	0.9 km NE from intake

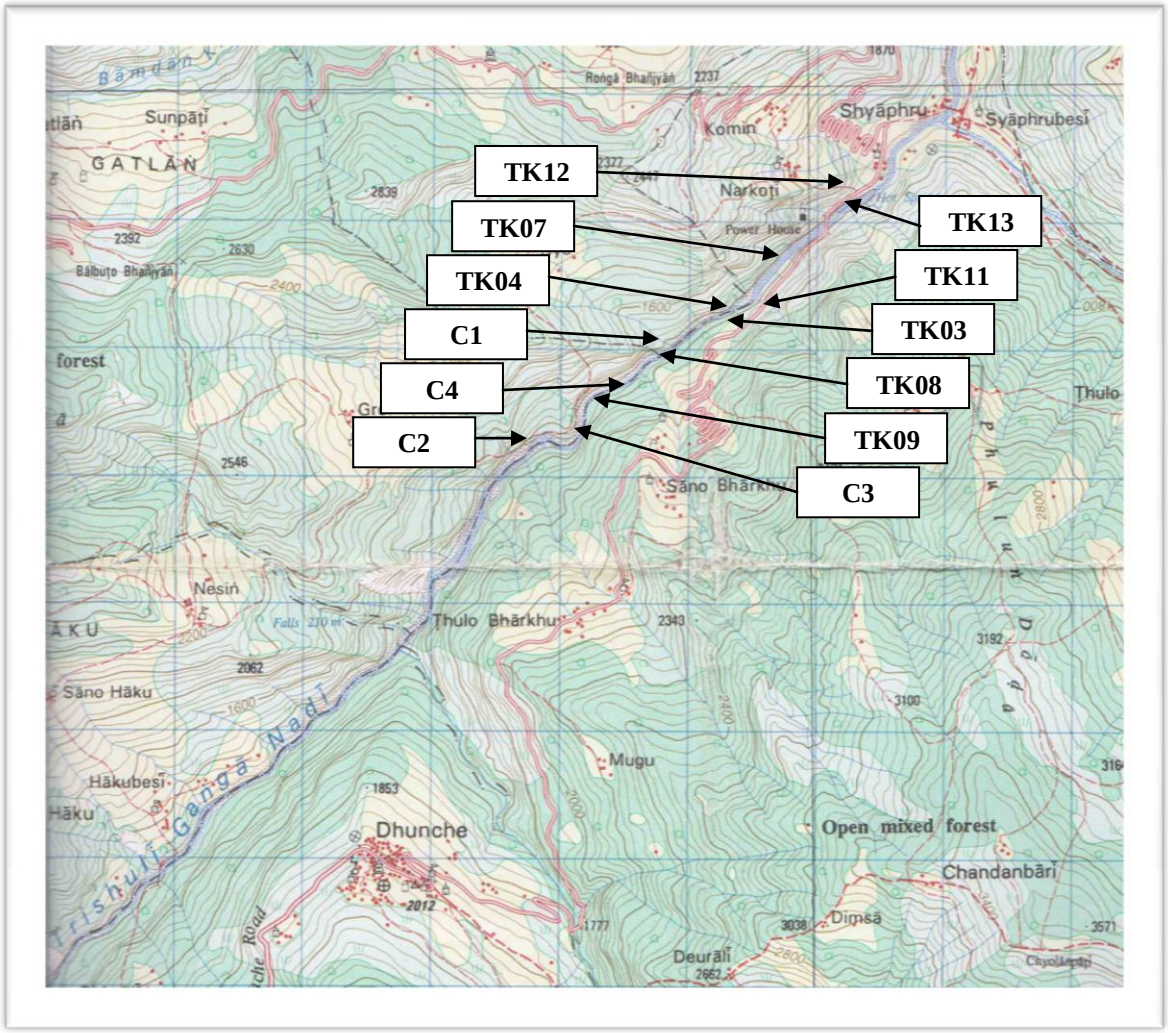

Fig. 7.1 Location map for Construction Material

7.2 Muck Disposal Area

Large amount of muck will be extract from the underground structures during excavation. The excavated muck can be deposited along the river bank of the Bhote Koshi River. The location for mucking is presented in Table 7.2 and Fig. 7.2.

Table 7.2 Location for Muck Disposal

S.N	Location	Area (m^2)	Stability Condition	Hydrological Condition	Distance from the Adit Area
M1	Chhokal	200 × 50	Stable	Wet	1.5 km upstream from adit-1
M2	Gum Village	200 × 50	Stable	Wet	1 km upstream from adit-2 and 3
M3	Bhote Koshi River	200 × 20	Stable	Wet	0.5 km upstream from adit-2
M4	Bhote Koshi River	350 × 10	Stable	Wet	0.3 km upstream from adit-2

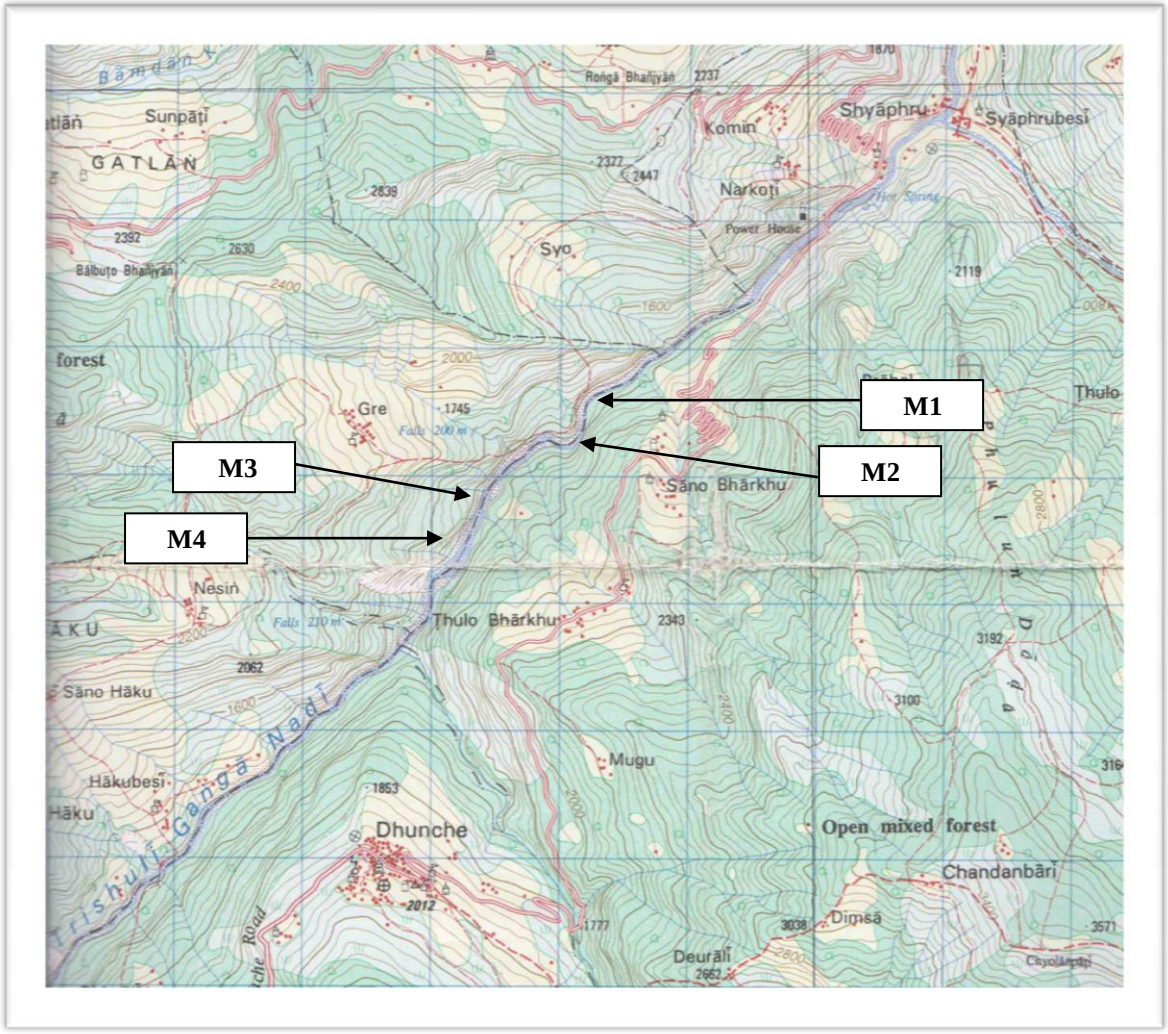

Fig. 7.2 Location map for Muck Disposal

CHAPTER 8

CONCLUSIONS

Based on geological, engineering geological, geotechnical and geophysical studies, their analysis and interpretation the following conclusions are made:

- The rocks of the study area belong to Ranimatta Formation, Lesser Himalaya. They comprise quartzite, phyllite and schist.
- Most of the underground structures lie on fair rocks (Quartzite >>Phyllite). Only the tunnel in the section Tasangi to Khahare Khola lie on poor Rocks (Quartzite << Phyllite).
- MCT lie on 3 km north of the proposed weir axis area and about 7 km south from powerhouse area.
- The headrace tunnel passes through two local passive faults i.e. Syo Khola Fault and Gre Khola Fault.
- The average attitude of the foliation plane is N 50° W / 38° NE.
- Alluvial deposits in the study area consist of gneiss, quartzite, phyllite and schist in the form of boulder, cobble and pebble and sand.
- Average in-situ deformation modulus obtained along the underground structures ranges between 6.7865 and 22.719.
- Vertical and horizontal stress as well as horizontal to vertical stress ratio along the underground structures range from 0.74-3.9394 MPa, 1.5029-5.7050 MPa and 0.623- 3.262 respectively.
- Uniaxial compressive strength of the rock along the underground structures varies from 93.264 to 137.344 MPa.
- Damage index varies from 0.0367 to 0.1158. Hence, rock show elastic behavior.
- Rock support design based on different systems suggests the combination of systematic bolting and reinforcement shotcrete as per requirement.
- 2D resistivity survey for subsurface investigation indicates the presence of thick layer of overburden ranging from 15 m to 60 m.
- Construction materials can be extracted from 14 sites in the vicinity of the project area.
- Muck disposal can be done in 4 sites in the vicinity of the project area.

REFERENCES

Arita, K., 1983. Origin of the inverted metamorphism of the lower Himalayas, Central Nepal. Tectonophysics 95 (1-2): 43-60.

Auden, J.B., 1935. Traverses in the Himalaya. Record of Geological Survey of India, 69, pp. 123-167.

Barton, N., Lien, R., Lunde, J., 1974. Engineering classification of rock masses for the design of rock support. Rock Mechanics, 6, pp. 189-236.

Bieniawski, Z.T., 1978. Determining rock masses deformability-experience from the case histories. Int. J. Rock Mech. Min. Sci. and Geomech, Abstr, 15, pp. 237-247.

Bieniawski, Z.T., 1989. *Engineering rock mass classifications*. John Wiley and Sons, New York, 251 p.

Bordet, P., Colchen, M., Le Fort, P., 1972. Some features of the geology of the Annapurna range Nepal Himalaya. Himalayan Geology, 2, pp. 537-563.

Corvinus, G., 1988. The Mio-Plio-Pleistocene litho- and bio-stratigraphy of the the Surai Khola Siwaliks in the West Nepal: first results. Comptes rendus des séances de 1´Academie des Sciences Paris Série, D 306, pp. 1471-1477.

Dahal, 2006. Geological map of Nepal, scale: 1:500,000.

Deere, D. U., 1964. Technical description of rock cores for engineering purposes. Rock Mechanics and Engineering Geology, Vol. 1, N.1, pp 17-22.

Deere, D. U., Peck, R.B., Parker, H., Monsees, J.E., Schmidt, B., 1970. Design of the tunnel support systemsHigh Res. Rec., 339, pp. 26-33.

D.M.G., 1987. Geological map of Central Nepal (1:250,000).

Fuchs, G., Widder, R.W., Tuladhar, R. (1988). Contributions to the geology of the Annapurna range (Manang area Nepal). *Jahrbuch der Geologischen Bundesanstalt.* 131. pp. 593-607.

Gansser, A., 1964. *Geology of the Himalayas*. Interscience Publishers, John Wiley and Sons, London, 289p.

Grimstad, E., and Barton, N., 1993. Updating of the Q-system for NMT. Proc. Int. Symp. on theSprayed Concrete., Norwegian Geotechnical Institute. Norway, pp. 1-10.

Guillot, S., 1999. An overview of the metamorphic evolution in Central Nepal. Journal of Asian Earth Sciences 17 (5-6): 713-725.

Hagen, T., 1969. Report on the Geological Survey of Nepal. Preliminary reconnaissance Denkschriften der Schweizerischen Naturforchenden Gesellschaft, Memoires de la Societte Helvetique des Sciences natures, Zurich, 86, 185 p.

Heim, A., and Gansser, A., 1939. Central Himalaya: Geological observations of the Swiss expedition 1936. Memoires de la Societte Helvetique des Sciences natures, Zurich, 73 (1), pp. 1-245.

Hoek, E., Brown, E.T., 1980, *Underground Excavation in Rock*. The Institution of Mining and Metallurgy, London, 527 p.

Hoek, E., Kaiser, P.K. Bawden, W.F., 1995. *Support of Underground Excavation in Hard Rock*. Oxford and IBH Publishing Co. Pvt. Ltd., New Delhi, 185 p.

Kohn M.J., Wieland M.S., Parkinson C.D. and Upreti B. N, 2005. Five generations of monazite in Langtang gneisses: implications for chronology of the Himalayan metamorphic core, J. metamorphic Geol., 23, pp. 399–406.

Laubscher, D.H., 1975. Geomechanics classification of jointed rock masses – mining applications. Trans. Instn. Min. Metall. 86, A1-8.

Lauffer, H. 1958. Gebirgsklassifizierung fűr den Stollenbau. Geol. Bauwesen 24 (1), 46-51.

Le Fort, P., 1975. Himalaya: the collided range present knowledge of the continentalarc. Am. J. Sci., 275 A, pp. 1-44.

Liu, G., Einsele, G., 1994. Sedimentary history of the Tethyan basin in the Tibetan Himalaya. *Geologischen Rundschau* 83: 32-61.

Macfarlane, A.M., 1992. The tectonic evolution of the core of the Himalaya, Langtang National Park, Central Nepal, (Ph.D. Thesis), Cambridge Institute of Technology.

Marinos, Hoek, E., 2001. Estimating the geotechnical properties of heterogeneous rock masses such flysch, Bull. Engg. Geol. Env. Vo. 60, pp. 85-92.

Medlicott, H.B., 1875. Note on the Geology of Nepal. Records of the Geological Survey of India 8, pp. 93-101.

Munthe, J., Dongol, B., Hutchison., J.H., Keans, W.F., Munthe, K., West, R.M., 1983. New fossil discoveries from the Miocene of Nepal include a hominoid. Nature, 303, pp. 331-333.

Palmstrőm, A., 2000. Recent developments in rock support estimates by the RMi. Journal of rock mechanics and tunnelling technology, vol. 6, No. 1, pp. 1-19.

Parrish, R.R. and Hodges, K.V., 1996. Isotopic constraints on the age and provenance of the Lesser and Greater Himalayan Sequences, Nepalese Himalaya. Geological Society of America, Bull. pp. 904-911.

Pêcher, A. and Le Fort, P., 1986. The Metamorphism in Central Himalaya, its relations with the thrust tectonic. In Le Fort, P., Colchen, M. and Montenat, C.. *Évolution des Domains Orogénique d'Asie Méridionale (de la Turquie à la Indoneasie)*. Science Terre. 47. pp. 285–309.

Rai, S.M., 1998. étude structural, métamorphique, géochimique et radiochronologique des nappes de Katmandou et du Gosainkund, Himalaya de Népal central (Thés d´université thesis), Univ Joseph-Fourier, Grenoble, 244 p.

Rai, S.M., 2001. Geology, geochronology and radio chronology of the Kathmandu and Gosainkunda Crystalline Nappe, Central Nepal Himalaya. Journal of Nepal Geological society, vol. 25 (Sp. Issue), pp. 135-155.

Romana, M., 1985. New Adjustment Rating for application of the Bieniawski Classification to Slopes. Proc. Int. Sym. Rock Mech. Min. Civ. Works, ISRM, Zacatecas, Mexico, pp. 59-69.

Seraphim, J.L. and Pereira, J.P., 1983. Consideration of the Geomechanical Classification of Bieniawski. Proc. Int. Symp. on Engineering Geology and Underground Construction, Lisbon, 1(II), pp. 33-44.

Sheory, P.R., 1994. A theory for in-situ stresses in isotopic and transversely isotropic rock. Int. J. Rock Mech. Min. Sci. and Geomech., Abstr., 31(1), pp. 23-34.

Stöcklin, J., 1980. Geology of Nepal and its regional Frame. Journal of the Geological Society of London, 137, pp. 1-34.

Stöcklin, J. and Bhattarai, K.D., 1977. Geology of the Kathmandu area and Central Mahabharat Range, Nepal Himlaya. Report of Department of Mines and Geology/UNDP (unpublished), 86p.

Takagi, Arita, K., Sawaguchi, Kobayashi and Awaji, D., 2003. Kinematic History of the Main Central Thrust Zone in the Langtang area, Nepal. Technophysics. Vol. 366 pp. 151-163.

Terzaghi, K., 1946. Rock defects and loads on tunnel supports. In rock tunnleing with steel supports, (eds R.V. Proctor and T.L. White) 1, 17-99. Younstown, OH: commercial Shearing and Stamping Company. pp. 17-99.

Upreti, B.N., 1999. An overview of the stratigraphy and tectonics of the Nepal Himalaya. Journal of Asian earth Science, Vol. 17, pp. 577-606.

WECS, 2011. Water resources of Nepal in the context of climate change. pp. 49-55.

West, R.M., Munthe, J., Lukacs, J.R., Shrestha, T.B., 1975. Fossil mollusc from the Siwaliks of Eastern Nepal. Current Scence, 44, pp. 497-498.

West, R.M., Munthe, J., Lukacs, J.R., Shrestha, Hussian, S.T., 1978. Vertebrate fauna from Neogene Siwalik Group, Dang Valley, Western Nepal. Journal of Paleontology, 52, pp. 1015-1022.

West, R.M., Munthe, J., 1981. Neogene vertebrate paleontology and stratigraphy fo Nepal. Journal of Nepal Geological Society, 1, pp. 1-14.

Wickham, G.E., Tiedeman H.R., and Skinner, E.H., 1972. Support Determination based on Geological prediction. Proc. Rapid Excav. Tunnelling Conf. AIME, New York, pp. 43-64.

LIST OF ANNEXES

ANNEX-I

SALIENT FEATURES OF THE UPPER TRISHULI – 2 HYDROELECTRIC PROJECT, RASUWA

UPPER TRISHULI – 2 HYDROELECTRIC PROJECT (100 MW), RASUWA

SALIENT FEATURES

S. N.	Name	Unit	Quantity	Remark
A	***Hydrology***			
1	Catchment above the dam site	km^2	4064 (dam site)	4074 (powerhouse site)
2	Utilized Hydrology	year	40	
3	Multi-year mean annual runoff	100,000,000 m^3	54.7	
4	Indicated runoff			
	Multi-year mean runoff	m^3/s	176	
	Designed flood runoff (P = 1%)	m^3/s	3260 (dam site)	
	Check flood runoff (P = 0.1%)	m^3/s	4140 (dam site)	
	Construction diversion flood runoff (P = 10%)	m^3/s	396 (dam site)	
5	Sediment			
	Multi-year mean suspended load annual transfer quantity	10,000 t	302	
	Multi-year annual sediment concentration	kg/ m^3	0.544	Flood season 0.69
	Multi-year mean bed load annual transfer quantity	10,000t	60	
B	***Reservoir***			
1	Water level of the reservoir			
	Check flood level	m	1382.1	
	Design flood level	m	1380.3	
	Normal water level	m	1372	

Contd…

S. N.	Name	Unit	Quantity	Remark
2	Catchment area of the normal water level	km^2	0.0247	
3	Reservoir volume			
	Volume below the normal water level	10,000 m^3	13.5	
4	Regulating characteristics		None	
C	***Let down flow quantity and its relative downstream water level***			
1	Unit whole running maximum quotative runoff	m^3/s	112.8	
2	Relative downstream water level	m	1260.18	
D	***Project performance indicator***			
1	Total installed capacity	MW	100	
2	Guaranteed output	MW	29.4	
3	Multi-year mean power generating quantity	100,000,000kW·h	5.85	
4	Annual utilized hours of the unit	h	5854	
E	***Land requisition and resettlement***			
1	Flooded cultivated land	mu	-	
2	Flooded woodland	mu	6.3	
3	Transferred people	person	-	
4	Dismantled houses	m^2	-	

Contd…

S. N.	Name		Unit	Quantity	Remark
F	***Main building and facilities***				
1	Water block building				
	Main Dam	Dam type		Concrete gate dam	
		Dam crest	m	1383.5	
		Maximum height of the dam	m	31.5	
		Length of the dam top	m	123.1	
	Seismic peak acceleration			0.25	
2	Water discharge buildings				
	Water discharge sand sluicing gate	Number of the orifice-dimension of the orifice mouth	m×m	3-4.5 ×6	w×h
		Intake invert elevation	m	1355	
		Maximum discharge quantity	m^3/s	1041	
		Energy dissipation mode		underset	
	Spillway dam	Cofferdam crest elevation	m	1372	
		Length of the dam crest	m	54.5	
		Maximum discharge	m^3/s	3099	
		Energy dissipation mode		underset	

Contd…

S. N.	Name		Unit	Quantity	Remark
3	Water conveying buildings				
	Water intake	Type of the intake		bank-tower	
		Underset elevation of the intake	m	1362	
	Diversion tunnel	Design flow quantity	m^3/s	112.8	
		Tunnel lining		part concrete	
		Quantity of the pressure pipe	pipe	1	
		Diversion tunnel diameter/length	m	7/3600	Diameter after concrete lining
	Sediment basin	Type		Underground sediment basin-continuous flushing type	
		Dimension inside the project area	m	130×15×10.3	L, W and H
	Surge shaft	Diameter	m	11	
		Height	m	59.5	
	Pressure pipe	Diameter	m	5	
		Length	m	155	
4	Powerhouse				
	Type of the powerhouse			underground	
	Dimension		m	70×17.6×44.8	L, W and H
	Installed elevation of the turbine		m	1253.2	

Contd…

S. N.	Name		Unit	Quantity	Remark
5	Tailrace tunnel				
	Type			pressure	
	Diameter		m	4.5	
	Length		m	135	
6	Switchyard				
	Type			Indoor GIS	
	Area of the transmission line outgoing yard		m×m	30×17.5	
7	Main electromechanical equipments				
	Quantity of turbine		unit	2	
	Rated water head		m	98	
	Rated output		MW	100	
	Quantity of the generator		unit	2	
	Capacity of the generator per unit		MW	50	
	Transmission voltage		kV	220	
	Quantity of the circuit		loop	2	
G	***Construction***				
1	Main work quantity	Soil and stone excavation	m^3	1,135,675	
		Excavation of the stone tunnel	m^3	466,461	
		Soil and stone filling	m^3	29,576	
		Concrete	m^3	187,433	
		Rebar	t	8,943	
		Reinforced material	t	813	

Contd…

S. N.	Name		Unit	Quantity	Remark
		Curtain grouting	m	1370.6	
		Consolidation grouting	m	96,983	
2	Transportation		km	307	
3	Construction diversion				
	Type			Stage diversion	
				Soil and stone cofferdam and geomembrane, set sprinkler grouting	
	Class			Class building	Once every decade flood
4	Construction duration				
	Preparation duration		month	3	
	Put into production duration of the first unit		month	46	
	Total construction duration		month	48	

ANNEX-II

PHOTOGRAPHS OF THE PROJECT AREA

Photograph 1: Reservoir Area, old alluvial deposits on the both banks of Bhote Koshi River

Photograph 2: Middle Dam Site area showing rocks on the right bank and alluvial deposits on the left bank of Bhote Koshi River.

Photograph 3: Overall view of Headworks Site (Option II)

Photograph 4: Depressed area of Syo Khola

Photograph 5: Bedrocks exposed along the Tunnel Alignment Area

Photograph 6: Fold developed in the bedrocks along the Tunnel Alignment Area

Photograph 7: Bedrocks observed in the Powerhouse Area

Photograph 8: Construction material on the riverbed of Bhote Koshi River at Gum village

Photograph 9: Red clay deposit along the road section at Betrawati village

Photograph 10: Red clay deposit along the road section at Battar village

ANNEX-III

GEOMECHANICAL PARAMETERS OF ROCK MASS OF THE PROJECT AREA

Location	Weather-ing	Continuity (m)				Spacing (m)				Roughness				Weaviness				Opening (mm)				Filling material				Rock type	Mineral type
		F	J_1	J_2	J_3	F	J_1	J_2	J_3	F	J_1	J_2	J_3	F	J_1	J_2	J_3	F	J_1	J_2	J_3	F	J_1	J_2	J_3		
Intake and Weir Axis Area																											
Right bank	F-S	>20	3-10	3-10	-	>2	>2	>2	-	R	R	R	-	U	ST	ST	-	<2	2 to 6	2 to 6	-	SA	SC	SC	-	Q>>P	Qtz/Fs
Approach/Diversion Tunnel Alignment, Desander Basin and Portal Inlet Area																											
Right bank	F-S	>20	3-10	3-10	3-10	>2	>2	>2	>2	R	R	R	R	ST	ST	ST	ST	<2	2 to 6	2 to 6	2 to 6	SA	SC	SC	SC	Q>>P	Qtz/Fs
HeadraceTunnel Alignment Area																											
Portal Inlet to Syo Khola	F-S	>20	3-10	3-10	3-10	0.5 - 2	0.5 - 2	>2	>2	R	R	R	R	ST	ST	ST	ST	<2	2 to 6	2 to 6	2 to 6	SA	SC	SC	SC	Q>>P	Qtz/Fs
Syo Khola to Gre Khola	F-S	>20	3-10	3-10	3-10	0.5- 2	>2	>2	>2	R	R	R	R	ST	ST	ST	ST	<2	2 to 6	2 to 6	2 to 6	SA	SC	SC	SC	Q>>P	Qtz/Fs
Gre Khola to Tasangi Khola	F-S	>20	3-10	3-10	3-10	>2	>2	>2	>2	R	R	R	R	PL	PL	PL	ST	<2	2 to 6	2 to 6	2 to 6	SA	SC	SC	SC	Q>>P	Qtz/Fs
Tasangi Khola to Khahare Khola	F-S	>20	3-10	3-10	3-10	>2	>2	>2	>2	R	R	R	R	PL	PL	PL	PL	<2	2 to 6	2 to 6	2 to 6	SA	SC	SC	SC	Q<<P	Qtz/Fs
Khahare Khola to Surge Tank	F-S	>20	3-10	3-10	3-10	>2	>2	>2	>2	R	R	R	R	ST	ST	ST	ST	<2	2 to 6	2 to 6	2 to 6	SA	SC	SC	SC	Q>>P	Qtz/Fs
Surge tank, Powerhouse and Tailrace Tunnel Alignment Area																											
Right bank	F-S	>20	3-10	3-10	3-10	>2	>2	0.5 - 2	>2	R	R	R	R	U	PL	PL	ST	<2	2 to 6	2 to 6	2 to 6	SA	SC	SC	SC	Q>>P	Qtz/Fs

F- Fresh, S- Slightly Weathered, R- Rough, U- Undulating, ST- Stepped, PL- Planar, SA- Surface Alteration, SC- Silty Clay, Q- Quartzite, P- Phyllite, Qtz- Quartz, Fs- Feldspar